COMISION NACIONAL DE ENERGIA ATOMICA
DEPENDIENTE DE LA PRESIDENCIA DE LA NACION

MICROSCOPIC ASPECTS OF PHASE TRANSFORMATIONS IN ALLOYS

Compilación de artículos del

Dr. PHILIP C. CLAPP
(Ledgemont Laboratory, Kennecott Copper Corporation, Lexington, Massachusetts)

para uso de los

alumnos del Curso de Actualización

dictado en la Gerencia de Tecnología de CNEA

Buenos Aires, Argentina
1972

COMISION NACIONAL DE ENERGIA ATOMICA
DEPENDIENTE DE LA PRESIDENCIA DE LA NACION

MICROSCOPIC ASPECTS OF PHASE TRANSFORMATIONS IN ALLOYS

Compilación de artículos del

Dr. PHILIP C. CLAPP
(Ledgemont Laboratory, Kennecott Copper Corporation, Lexington, Massachusetts)

para uso de los

alumnos del Curso de Actualización

dictado en la Gerencia de Tecnología de CNEA

Buenos Aires, Argentina
1972

MICROSCOPIC ASPECTS OF PHASE TRANSFORMATIONS IN ALLOYS

Philip C. Clapp

Lecture Outline

Lecture I

1. The General Problem of Phase Transformations
   a) How is a phase characterized, both theoretically and experimentally?
   b) How are phase transformations detected?
   c) How can phase transformations be predicted and controlled?

2. Specific Examples of Phase Transformations
   a) Gas-Liquid
   b) Liquid-Solid
   c) Ferromagnetic
   d) Displacive (Martensitic)
   e) Alloy Order-Disorder
   f) Rush Hour Traffic
   g) Life-Death
   h) Marriage

3. Alloy Order-Disorder Transformations: Description and Characterization

———————————— o ————————————

Lecture II

4. Atomic Pair Correlations as a Statistical Description of an Ordering or Clustering System
   a) The Warren-Cowley Short Range Order Parameters: Meaning and Use.

5. Measurement of Pair Correlations

a) X-ray Diffraction

b) Neutron Diffraction

c) Electron Diffraction

d) Field Ion Microscope

6. Theory of Pair Correlations

a) The Ising Model

b) Bragg-Williams Approximation

c) Cowley's Equations

d) Clapp-Moss Approximation

e) Cook-deFontaine model and the relationship between Spinodal Decomposition and Ordering Transformations.

———————————— o ————————————

Lecture III

7. Atomic Configurations of Disordered Phases

a) Computer Modelling from Experimental Data - (Cohen, Gehlen, Gragg)

b) Microdomain Models - (Moss, Thomas, Okamoto, Warlimont)

c) Cluster Frequency Distributions from Experimental Data - (Clapp)

8. Metallurgical Effects

a) k-state Alloys

b) Resistance Anomalies

c) Hardening Behaviour

d) "Tweed" structure

e) Frozen microdomains

———————————— o ————————————

Lecture IV

9. Possible Alloy Ordered Phases
   a) Clapp-Moss Diagrams
   b) Richards-Cahn Diagrams
10. Possible Mechanisms of Ordering or clustering
   a) Nucleation and Growth
   b) Spinodal Decomposition (Cahn, Cook - deFontaine)
   c) Continuous Ordeing (Cook - de Fontaine, Richards - Cahn)

Lecture V

11. Complex Ordering Transformations
   a) Long Period Super Lattices: (Sato-Toth, Moss)
12. Theories of Complex Ordering
   a) Long range interactions
   b) Pseudopotential Calculations
   c) Fermi Surface Effects
   d) Charge Transfer
13. Critique of Pairwise Interaction Models
   a) Strain Displacement Forces
   b) n-body Interactions
   c) CuPt
14. Directions for the Future

REFERENCE LIST

1. J.W. Christian, "The Theory of Transformations in Metals and Alloys" (Pergamon, Oxford, 1965)

2. "Phase Stability in Metals and Alloys", P.S. Rudman, J. Stringer, R.I. Jaffee editors (McGraw-Hill, N.Y., 1967)

3. L. Guttman, Solid State Physics 3, 145 (1956)

4. B.E. Warren, "X-Ray Diffraction" (Addison-Wesley, Reading Mass, 1969)

5. J.M. Cowley, Phys. Rev. 77, 669 (1950); 120, 1648 (1960); 138, A1384 (1965)

6. P.C. Clapp and S.C. Moss, Phys. Rev. 142, 418 (1966); 171 754, 764 (1968)

7. H.E. Cook and D. deFontaine, Acta Met. 17, 915 (1969); 19, 607 (1971)

8. P.C. Gehlen and J.B. Cohen, Phys. Rev. 139, A844 (1965)

9. J.E. Gragg and J.B. Cohen, Acta Met. 19, 507 (1971)

10. S.C. Moss, A.I.M.E. Metallurgical Society Conferences; 36, 95 (1966)

11. H. Warlimont and G. Thomas, Metal Sci. J. 4, 47 (1970)

12. P. Okamoto and G. Thomas, Acta Met. 19, 825 (1971)

13. P.C. Clapp, J. Phys. Chem. Sols. 30, 2589 (1969); Phys. Rev. B 4, 255 (1971)

14. J.B. Cohen and M.E. Fine, J. Phys. Radium 23, 749 (1962); Acta Met. 11, 1106 (1963)

15. M.J. Richards and J.W. Cahn, Acta Met. 19, 1263 (1971)

16. H. Sato and R.S. Toth in "Alloying Behaviour and Effects in Concentrated Solid Solutions" edited by T.B. Massalski (Gordon and Breach, N.Y., 1965)

17. S.C. Moss, Phys. Rev. Letts. 22, 1108 (1969)

18. P.C. Clapp in "Ordered Alloys: Structural Applications and Physical Metallurgy" edited by B.H. Kear et al. (Claitor's Baton Rouge, La., 1970)

J. Phys. Chem. Solids Pergamon Press 1966. Vol. 27, pp. 391–393. Printed in Great Britain.

AN INTERPRETATION OF THE COWLEY AND CHRISTY–HALL THEORIES FOR BINARY ALLOY SHORT-RANGE ORDER PARAMETERS

PHILIP C. CLAPP

Ledgemont Laboratory, Kennecott Copper Corporation, Lexington, Massachusetts

(*Received* 4 *August* 1965)

Abstract—It is shown that the statistical mechanics employed by Cowley in deriving his equations for the Warren short-range order parameters (α_{ij}) of a binary alloy implies a different definition for α_{ij} at each stage of the derivation. These definitions are made explicit here and provide an answer to the major criticisms of Cowley's theory made by Hall and others. It is also shown that Cowley's theory does include contributions to α_{ij} from all sites in the alloy which affect α_{ij} in an approximately correct way, whereas the theory of Christy–Hall includes only the direct i, j interaction. It is concluded that Cowley's theory is an approximate solution of an N-body problem and the Christy–Hall theory is the solution of a simple two-body problem which has none of the important cooperative effects of an N-body problem.

SINCE the first appearance of Cowley's derivation[1] of a theory for the Warren short-range order parameters of a binary alloy, various doubts have been raised as to the validity of this derivation. Cowley himself has published two subsequent derivations[2,3] but neither of these new derivations have completely answered the main criticism which has been made by HALL[4,5] and others in regard to the energy expression which appears in Cowley's theory. It will be our purpose here to offer a new justification for Cowley's energy term and to show that the alternate form of the energy term proposed by HALL *et al.*[4,5] is considerably less exact, contrary to their claim of complete exactness.

For purposes of mathematical simplicity the discussion is confined to a 50–50 binary alloy although there is no inherent difficulty in generalizing the following arguments to the case of an alloy of arbitrary composition.

The configurational energy of a particular state of an AB binary alloy is given by:

$$E(\sigma) = \tfrac{1}{2}\sum_{i,j} V_{ij}\sigma_i\sigma_j \qquad (1)$$

where the double sum is over the N sites i of the crystal and the variable σ_i is $+1$ or -1 according to whether an A atom or a B atom occurs at site i for the specific configuration in question.

The Warren short-range order parameter α_{ij} may be shown to be equivalent to the grand canonical average of the binary variable $\sigma_i\sigma_j$, i.e.

$$\alpha_{ij} = \langle\sigma_i\sigma_j\rangle = \sum_{\sigma_k=\pm}^{k=1,N} \frac{\sigma_i\sigma_j \exp(-\beta E(\sigma))}{\sum_{\sigma_k=\pm}^{k=1,N} \exp(-\beta E(\sigma))} \qquad (2)$$

where β is the Boltzmann factor $(kT)^{-1}$ and the sum is over the two values of σ_k for $k = 1$ to N (i.e. over the 2^N states of the grand canonical ensemble).

Cowley uses α_{ij} in three separate ways with no symbolic distinction and therein lies the confusion. We shall label these separate quantities α_{ij}, $\overset{1}{\alpha}_{ij}$ and $\overset{s}{\alpha}_{ij}$. $\overset{1}{\alpha}_{ij}$ is the value of $(\sigma_i\sigma_j)$ in a particular configuration. $\overset{s}{\alpha}_{ij}$ is the average of $\overset{1}{\alpha}_{ij}$ over a certain subset of states in the grand canonical ensemble, which will be specified below. Finally, α_{ij} is the average of $\overset{1}{\alpha}_{ij}$ over the entire grand canonical ensemble as defined above by equation (2).

Cowley's procedure may now be interpreted as follows: a particular site 0 is chosen as origin and

the energy of a configuration (given by equation 1) may be exactly rewritten as:

$$E(\sigma) = \tfrac{1}{2}\sum_{i,j} V_{ij}(\sigma_0\sigma_i)(\sigma_0\sigma_j) = \tfrac{1}{2}\sum_{i,j} V_{ij}\alpha^1_{0i}\alpha^1_{0j} \quad (3)$$

since $\sigma_0\cdot\sigma_0 = 1$ identically. Equation (3) may be identified with Cowley's energy expression appearing in Ref. 1.

$$U - U_0 = \tfrac{1}{2}\sum_i\sum_j V_{ij}\alpha_i\alpha_j \quad (C1)$$

Interpreted as the energy of a single configuration the expression is exact. The point in writing the energy in this manner is that it is now expressed entirely in terms of independent variables. In specifying a particular configuration N numbers are needed. These may be the values of the N σ_k's or alternatively the values of the $N-1$ α^1_{0k}'s and σ_0. Consequently once the α^1_{0k}'s are chosen $\alpha^1_{ij}(i,j \neq 0)$ is a dependent variable whose value is given by $\alpha^1_{0i}\cdot\alpha^1_{0j}$. It is apparent then that equation (1) written in terms of the α_{ij}'s, i.e.

$$E = \tfrac{1}{2}\sum_{i,j} V_{ij}\alpha^1_{ij} \quad (1a)$$

contains mostly dependent variables and this will be an important reason for avoiding its use in the following development, since the variational procedure used by Cowley and Christy–Hall requires independent variables.

We now introduce a set of states by considering a shell of sites around the origin at some constant radius. The nth shell contains C_n sites and the value of α^1_{0n} averaged over this shell for a particular configuration will be called α^s_{0n} and is given by:

$$\alpha^s_{0n} = \frac{1}{C_n}(\alpha^1_{0n_1} + \alpha^1_{0n_2} + \cdots + \alpha^1_{0n_{C_n}}) \quad (4)$$

The allowed values of $\alpha^1_{0n_i}$ are ± 1 so that α^s_{0n} will range between $+1$ and -1. Now imagine all possible rearrangements of this configuration which maintain α^s_{0n} for each shell constant. This is a subset of states in the grand canonical ensemble and is uniquely specified by the α^s_{0n} parameters. The grand canonical ensemble will be exhausted by ranging α^s_{0n} over its possible values for each shell n. The number of states in such a subset is given by

$$W(\alpha^s) = \prod_{n=1,M} \frac{C_n!}{[(C_n/2)(1-\alpha^s_{0n})]\,![(C_n/2)(1+\alpha^s_{0n})]!} \quad (5)$$

where the product is taken over the M shells in the lattice. Equation (5) corresponds to Cowley's calculation[1] of the number of possible arrangements if his α_{0n} is interpreted as α^s_{0n}. Consequently the entropy $S(\alpha^s)$ of a subset may be calculated from

$$S(\alpha^s) = -k \ln W(\alpha_s) \quad (6)$$

Cowley now used equation (C1) as the 'average' energy to put with the above entropy term in a calculation of the free energy. CHRISTY and HALL[4] assume that Cowley means the average energy of the grand canonical ensemble and point out quite correctly that this usage would be in considerable error. However, since Cowley combines this energy term with the entropy term of a subset he is, in fact, using it as *the average energy of a subset*. To calculate the average energy of a subset, it is necessary to calculate the subset average of $\alpha^1_{0i}\alpha^1_{0j}$ in equation (3). Since the α^1_{0n}'s on different shells are independent variables, the average of their product is the product of their averages, i.e.

$$\langle\alpha^1_{0i}\alpha^1_{0j}\rangle_s = \langle\alpha^1_{0i}\rangle_s\langle\alpha^1_{0j}\rangle_s = \alpha^s_{0i}\cdot\alpha^s_{0j} \quad (7a)$$

For the same subshell α^1_{0i} and $\alpha^1_{0i'}$ are not quite independent since they are subject to the constraint in equation (4), but to a good approximation (especially for shells with many sites) one may write:

$$\langle\alpha^1_{0i}\alpha^1_{0i'}\rangle_s \simeq \langle\alpha^1_{0i}\rangle_s\langle\alpha^1_{0i'}\rangle_s \quad (7b)$$

and hence, the average energy of the subset is closely approximated by

$$E(\alpha^s) = \tfrac{1}{2}\sum_{i,j} V_{ij}\alpha^s_{0i}\alpha^s_{0j} \quad (8)$$

The free energy of a subset is then:

$$F(\alpha^s) = E(\alpha^s) - T\cdot S(\alpha^s) \quad (9)$$

This expression is a function of the *independent variables* α^s_{0n} so that the free energy may be minimized with respect to each α^s_{0n} separately by setting $\partial F(\alpha^s)/\partial\alpha^s_{0n}$ equal to zero for $n = 1, \ldots, M$. The values of α^s_{0n} so determined may be identified

with the grand canonical average α_{0n} by the classical argument that those subsets of states which have the lowest free energy will provide the dominant contribution to the grand canonical average.

Up to this point all that has been determined from minimizing equation (9) are the grand canonical averages of the correlation α_{0n} between the origin site and the other $N-1$ sites of the lattice, and correlations such as $\alpha_{ij}(i,j\neq 0)$ are as yet undetermined. If the values of α_{0n} which minimized equation (9) belonged to a single subset, the relation $\alpha_{ij} = \alpha_{0i}\cdot\alpha_{0j}$ would still hold but, in general, the equilibrium values of α_{0n} are an average over a group of subsets and hence α_{ij} cannot be calculated from this relation. It is possible to argue, however, that the grand canonical average must have the same translational invariance as the lattice and therefore $\alpha_{ij} = \alpha_{0n}$ where i and j are separated by the same vector distance in the lattice as 0 and n. This translational invariance *does not*, in general, hold for a given subset of the grand canonical ensemble.

The primary error in the attempt of Christy and Hall[4] to improve on Cowley's theory is that they have misinterpreted Cowley's energy expression in equation (9) as a grand canonical average, rather than the energy of a subset, which it must be in order for the variational procedure in which it is used to have any sense. This error in interpretation leads them to a replacement of Cowley's energy expression (equation 8) by the expression

$$E(\alpha) = \tfrac{1}{4}\sum_{i,j} V_{ij}\alpha_{ij} \qquad \text{(CH1)}$$

in the free energy equation (equation 9). They claim this expression to be exact, which it is, whether one takes it to be the energy for a single configuration, for a subset average or as the grand canonical average with the appropriate interpretation of α_{ij} in each case. However, to remove the dependent variables (the α_{ij}'s where neither i or $j = 0$) from their energy expression they use the translational invariance $\alpha_{ij} = \alpha_{0n}$ appropriate only to the grand canonical interpretation. Since, for the variational calculation which is the next step in their development, $E(\alpha)$ must be interpreted as a subset energy, this assumption of translation equivalence is a serious error and is primarily responsible for the poorness of their result. This error is tantamount to discarding all tems in equation (8) which represent interactions between shell sites, i.e. equation (8) is reduced to

$$E(\alpha) = \tfrac{1}{4}\sum_{i} V_{0i}\alpha^{s}_{0i} \qquad (10)$$

The effect of this is that the correlation which they calculate between sites 0 and i depends only upon the direct interaction between these two sites and, in fact, one can derive their equations for α_{0i} by discarding all the other sites and interactions in the crystal and retaining only the two sites 0 and i and the direct interaction V_{0i}. Consequently, their solution is equivalent to a two body solution and retains none of the more complex features of an N body problem.

A previously published letter by the author[6] has given an exact expansion of α_{0n} of an AB alloy which makes a direct comparison between the theories of Cowley and Christy–Hall possible, term by term. In a forthcoming publication by S. C. Moss and the author,[7] an exact expansion for α_{n0} for the general case of an alloy of arbitrary composition and range of interaction is derived. This is used to analyze the theories of Zernike and Cowley and to suggest a new expression for the α_{0n}'s.

Acknowledgement—I wish to express my thanks to S. C. Moss for a number of illuminating discussions.

REFERENCES

1. Cowley J. M., *Phys. Rev.* **77,** 669 (1950).
2. Cowley J. M., *Phys. Rev.* **120,** 1648 (1960).
3. Cowley J. M., *Phys. Rev.* **138,** A1384 (1965).
4. Christy D. O. and Hall G. L. *Phys. Rev.* **132,** 1959 (1963).
5. Hall G. L. and Philhours J., *Phys. Rev.* **139,** A160 (1965).
6. Clapp P. C., *Phys. Lett.* **13,** 305 (1964).
7. Clapp P. C. and Moss S. C. (submitted to ***The Physical Review***).

NECESSITY OF SECOND-NEIGHBOR INTERACTIONS IN ISING THEORIES OF ORDERED ANTIFERROMAGNETS AND ALLOYS ON FACE-CENTERED CUBIC LATTICES

Philip C. Clapp

Ledgemont Laboratory, Kennecott Copper Corporation, Lexington, Massachusetts
(Received 8 March 1966)

A number of recent advances have been made in discussing the ordering of face-centered cubic lattices within the framework of a nearest-neighbor Ising model.[1-5] The purpose of this Letter is to point out that second-neighbor interactions must be included in the theory, if the theory is to be used for predicting the properties of real systems.

Danielian[1] has shown that assuming a positive value for the nearest-neighbor interaction and neglecting higher-neighbor interactions, the ground state of a face-centered lattice is degenerate and may be described as having one of two possible configurations for each 100 plane normal to, say, the x direction. The two configurations, denoted by I and II, are shown in Fig. 1.

This leads to a "ground state" which is 2^R-fold degenerate, where R is the number of 100 planes ($\cong N^{1/3}$ in a lattice of N sites). This state is partially ordered in that it possesses perfect long-range order in directions within a plane but is completely disordered in directions out of a plane.

The question now arises as to whether physical systems (such as binary alloys) which are well described by an Ising Hamiltonian might show a transition at some temperature to this partially ordered state, and then perhaps show a second transition to a perfectly ordered state at a lower temperature due to very weak higher-neighbor interactions. Such double transitions are theoretically expected[6] and do occur in body-centered A_3B alloys (e.g., Fe_3Al[7]).

Since higher-neighbor interactions are probably always present to some degree in real systems, theoretical predictions based on nearest-neighbor calculations are tenable only if inclusion of very weak higher-neighbor inter-

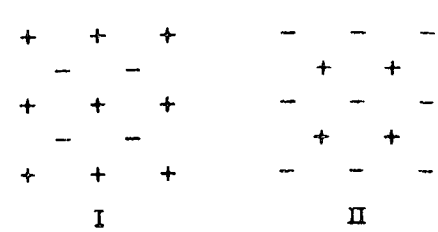

FIG. 1. The two possible configurations of a 100 phase in the ground state of an fcc antiferromagnet.

actions does not alter the results significantly. We shall now show that consideration of higher-neighbor forces radically changes the low-temperature properties of this lattice. Introducing a second-neighbor interaction V_2 ($|V_2/V_1| \ll 1$), the energies of the 2^R degenerate states are changed by the amount

$$\Delta E = N^{2/3} V_2 \sum_{i=1}^{R} S_i S_{i+2} + 2NV_2, \qquad (1)$$

where $S_i = +1$ if the ith layer is in configuration I and -1 if in configuration II. This is readily recognizable as the Hamiltonian of two interpenetrating Ising linear chains having nearest-neighbor forces with an added constant energy due to interactions within the 100 planes.

This splitting of the 2^R states is so strong (due to the $N^{2/3}$ factor) that only the lowest energy state of these 2^R states need be considered in any thermodynamic average for this lattice. This may be seen by comparing the free energy of the lowest energy state (F_0) to that of the rest of the 2^R states (F_e). One has

$$F_e - F_0 = (E_e - E_0) - kT \ln(g_e/g_0) \geq N^{2/3}|V_2| - kTN^{1/3} \ln 2. \qquad (2)$$

The inequality has been calculated by letting all the $(2^R - 1)$ excited states have the energy of the first excited state. g_e and g_0 are the number of excited and ground states, respectively. The statistical weight of all the excited states relative to that of the ground state in a thermodynamic average is

$$\exp\left\{-\frac{1}{kT}(F_e - F_0)\right\} \leq \exp\left\{-N^{2/3}\left[\frac{|V_2|}{kT} - \frac{\ln 2}{N^{1/3}}\right]\right\}, \qquad (3)$$

which becomes arbitrarily small as the limit of $N \to \infty$ is taken, regardless of temperatures. It is seen that $|V_2|$ need only be greater than $N^{-1/3}$ for this result to be valid, a very weak interaction indeed.

Two points can be made in conclusion. Double transitions of the type we have described are thermodynamically impossible for face-centered cubic lattices. Secondly, some method should be used in calculations of the low-temperature properties of such lattices to be sure that the partially ordered states have no effect on the result. These conclusions are true for A_3B alloys as well by simple extensions of the above arguments.

It may be remarked that Danielian's low-temperature partition function for this lattice[2] can be easily modified to conform to the above restrictions by eliminating the factor 2^R which appears there.

[1]A. Danielian, Phys. Rev. Letters 6, 670 (1961).
[2]A. Danielian, Phys. Rev. 133, A1344 (1964).
[3]A. Danielian, Physica 29, 67 (1963).
[4]Y. Y. Li, Phys. Rev. 84, 721 (1951).
[5]D. D. Betts and C. J. Elliott, Phys. Letters 18, 18 (1965).
[6]S. Matsuda, J. Phys. Soc. Japan 8, 20 (1953).
[7]R. H. Fowler and E. A. Guggenheim, Statistical Thermodynamics (Cambridge University Press, New York, 1939), p. 589.

Reprinted from THE PHYSICAL REVIEW, Vol. 164, No. 3, 1018–1020, 15 December 1967
Printed in U. S. A.

Exact Relations between Triplet Probabilities and Pair Correlations in AB Binary Alloys and Ising Spin-$\frac{1}{2}$ Systems

PHILIP C. CLAPP
Ledgemont Laboratory, Kennecott Copper Corporation, Lexington, Massachusetts
(Received 21 June 1967)

The probabilities for triplet occupation in an AB binary alloy (or spin one-half Ising magnet) are found to be exactly expressible as linear combinations of the three pair correlations if the configurational energy of the system possesses a certain symmetry. The required symmetry is that the energy be invariant when all A atoms are replaced by B atoms and vice versa (or all spins are flipped). Systems having only pairwise or even particle interactions satisfy this requirement. Roberts's values for the pair correlations in CuAu at various temperatures are used to calculate the probabilities of several triplet configurations. The results are somewhat paradoxical and can probably be attributed to the lack of a size-effect correction in Roberts's data. Equations for the triplet probabilities in alloy compositions other than 50–50 are also given; but these require a fourth parameter, the triplet correlation, which is not yet available experimentally.

SINCE the first detailed measurement by Cowley[1] of the pair correlations [or Warren short-range-order (SRO) parameters] for Cu_3AU, it has become possible to experimentally determine the pair correlations in favorable alloy systems up to distances of the order of tenth nearest neighbors. It has long been known that a knowledge of the alloy composition and the Warren SRO parameter α_{ij} was sufficient to determine the four pair probabilities $P_{ij}{}^{AA}$, $P_{ij}{}^{AB}$, $P_{ij}{}^{BA}$, $P_{ij}{}^{BB}$, and to thus provide a partial description of the atomic arrangement in the alloy. What has not been generally realized is that for the special case of a 50-50 composition alloy, the eight triplet probabilities $P_{ijk}{}^{AAA}$, $P_{ijk}{}^{AAB}$, etc., are also directly determinable from the pair correlations α_{ij}, α_{ik}, and α_{jk} provided that the configurational energy of the alloy is a sum of only even number particle interactions. It is normally assumed that the configurational energy is a sum of pairwise interactions, in which case the equalities to be derived below are valid. Conversely, if it becomes possible to measure triplet correlations (as suggested by Cowley[2]), an observed violation of the equations would indicate the importance of three-particle (or higher odd number) interactions.

We shall use the occupation numbers σ_i to describe any state of the alloy or spin system where σ_i $(+1, -1)$ if site i is occupied by an (A,B) atom or equivalently an (up, down) spin. We will not continue to discuss the spin problem explicitly but it will be understood that all the subsequent arguments apply to the spin problem by replacing (A,B) atoms by (up, down) spins.

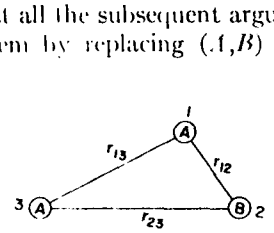

FIG. 1. Illustration of a configuration which would contribute to $P_{123}{}^{ABA}$. Site 1 can be taken as any of the N sites in the crystal but sites 2 and 3 must always have the same orientation and distance relative to site 1.

[1] J. M. Cowley, Phys. Rev. **77**, 669 (1950).
[2] J. M. Cowley, J. Australian Inst. Metals **11**, 258 (1966).

We note the following useful relations:

$\sigma_i{}^A \equiv \frac{1}{2}(1+\sigma_i) = (1,0)$ if an (A,B) atom is at site i,

$\sigma_i{}^B \equiv \frac{1}{2}(1-\sigma_i) = (0,1)$ if an (A,B) atom is at site i.

It is now possible to write definitions for the pair and triplet probabilities in a general form

$$P_{12}{}^{XY} \equiv \sum_\gamma \langle\gamma|\rho(\gamma)\frac{1}{N}\sum_{\tau=0}^{N-1}\sigma_{1+\tau}{}^X\sigma_{2+\tau}{}^Y|\gamma\rangle, \quad (1)$$

$$P_{123}{}^{XYZ} \equiv \sum_\gamma \langle\gamma|\rho(\gamma)\frac{1}{N}\sum_{\tau=0}^{N-1}\sigma_{1+\tau}{}^X\sigma_{2+\tau}{}^Y\sigma_{3+\tau}{}^Z|\gamma\rangle, \quad (2)$$

where X, Y, Z can each be assigned A or B. One of the four possibilities in (1) is $P_{12}{}^{AB}$ which then means the statistically averaged probability that an A-B pair will be found separated by the distance r_{12}. One of the eight possibilities in (2) is $P_{123}{}^{ABA}$ which is the probability that a triangle of sides r_{12}, r_{23}, and r_{31} will be occupied in the manner shown in Fig. 1.

The summation over γ refers to a sum over all the possible individual configurations of the alloy on the N sites of the crystal, there being $N!/(N/2)!^2$ such possibilities for an AB alloy. $\rho(\gamma)$ is the usual thermodynamic weight factor $e^{-\beta H}/\sum_\gamma e^{-\beta H}$. The sum over τ is used to average over all pair sites separated by a fixed distance r_{12} or, in the case of Eq. (2), over all triplet sites which form a triangle of fixed dimensions r_{12}, r_{23}, and r_{31}. The notation $\langle\gamma|\cdots|\gamma\rangle$ merely implies that the value of the quantity inside the brackets is to be calculated for the configuration γ.

As an example, consider the probability $P_{123}{}^{ABA}$ given by Eq. (2) as follows:

$$P_{123}{}^{ABA} = \sum_\gamma \langle\gamma|\rho(\gamma)N^{-1}\sum_{\tau=0}^{N-1}\sigma_{1+\tau}{}^A\sigma_{2+\tau}{}^B\sigma_{3+\tau}{}^A|\gamma\rangle.$$

The product $\sigma_{1+\tau}{}^A\sigma_{2+\tau}{}^B\sigma_{3+\tau}{}^A$ will have the value 1 only if the three sites are simultaneously occupied in the fashion indicated, otherwise the product vanishes. Thus, summing this operator product over τ counts

precisely the number of triplets for the γ configuration (out of a possible total of N) that are occupied in the required way. The summation over γ then accomplishes the thermodynamic averaging of all configurations.

We shall now postulate two separate conditions: I: For every configuration γ in the ensemble there exists an inverse ($\bar{\gamma}$) obtained by replacing every A atom by a B atom and vice versa (i.e., all the σ_i's change sign). II: The thermodynamic weight factor has the symmetry property $p(\gamma)=p(\bar{\gamma})$, i.e., $H(\gamma)=H(\bar{\gamma})$.

Condition I is clearly satisfied for the ensemble of possible configurations of an AB alloy but will not be satisfied for canonical ensembles of other compositions.

A specific example of a Hamiltonian that satisfies condition II would be the general n-particle interaction Hamiltonian

$$H=\sum_{i,j}^{N} V_{ij}\sigma_i\sigma_j+\sum_{i,j,k}^{N} V_{ijk}\sigma_i\sigma_j\sigma_k + \sum_{i,j,k,l}^{N} V_{ijkl}\sigma_i\sigma_j\sigma_k\sigma_l+\cdots, \quad (3)$$

if the terms containing odd numbered products of σ's vanish. The usual pairwise interaction model assumes all but the first term are negligible.

Proceeding to a calculation of the pair and triplet probabilities by using the relations for σ_i^A and σ_i^B in terms of σ_i, and using the notation

$$\langle\sigma_1\sigma_2\sigma_3\rangle=\sum_{\gamma}\langle\gamma|\,p(\gamma)\frac{1}{N}\sum_{\tau=0}^{N-1}\sigma_{1+\tau}\sigma_{2+\tau}\sigma_{3+\tau}|\gamma\rangle,$$

we have

$$P_{12}^{AA}=\tfrac{1}{4}(1+\langle\sigma_1\rangle+\langle\sigma_2\rangle+\langle\sigma_1\sigma_2\rangle).$$

But $\langle\sigma_1\rangle=\langle\sigma_2\rangle=0$, because this is simply the difference in the fraction of A and B atoms in the crystal. Hence, by omission of such terms one has

$$P_{12}^{AA}=\tfrac{1}{4}(1+\langle\sigma_1\sigma_2\rangle), \quad (4a)$$

$$P_{12}^{AB}=\tfrac{1}{4}(1-\langle\sigma_1\sigma_2\rangle), \quad (4b)$$

$$P_{12}^{BA}=\tfrac{1}{4}(1-\langle\sigma_1\sigma_2\rangle), \quad (4c)$$

$$P_{12}^{BB}=\tfrac{1}{4}(1+\langle\sigma_1\sigma_2\rangle). \quad (4d)$$

The pair correlation is simply the Warren short-range-order parameter α_{12} and the equations state the familiar fact that all four pair probabilities depend on a single experimentally determined parameter.[3]

The triplet probability P_{123}^{AAA} becomes

$$P_{123}^{AAA}=\tfrac{1}{8}(1+\langle\sigma_1\rangle+\langle\sigma_2\rangle+\langle\sigma_3\rangle+\langle\sigma_1\sigma_2\rangle+\langle\sigma_2\sigma_3\rangle+\langle\sigma_3\sigma_1\rangle+\langle\sigma_1\sigma_2\sigma_3\rangle)$$

and we note that the triplet correlation $\langle\sigma_1\sigma_2\sigma_3\rangle$ vanishes, because for every contribution to the sum from γ there is an exactly cancelling contribution from $\bar{\gamma}$, i.e., $p(\gamma)=p(\bar{\gamma})$ but $\langle\gamma|\sigma_1\sigma_2\sigma_3|\gamma\rangle=-\langle\bar{\gamma}|\sigma_1\sigma_2\sigma_3|\bar{\gamma}\rangle$. As a consequence, the eight triplet probabilities can be written entirely in terms of the pair correlations α_{ij} as follows:

$$P_{123}^{AAA}=P_{123}^{BBB}=\tfrac{1}{8}(1+\alpha_{12}+\alpha_{23}+\alpha_{31}), \quad (5a)$$

$$P_{123}^{AAB}=P_{123}^{BBA}=\tfrac{1}{8}(1+\alpha_{12}-\alpha_{23}-\alpha_{31}), \quad (5b)$$

$$P_{123}^{BAA}=P_{123}^{ABB}=\tfrac{1}{8}(1-\alpha_{12}+\alpha_{23}-\alpha_{31}), \quad (5c)$$

$$P_{123}^{ABA}=P_{123}^{BAB}=\tfrac{1}{8}(1-\alpha_{12}-\alpha_{23}+\alpha_{31}). \quad (5d)$$

For the more general situation where either condition I or II or both are violated, $\langle\sigma_1\sigma_2\sigma_3\rangle$ need not be zero and the triplet probabilities now depend on five parameters as follows:

$$P_{123}^{AAA}=\tfrac{1}{8}(1+3c+\alpha_{12}'+\alpha_{23}'+\alpha_{31}'+\tau_{123}), \quad (6a)$$

$$P_{123}^{BBB}=\tfrac{1}{8}(1-3c+\alpha_{12}'+\alpha_{23}'+\alpha_{31}'-\tau_{123}), \quad (6b)$$

$$P_{123}^{AAB}=\tfrac{1}{8}(1+c+\alpha_{12}'-\alpha_{23}'-\alpha_{31}'-\tau_{123}), \quad (6c)$$

$$P_{123}^{BBA}=\tfrac{1}{8}(1-c+\alpha_{12}'-\alpha_{23}'-\alpha_{31}'+\tau_{123}), \quad (6d)$$

$$P_{123}^{BAA}=\tfrac{1}{8}(1+c-\alpha_{12}'+\alpha_{23}'-\alpha_{31}'-\tau_{123}), \quad (6e)$$

$$P_{123}^{ABB}=\tfrac{1}{8}(1-c-\alpha_{12}'+\alpha_{23}'-\alpha_{31}'+\tau_{123}), \quad (6f)$$

$$P_{123}^{ABA}=\tfrac{1}{8}(1+c-\alpha_{12}'-\alpha_{23}'+\alpha_{31}'-\tau_{123}), \quad (6g)$$

$$P_{123}^{BAB}=\tfrac{1}{8}(1-c-\alpha_{12}'-\alpha_{23}'+\alpha_{31}'+\tau_{123}), \quad (6h)$$

where c is the difference in the fraction of A and B atoms, α_{ij}' is the quantity $(1-c^2)\alpha_{ij}+c^2$ and is identical to $\langle\sigma_i\sigma_j\rangle$, and $\tau_{123}\equiv\langle\sigma_1\sigma_2\sigma_3\rangle$. It is apparent that various pairwise combinations of the triplet probabilities can be found that are independent of τ_{123}, but this is not as useful for describing a state of order.

As an application of Eqs. (5a)–(5d), we consider the alloy CuAu. Roberts[4] has measured the α_{ij}'s out to eighth-neighbor separations at several temperatures above T_c. Unfortunately, the α_{ij}'s were not corrected for size effects, which are large in this system as shown explicitly by Borie.[5] Thus, the α_i's reported by Roberts should not be taken too literally, and we shall use them here primarily for purposes of illustration. They are

TABLE I. Pair correlations (α_i) for CuAu ($T_c=408$°C).

Neighbor distance, i	Perfect order	Quenched from 500°C	Held at 425°C	Held at 525°C	Perfect disorder
1	$-\frac{1}{2}$	−0.158	−0.123	−0.118	0.000
2	+1	+0.210	+0.048	−0.002	0.000
3	$-\frac{1}{2}$	−0.048	0.00	0.00	0.000
4	+1	+0.153	+0.07	+0.05	0.000
5	$-\frac{1}{2}$	−0.050	−0.03	−0.03	0.000
6	+1	+0.093	+0.03	+0.03	0.000
7	$-\frac{1}{2}$	−0.035	−0.02	−0.02	0.000
8	+1	+0.070	+0.02	0.00	0.000

[3] P. C. Clapp and S. C. Moss, Phys. Rev. 142, 418 (1966).

[4] B. W. Roberts, Acta Met. 2, 597 (1954).

[5] B. Borie, Acta Cryst. 14, 472 (1961).

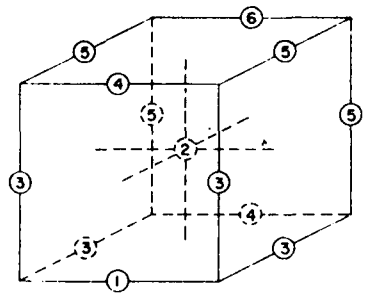

FIG. 2. Sites used for the calculation of triplet probabilities in CuAu.

listed in Table I along with the α_{ij}'s for perfectly ordered and perfectly disordered samples.

CuAu is an interesting example to study because the symmetry of the crystal changes from cubic to tetragonal upon ordering. The ordered phase may be described as even-numbered 100 planes of a face-centered cubic lattice occupied by one type of atom and odd-numbered 100 planes occupied by the other type. Since three points are required to define a plane, the triplet probabilities have an advantage over the binary probabilities in that they can provide an answer to the question of whether such layering occurs on a small scale in the disordered state, in anticipation of the ordered structure.

Although we could, in principle, calculate probabilities of any triplet which did not contain a pair separated by more than eighth-neighbor distances, we shall confine our attention to the cluster of sites shown in Fig. 2. All the sites of the cluster are nearest neighbors of site 2, and we shall calculate the triplet probabilities for the case when sites 1 and 2 are occupied by A atoms.

TABLE II. Triplet conditional probabilities $[P(_j{}^B|_{12}{}^{AA})]$ for CuAu.

Cluster site j	Perfect order	Quenched from 500°C	Held at 425°C	Held at 525°C	Perfect disorder
3	1	0.688	0.640	0.634	0.500
4	0	0.469	0.543[a]	0.568[a]	0.500
5	1	0.622	0.570	0.567	0.500
6	0	0.503[a]	0.530[a]	0.539[a]	0.500

[a] Values which are paradoxical in the sense that they do not lie between the perfectly ordered and perfectly disordered values.

Equations (5a) and (5b) yield

$$P_{12_j}{}^{AAA}=\tfrac{1}{8}(1+2\alpha_1+\alpha_{1j}),$$
$$P_{12_j}{}^{AAB}=\tfrac{1}{8}(1-\alpha_{1j}).$$

In particular we shall calculate the conditional probability $P(_j{}^B|_{12}{}^{AA})$ of a B atom at j given an A atom at 1 and 2, i.e.,

$$P(_j{}^B|_{12}{}^{AA})\equiv\frac{P_{12_j}{}^{AAB}}{P_{12_j}{}^{AAA}+P_{12_j}{}^{AAB}}=\frac{1-\alpha_{1j}}{2+2\alpha_1}.$$

Since sites 3, 4, 5, and 6 in Fig. 2 are first, second, third, and fourth neighbors of site 1, we have $\alpha_{13}=\alpha_1$; $\alpha_{14}=\alpha_2$; $\alpha_{15}=\alpha_3$; $\alpha_{16}=\alpha_4$. The calculated values of $P(_j{}^B|_{12}{}^{AA})$ appear in Table II. We see from the column of values for the ordered structure that placing an A atom on sites 1 and 2 resolves the ambiguity of whether the layering occurs on the 100, 010, or 001 planes, in that sites 4 and 6 are forced to contain A atoms, and sites 3 and 5 are forced to have B atoms. If layering also occurs in the disordered state this should appear as a value of less than 0.5 in the table for sites 4 and 6 and a value greater than 0.5 for sites 3 and 5. Only the quenched sample seems to come close to satisfying these conditions. The values in the table marked with a letter are those that do not satisfy the layering condition and we note that although 3 and 5 are preferred B sites in all cases, the paradoxical result emerges that at 425 and 525°C locations 4 and 6 also appear to be preferred B sites.

However, as we noted before, Roberts's results do contain significant errors and he comments that α_2 in particular is probably much too small. Increasing α_2 in our equations would affect only site 4 and change it in the direction of being a preferred A site.

In conclusion, it may be said that the results for CuAu are ambiguous and that a better picture of the disordered state in this system will have to wait for more accurate values of the α_{ij}'s. When such measurements are available for this and other AB alloys, the triplet probabilities should provide a critical test for the importance of higher particle interactions in ordering processes when the direct measurement of triplet probabilities becomes feasible.

Reprinted from THE PHYSICAL REVIEW, Vol. 142, No. 2, 418–427, 11 February 1966
Printed in U. S. A.

Correlation Functions of Disordered Binary Alloys. I

PHILIP C. CLAPP
Lockwood Laboratory, Kennecott Copper Corporation, Lexington, Massachusetts
AND
SIMON C. MOSS*
Department of Metallurgy, Massachusetts Institute of Technology, Cambridge, Massachusetts
(Received 9 August 1965; revised manuscript received 4 October 1965)

An exact expression for the correlation functions (or Warren short-range order parameters) of an alloy of arbitrary composition and range of interaction is derived in terms of the Flinn operators. An approximate method of solution is found by replacing certain operators by their averages. One such choice leads to the equations formerly deduced by Cowley, and constitutes an alternative derivation of Cowley's theory. A second choice yields Zernike's equations and provides a method of comparing the approximations inherent in these two theories. Finally, a third solution is suggested which appears to have the same order of accuracy as the former two, but which has the advantage of being exactly soluble. It also provides an inversion formula which, in theory, can be used to infer the form of the two-particle interaction energy as a function of distance in the crystal. The theory is valid only above the ordering temperature of an alloy, but may be used with equal facility for a variety of alloys with differing compositions and ranges of interaction.

I. INTRODUCTION

THE central problem considered in this paper is that of determining theoretically the correlation functions of a binary alloy. The more familiar question of finding the long- and short-range order parameters of an alloy is a special case of this general problem. We confine ourselves to the assumption that the configurational energy of the alloy is adequately approximated by the following pair Hamiltonian

$$H = \tfrac{1}{2}\sum_{i,j}\{V_{ij}^{AA}\sigma_i^A\sigma_j^A + V_{ij}^{BB}\sigma_i^B\sigma_j^B + V_{ij}^{AB}(\sigma_i^A\sigma_j^B + \sigma_i^B\sigma_j^A)\}, \quad (1)$$

where i, j refer to the sites of a regular rigid lattice and σ_i^A, σ_i^B are the occupation numbers for each site. If, in a particular state of the crystal, site i is occupied by an A atom, $\sigma_i^A = +1$, $\sigma_i^B = 0$ and if by a B atom, $\sigma_i^A = 0$, $\sigma_i^B = +1$. V_{ij}^{AB} is the energy of interaction between an A atom on site i and a B atom on site j, and is assumed symmetric with respect to the interchange of site labels.

The correlation functions we seek are the thermodynamic averages $\langle\sigma_i^A\sigma_j^B\rangle$, $\langle\sigma_i^A\sigma_j^A\rangle$ etc., and are defined as follows:

$$\langle\sigma_i^A\sigma_j^B\rangle = \sum_\gamma \sigma_i^A\sigma_j^B e^{-\beta H_\gamma} \Big/ \sum_\gamma \langle\gamma|e^{-\beta H}|\gamma\rangle, \quad (2)$$

where $\beta = 1/kT$ and k and T are the Boltzmann constant and temperature. The states of the system $|\gamma|$ correspond to all possible configurations of N_A A atoms and N_B B atoms arranged on N sites. The total number of different states is therefore $N!/N_A!N_B!$ with $N_A + N_B = N$.

The theory of binary alloys based on the Hamiltonian given above is mathematically equivalent in most respects to the Ising theory of magnetic systems so that many of the results obtained for the spin-spin correlation functions in magnetic systems can be translated into predictions for the alloy correlation functions. Since an exact solution for the Ising linear chain with magnetic field has been obtained for the case of nearest-neighbor interactions only, this constitutes an exact solution for a one-dimensional binary alloy of any composition with the same restriction on range of interaction. Similarly, Onsager's exact solution[1] of the two-dimensional Ising lattice with nearest-neighbor interactions in zero magnetic field is equivalent to a complete description of a two-dimensional binary alloy of 50–50 composition.

There are no complete solutions for three-dimensional lattices and so one must resort to either so-called cluster approximations which give a solution in closed form at all temperatures or else some form of high- or low-temperature expansion[2] which is valid only in a limited temperature range. Although these expansions have the satisfying feature of exactness (apart from truncation errors) they are very tedious to carry out for interactions which have a range greater than nearest-neighbor distances. Furthermore, a new expansion must be computed for each correlation function, for each lattice type, and for each composition. The only high-temperature expansions for more than first neighbor correlation functions that we are aware of are contained in the work of Oguchi.[3] Oguchi gives expansions for the correlation functions in the 100 direction of an AB alloy with a simple cubic lattice. It is clear that a single expression for the correlation functions would be extremely useful for experimental analysis if it were reasonably accurate. For this reason our development will be more akin to the cluster approach.

Work in this direction on the correlation functions has previously been done by Zernike[4] and Cowley.[5] The

* Supported by a grant from the U. S. Atomic Energy Commission.

[1] L. Onsager, Phys. Rev. 65, 117 (1944).
[2] See for example C. Domb, Advan. Phys. 9, 149 (1960).
[3] J. Phys. Soc. Japan 6, 31 (1951).
[4] F. Zernike, Physica 7, 565 (1940).
[5] J. M. Cowley, Phys. Rev. 77, 669 (1950); 120, 1648 (1960); 138, A1384 (1965).

recent work of Christy and Hall[6] is closely related to Cowley's theory, and the theory of Elliott and Marshall[7] as it applies to alloy systems is directly related to Zernike's work. Although Zernike and Cowley appear to have approached the problem from quite different directions, it will be part of our purpose to show that their approximations are quite closely related.

The above fact will emerge in the mathematical development presented in Sec. III of a general expression for the correlation functions of a binary alloy with arbitrary composition and range of interaction. This expression is exact and may be solved approximately by replacing certain operators by their averages, the choice being guided to some extent by physical arguments. It will be shown that one choice leads to Cowley's theory and a second more complex choice to Zernike's theory. Also, it will be possible to judge qualitatively the conditions under which each of these two theories constitutes a reasonable approximation.

In Sec. IV a third approximation to the exact correlation function equation is proposed which leads to a new theory of correlations in alloy systems, and which appears to have the same order of accuracy as the approaches of Cowley and Zernike. Furthermore, this theory gives a linear set of equations which may be solved in closed form, unlike the equations of the two preceding theories. It has, however, the disadvantage that the theory is valid only above the ordering temperature.

Section II introduces the operators, the statistics, and the transformations necessary for Secs. III and IV.

In a succeeding paper[8] (Part II) it is intended to apply the theory outlined in Sec. IV of this paper to current experimental results for Cu_3Au and, possibly, CuZn.

II. MATHEMATICAL DEVELOPMENT

A. The Grand Canonical Ensemble

The Hamiltonian given in Eq. (1) can be rewritten in a more compact and useful form by introducing operators ($\bar{\sigma}_i$) which are called spin-deviation operators in magnetism and Flinn operators[6,9] in alloy theory. They are defined here as

$$\bar{\sigma}_i = 2(\sigma_i{}^A - m_A) \equiv 2(m_B - \sigma_i{}^B), \tag{3}$$

where $m_A = N_A/N$ and $m_B = N_B/N$. These operators have the property that $\bar{\sigma}_i = 2m_B$ if there is an A atom at i and $\bar{\sigma}_i = -2m_A$ if a B atom is at site i.[10] Introduction of these operators in Eq. (1) yields

$$H = +\tfrac{1}{4}\sum_{i,j}^{N}[V_{ij}{}^0 + V_{ij}{}^1(\bar{\sigma}_i + \bar{\sigma}_j) + V_{ij}\bar{\sigma}_i\bar{\sigma}_j] \tag{4}$$

with

$$V_{ij}{}^0 = \tfrac{1}{2}(V_{ij}{}^{AA} + V_{ij}{}^{BB} + 2V_{ij}{}^{AB}),\ \tfrac{1}{2}V_{ij}{}^1 = (V_{ij}{}^{AA} - V_{ij}{}^{BB})$$

and

$$V_{ij} = \tfrac{1}{2}(V_{ij}{}^{AA} + V_{ij}{}^{BB} - 2V_{ij}{}^{AB}).$$

Since $\sum_{i=1}^{N}\bar{\sigma}_i$ has the same value for all states of the system (in this case equal to zero), the terms in (4) containing $V_{ij}{}^1$ can be dropped. The $V_{ij}{}^0$ term may be eliminated for the same reason and the resulting Hamiltonian (5) will give all the essentials of the problem.

$$H = +\tfrac{1}{4}\sum_{i,j}^{N} V_{ij}\bar{\sigma}_i\bar{\sigma}_j. \tag{5}$$

If V_{ij} is positive the system prefers unlike atoms on sites i and j, and like atoms if V_{ij} is negative.

Before we attempt to evaluate thermodynamic averages such as (2), the task will be made simpler by changing from a canonical ensemble to a grand canonical ensemble. This will mean changing the set of allowable states from all configurations of N_A A atoms and N_B B atoms on N sites to the larger set of all configurations in which each site has either an A atom or a B atom with probability m_A and m_B, respectively. An average in the grand canonical ensemble of some arbitrary function, $F(\bar{\sigma}_i)$, of the $\bar{\sigma}_i$'s, is defined as

$$\langle F(\bar{\sigma}_i)\rangle = \sum_{\bar{\sigma}_k=\pm} F(\bar{\sigma}_i)\cdot\omega(\bar{\sigma}_1)\omega(\bar{\sigma}_2)\cdots\omega(\bar{\sigma}_N)e^{-\beta H'} \Big/ \sum_{\bar{\sigma}_k=\pm}\omega(\bar{\sigma}_1)\cdots\omega(\bar{\sigma}_N)e^{-\beta H}, \tag{6}$$

where $\sum_{\sigma_k=\pm}$ implies summing each of the $\bar{\sigma}_k$'s over the two possible values $+2m_B$ and $-2m_A$, and the weighting factors $\omega(\bar{\sigma}_i)$ account for the fact that the $+$ and $-$ values should occur with the relative frequency m_A and m_B, respectively. Hence, $\omega(\bar{\sigma}_i = +2m_B) = m_A$ and $\omega(\bar{\sigma}_i = -2m_A) = m_B$. We may write $\omega(\bar{\sigma}_i)$ as $(m_A)^{\sigma_i{}^A}(m_B)^{\sigma_i{}^B}$ and

$$\prod_{i=1}^{N}\omega(\bar{\sigma}_i) = (m_A)^{\Sigma\sigma_i{}^A}(m_B)^{\Sigma\sigma_i{}^B} \tag{7a}$$

or

$$\prod_{i=1}^{N}\omega(\bar{\sigma}_i) = (m_A)^{m_A N}(m_B)^{m_B N}\left[\left(\frac{m_A}{m_B}\right)^{1/2}\right]^{\Sigma\sigma_i}. \tag{7b}$$

Equation (7b) follows from Eq. (3). Henceforth $\sum$ without summation indices will imply a summation over the N sites of the crystal. Finally, we may write Eq. (6) as

$$\langle F(\bar{\sigma}_i)\rangle = \sum_{\bar{\sigma}_k=\pm} F(\bar{\sigma}_i)e^{\lambda\Sigma\bar{\sigma}_i}e^{-\beta H} \Big/ \sum_{\bar{\sigma}_k=\pm} e^{\lambda\Sigma\bar{\sigma}_i}e^{-\beta H}, \tag{8}$$

where $e^{\lambda} \equiv (m_A/m_B)^{1/2}$ and the factor $e^{\lambda\Sigma\bar{\sigma}_i}$ is analogous to the term $e^{-\mu N}$ which often appears in grand canonical

[6] D. O. Christy and G. L. Hall, Phys. Rev. 132, 1959 (1963).
[7] R. J. Elliott and W. Marshall, Rev. Mod. Phys. 30, 75 (1958).
[8] S. C. Moss and P. C. Clapp, Phys. Rev. (to be published).
[9] P. A. Flinn, Phys. Rev. 104, 350 (1956).
[10] Flinn's definition is $\bar{\sigma}_i = +m_B, -m_A$.

averages and is responsible for making the grand canonical and canonical averages equivalent in the limit of large N.

B. Correlations

We shall now be concerned with finding the correlation between the occupation of some site j and a second site O, which can be thought of as the origin of the lattice without loss of generality. This will be expressed in terms of statistical probabilities such as: the probability that site O is occupied by a B atom, given that site j is occupied by an A atom. This conditional probability is written $P_{Oj}{}^{BA}$ and the second subscript and superscript will always refer to the given condition. In general, $P_{Oj}{}^{BA}$ is not equal to $P_{jO}{}^{AB}$. $P_{Oj}{}^{BA}$ may be written exactly as

$$P_{Oj}{}^{BA}=\sum_{\bar\sigma_k=\pm 1}\sigma_O{}^B\sigma_j{}^A e^{-\beta H}e^{\lambda\Sigma\bar\sigma_i}\Big/\sum_{\bar\sigma_k=\pm 1}\sigma_j{}^A e^{-\beta H}e^{\lambda\Sigma\bar\sigma_i}. \quad (9)$$

$\sigma_j{}^A$ is, in effect, a projection operator that allows only those states for which j is occupied by an A atom to count in the summation. Similarly, $\sigma_O{}^B$ selects those states having a B atom on O.

We may write expressions analogous to Eq. (9) for each of the other three binary probabilities $P_{Oj}{}^{AA}$, $P_{Oj}{}^{BB}$, and $P_{Oj}{}^{AB}$. It is apparent that these four probabilities are not independent since the following relations must hold:

$$P_{Oj}{}^{BA}+P_{Oj}{}^{AA}=1 \quad (10a)$$

$$P_{Oj}{}^{AB}+P_{Oj}{}^{BB}=1 \quad (10b)$$

$$m_B P_{Oj}{}^{AB}=m_A P_{Oj}{}^{BA}. \quad (10c)$$

Equation (10c) follows from the fact that $m_B P_{Oj}{}^{AB}$ is the probability of the simultaneous occurrence of an A on O and a B on j, and $m_A P_{Oj}{}^{BA}$ is the probability of B on O and A on j. Thus these weighted probabilities differ only in an interchange of indices which, because of the assumed symmetry of the crystal, cannot affect their value.

The three relations among four unknowns allow us to write all four probabilities in terms of one arbitrary parameter, which is customarily taken to be the Warren short range order parameter, α_{Oj}.

The four probabilities in terms of α_{Oj} are given by Cowley[6] as

$$P_{Oj}{}^{AA}=m_A+m_B\alpha_{Oj}, \quad (11a)$$

$$P_{Oj}{}^{BA}=m_B-m_B\alpha_{Oj}, \quad (11b)$$

$$P_{Oj}{}^{AB}=m_A-m_A\alpha_{Oj}, \quad (11c)$$

$$P_{Oj}{}^{BB}=m_B+m_A\alpha_{Oj}, \quad (11d)$$

and by a simple computation, it may be discovered that

$$\langle\bar\sigma_O\bar\sigma_j\rangle=4m_A m_B\alpha_{Oj}. \quad (12)$$

Since only α_{Oj} is experimentally measurable it will be important to have our final results in terms of α_{Oj} alone, although it will turn out to be simpler to calculate each of the binary probabilities separately.

Equation (9) may be recast in a form which will allow us to obtain solutions in varying degrees of approximation. This is done by replacing $\sigma_O{}^B$ by its conditional average (i.e., the average of $\sigma_O{}^B$ when all other sites in the system are fixed and $\bar\sigma_O$ alone is allowed to vary). This may be seen to be

$$\langle\sigma_O{}^B\rangle_{\rm cond}\equiv\frac{\sum_{\bar\sigma_O=\pm}\sigma_O{}^B\exp\left[\left(-\frac{\beta}{2}\sum_f V_{Of}\bar\sigma_f\right)\bar\sigma_O\right]e^{\lambda\bar\sigma_O}}{\sum_{\bar\sigma_O=\pm}\exp\left[\left(-\frac{\beta}{2}\sum_f V_{Of}\bar\sigma_f\right)\bar\sigma_O\right]e^{\lambda\bar\sigma_O}} \quad (13)$$

and performing the sum gives

$$\langle\sigma_O{}^B\rangle_{\rm cond}=\frac{e^{-2m_A(\beta E_O+\lambda)}}{e^{-2m_A(\beta E_O+\lambda)}+e^{+2m_B(\beta E_O+\lambda)}}\equiv f_B(E_O), \quad (14)$$

where $E_O\equiv-\frac{1}{2}\sum_f V_{Of}\bar\sigma_f$ and may be thought of as the field which the atom at the origin sees as a result of some particular configuration of atoms around O (specified by the $\bar\sigma_f$'s).

We shall also need $\langle\sigma_O{}^A\rangle_{\rm cond}$ and it is calculated to be

$$\langle\sigma_O{}^A\rangle_{\rm cond}=\frac{e^{+2m_B(\beta E_O+\lambda)}}{e^{-2m_A(\beta E_O+\lambda)}+e^{+2m_B(\beta E_O+\lambda)}}\equiv f_A(E_O). \quad (15)$$

Using a theorem of statistics (which will be proven in the Appendix for our particular case), $\sigma_O{}^B$ may be replaced in Eq. (9) by $\langle\sigma_O{}^B\rangle_{\rm cond}$ without altering the exactness of the relation. Therefore, we have

$$P_{Oj}{}^{BA}=\sum_{\bar\sigma_k=\pm}f_B(E_O)\sigma_j{}^A\rho\Big/\sum_{\bar\sigma_k=\pm}\sigma_j{}^A\rho, \quad (16)$$

where $\rho\equiv e^{-\beta H}e^{\lambda\Sigma\bar\sigma_i}$, the grand canonical density operator.

It is important to realize what has been accomplished by this transformation. The correlation between site j and the origin has been written in terms of the correlation between j and the shells of sites around O which have a direct interaction (V_{Of}) with O, and the operator $\bar\sigma_O$ no longer appears in the expression. In essence, the effect of an A atom at site j on the occupancy of the origin is now represented in terms of the effect it has on the shells of sites around O, which, in turn, pass this information on to O via their direct interactions with

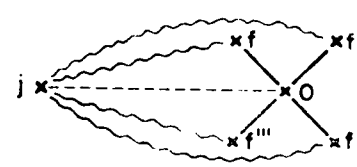

FIG. 1. The basic cluster for calculating the correlation between site j and the origin in terms of the correlations between site j and the neighbors of the origin.

the origin site. This is represented diagrammatically in Fig. 1 where the correlation between j and the origin (shown by a dashed line) has been replaced by the correlations between j and sites f, f', etc. (shown by wavy lines) and the direct interactions V_{Of} (indicated by solid lines) which these sites have with the origin site.

III. APPROXIMATE EQUATIONS FOR THE CORRELATION FUNCTIONS

In this section two methods will be developed for obtaining approximate solutions to the exact binary probability equation [Eq. (16)] which was given in Sec. II.

The first method involves the use of a frequency distribution function for E_O and by making a simple assumption about the behavior of this distribution function it is shown that the general equations previously derived by Cowley[5] result. Furthermore, if a somewhat more complex approximation is used for the distribution function, the theory of Zernike[4] is recovered. It then becomes possible to compare directly the basic approximations of these two theories and to determine under what conditions each should be a good approximation.

The second method for solving Eq. (16) approximately uses an exact expansion of the distribution function in terms of its moments. The theories of Zernike and Cowley are shown to be equivalent to certain approximations for the successive moments of this expansion. In addition, this expansion suggests a third approximation which would appear to have the same order of accuracy as the two other theories at temperatures above the ordering temperature, but has the advantage of yielding a set of linear equations for the correlation functions which are amenable to exact solution. This theory for correlation functions in alloy systems is discussed in detail in Sec. IV.

A. The Distribution Function

Returning to Eq. (16) we may write the right-hand side in the form of a sum over the set of discrete values $\{E_O\}$ which E_O is able to assume:

$$P_{Oj}^{BA}=\sum_{\{E_O\}} g_{j-A}(E_O)f_B(E_O), \tag{17}$$

where

$$g_{j-A}(E_O)=\sum_{\bar{\sigma}_k=\pm 1}\delta(E_O+\tfrac{1}{2}\textstyle\sum_f V_{Of}\bar{\sigma}_f)\sigma_j^A\rho/\sum_{\bar{\sigma}_k=\pm 1}\sigma_j^A\rho$$

and $\delta(E_O+\frac{1}{2}\sum_f V_{Of}\bar{\sigma}_f)=1$ if $E_O=-\frac{1}{2}\sum_f V_{Of}\bar{\sigma}_f$, and $=0$ otherwise.

$g_{j-A}(E_O)$ is simply the frequency distribution of the random variable E_O under the condition that site j is occupied by an A atom, and satisfies the normalization requirement of $\sum_{\{E_O\}} g_{j-A}(E_O)=1$. Complete knowledge of this frequency distribution would be tantamount to an exact solution for the correlation functions. This, in three dimensions, is one of the unsolved problems of lattice statistics and so we content ourselves with different possible approximations to $g_{j-A}(E_O)$.

One fact that can be immediately determined about $g_{j-A}(E_O)$ is the mean of $E_O(\langle E_O\rangle_{j-A})$ with respect to $g_{j-A}(E_O)$:

$$\begin{aligned}\langle E_O\rangle_{j-A}&=\sum_{\{E_O\}} E_O g_{j-A}(E_O)\equiv -\tfrac{1}{2}\sum_f V_{Of}\langle\bar{\sigma}_f\rangle_{j-A}\\&=-\tfrac{1}{2}\sum_f V_{Of}(+2m_B P_{fj}^{AA}-2m_A P_{fj}^{BA})\\&=-m_B\sum_f V_{Of}\alpha_{fj},\end{aligned} \tag{18}$$

where the last equality follows from Eq. (11). Similarly the mean with the complementary distribution function $g_{j-B}(E_O)$ is found to be $\langle E_O\rangle_{j-B}=+m_A\sum_f V_{Of}\alpha_{fj}$. Our treatment to this point has been exact and we now introduce an approximation which will yield a closed form solution to the problem and will be mathematically equivalent to Cowley's theory.

The approximation is

$$\langle(E_O)^n\rangle_{j-A}\equiv\sum_{\{E_O\}}(E_O)^n g_{j-A}(E_O)\cong(\langle E_O\rangle_{j-A})^n \tag{19a}$$

and

$$\langle(E_O)^n\rangle_{j-B}\equiv\sum_{\{E_O\}}(E_O)^n g_{j-B}(E_O)\cong(\langle E_O\rangle_{j-B})^n. \tag{19b}$$

Since a knowledge of all the moments of a distribution function is sufficient to determine the distribution function it can be shown that the form of $g(E_O)$ which satisfies Eq. (19) is a delta function, i.e.,

$$g_{j-A}(E_O)=\delta(E_O-\langle E_O\rangle_{j-A}) \tag{20a}$$

$$g_{j-B}(E_O)=\delta(E_O-\langle E_O\rangle_{j-B}). \tag{20b}$$

Equation (17) is now soluble and we obtain

$$P_{Oj}^{AA}=f_A(\langle E_O\rangle_{j-A}), \tag{21a}$$

$$P_{Oj}^{AB}=f_A(\langle E_O\rangle_{j-B}), \tag{21b}$$

$$P_{Oj}^{BA}=f_B(\langle E_O\rangle_{j-A}), \tag{21c}$$

$$P_{Oj}^{BB}=f_B(\langle E_O\rangle_{j-B}). \tag{21d}$$

Remembering the functional forms of f_A and f_B from Eqs. (14) and (15) and inserting the values of $\langle E_O\rangle_{j-A}$ and $\langle E_O\rangle_{j-B}$ from Eq. (18), the results of the calculation can be put in the following convenient combination

$$\begin{aligned}\frac{P_{Oj}^{AA}P_{Oj}^{BB}}{P_{Oj}^{AB}P_{Oj}^{BA}}&\equiv\frac{(m_A+m_B\alpha_{Oj})(m_B+m_A\alpha_{Oj})}{(1-\alpha_{Oj})^2 m_A m_B}\\&=\exp(-2\beta\sum_f V_{Of}\alpha_{fj}),\end{aligned} \tag{22}$$

which is the result of Cowley[5] with the difference that the site indices O, j are interchanged. Cowley arrived at Eq. (22) by arguments which, on the surface, appear

to be quite different from those used here although the two arrive at the same mathematical endpoint.

We shall now use the present derivation of Cowley's expression to determine under what conditions Eq. (22) should give a good fit to experimental results. In physical terms we have approached the problem of calculating the correlation between the origin and j by fixing the occupancy of site j (to be an A atom, say) and trying to ascertain how this affects the occupancy of the origin site. In terms of the operator $\bar{\sigma}_O$, before the occupancy of site j was fixed, the average of $\bar{\sigma}_O$ was zero, but now this average will be shifted slightly (by an amount $\langle\sigma_O\rangle_{j=A} = 2m_B\alpha_{Oj}$). We have shown that we are able to calculate the shift in $\langle\bar{\sigma}_O\rangle$ by another route (see Fig. 1) since α_{Oj} is directly affected only by the sites f with which it has an interaction V_{Of} so that the effect of j on O must be passed through these sites f. Consequently, fixing an A atom at j can be imagined to "polarize" slightly the sites around O which then causes a shift in $\langle\sigma_O\rangle$ from its random value. This second way of calculating $\langle\sigma_O\rangle_{j=A}$ was expressed by Eq. (16). The condition that the value of $\langle\bar{\sigma}_O\rangle_{j=A}$ be the same in both cases gives the set of equations for the α_{Oj}'s. The approximation of replacing $g(E_O)$ by a delta function means in physical terms that we have assumed that the origin "sees" its neighbors frozen in their *average* polarized configuration and does not follow their fluctuations about this average. There are two cases in which this makes good sense. The first is at temperatures well below an ordering temperature in which we know that the atoms really are frozen into a few highly ordered states. In the case of an AB alloy in a simple cubic lattice two states predominate, A on α sites with B on β sites or A on β sites with B on α sites. Choosing j to be an A site resolves this twofold degeneracy and makes the occupancy of the neighbors of O determinate. Consequently site O will see on the average essentially one configuration of its neighbors with decreasing fluctuations about that configuration as the temperature decreases.

The second case in which the distribution function can be well represented by a delta function is at temperatures above the ordering temperature when a large number of sites have an interaction with the origin. This will be the situation when V_{Of} is a long-range interaction and the dimensionality of the lattice is high. This may be seen by regarding the operators $\bar{\sigma}_f$ in $E_O = -\frac{1}{2}\sum_f V_{Of}\bar{\sigma}_f$ as random variables capable of taking each of two values with a certain probability. At temperatures well above the ordering temperature these variables will be only weakly correlated and it is known from the theory of independent random variables that a distribution function of a sum of such variables peaks more and more sharply about $\langle E_O\rangle$ as the number of variables increases and reaches a delta function form in the limit of an indefinitely large number of variables. Consequently, we suggest that Cowley's expression will be worst for lattices of low coordination numbers and short-range interactions and best for the converse.

In view of the foregoing, one of the chief criticisms that can be made of Cowley's approximation is that it takes no account of the fluctuations in E_O about its average value, which can be expected to cause appreciable effects near the ordering temperature. It is natural, therefore, to try to incorporate these fluctuations into the theory and give a finite width to $g(E_O)$. Zernike's theory[4] and the closely related theory of Elliott and Marshall[7] do just this by using a different approximation to $g(E_O)$ which we will now discuss.

Zernike makes the assumption that the operators occurring in E_O may be regarded as stochastically independent of each other so that if the relative probability of the two values which each operator is able to assume were known the probability of any configuration of the neighbors would be given by a simple product of the individual probabilities. In this way he is able to obtain a first approximation for the fluctuations in E_O about its average value and arrives at a distribution function with a finite width.

For the case of an AB alloy with nearest-neighbor interactions (which is the only case given by Zernike), any operator $\bar{\sigma}_k$ can take on the values $+1$ or -1. Let us further assume we are dealing with a square lattice (as in Fig. 1) and the neighbors f, f', f'', and f''' of O are labeled from 1 to 4. If there were no constraints $\bar{\sigma}_f$ would assume the values $+1$ and -1 with equal probability, but if the constraint that j be occupied by an A atom (i.e., $\bar{\sigma}_j = +1$) is introduced then these probabilities are no longer equal. From the definitions of Eq. (11) we have

$$P_{fj}^{AA} \equiv P(\bar{\sigma}_f = +1 \,|\, \bar{\sigma}_j = +1) = \tfrac{1}{2}(1+\alpha_{fj}), \quad (23a)$$

$$P_{fj}^{BA} \equiv P(\bar{\sigma}_f = -1 \,|\, \bar{\sigma}_j = +1) = \tfrac{1}{2}(1-\alpha_{fj}), \quad (23b)$$

which may be condensed to

$$P(\bar{\sigma}_f \,|\, \bar{\sigma}_j = +1) = \tfrac{1}{2}(1+\bar{\sigma}_f\alpha_{fj}), \quad (23c)$$

and similarly

$$P(\bar{\sigma}_f \,|\, \bar{\sigma}_j = -1) = \tfrac{1}{2}(1-\bar{\sigma}_f\alpha_{fj}). \quad (23d)$$

Using Zernike's assumption that each neighbor f of the origin is independently correlated with j, one may write that the probability of any of the 2^4 configurations of the neighbors of O is

$$P(\bar{\sigma}_1\bar{\sigma}_2\bar{\sigma}_3\bar{\sigma}_4 \,|\, \bar{\sigma}_j = \pm 1) = \frac{1}{2^4}\prod_{f=1,4}(1\pm\bar{\sigma}_f\alpha_{fj}). \quad (24)$$

Equation (24) provides the necessary information to calculate the frequency distribution

$$g_{j=A}(E_O = -\tfrac{1}{2}\textstyle\sum_f V_{Of}\bar{\sigma}_f)$$

in terms of the α_{fj}'s and it is apparent from Eq. (24) that since products of the α_{fj}'s occur, $g_{j=A}(E_O)$ will be nonlinear in the α_{fj}'s. We have drawn the distribution

functions $g_{j-A}(E_O)$ and $g_{j-B}(E_O)$ obtained from the Cowley and Zernike expressions in Fig. 2 for purposes of comparison. α_{fj} has been taken as 0.1 independent of f for the sake of illustration although it is unrealistic that the α_{fj}'s would be equal at unequal distances. The last step is to use Eq. (17) to obtain Zernike's equation relating α_{0j} to the α_{fj}'s and V_{0f} by performing the sum over E_O. The final result is

$$\alpha_{0j}=\frac{1}{2^4}(t_4+2t_2-2t_{-2}-t_{-4})(\alpha_{1j}+\alpha_{2j}+\alpha_{3j}+\alpha_{4j})$$
$$+\frac{1}{2^4}(t_4-2t_2+2t_{-2}-t_{-4})$$
$$\times(\alpha_{1j}\alpha_{2j}\alpha_{3j}+\alpha_{1j}\alpha_{2j}\alpha_{4j}+\alpha_{1j}\alpha_{3j}\alpha_{4j}+\alpha_{2j}\alpha_{3j}\alpha_{4j}), \quad (25)$$

where $t_n=\tanh(-n\beta V/2)$ and V is the common value of the nearest-neighbor interaction (i.e., $V=V_{01}=V_{02}$, etc.).

Since j in Eq. (25) may be taken as any of the N sites of the lattice (except the origin), Eq. (25) is, in fact, $N-1$ nonlinear equations in $N-1$ unknowns which must be solved by some further approximation. Zernike treats this problem in detail for the cubic simple, body-centered and face-centered lattices in his original paper.[4]

B. Moment Expansion for the Correlation Function

We will now give an expansion for the correlation functions which will put the theories of Cowley and Zernike in clearer perspective with respect to each other and will indicate where possible improvements can be made in the calculations.

Equation (17) can be written exactly in terms of the successive moments of the distribution function by using a Maclaurin expansion for $f_B(E_O)$ in the variable βE_O as follows:

$$P_{0j}^{BA}=\sum_{\{E_O\}} g_{j-A}(E_O)\left[f_B(0)+\beta E_O f_B'(0)+\frac{\beta^2 E_O^2}{2!}f_B''(0)+\cdots\right]$$
$$=f_B(0)+\beta f_B'(0)\langle E_O\rangle_{j-A}+\frac{\beta^2}{2!}f_B''(0)\langle E_O^2\rangle_{j-A}+\cdots+\frac{\beta^n}{n!}f_B^{(n)}(0)\langle E_O^n\rangle_{j-A}+\cdots, \quad (26)$$

where $f_B^{(n)}(0)$ is $\partial^n f_B(E_0)/\partial^n(\beta E_O)$ evaluated at $\beta E_O=0$.

We may write analogous expansions for the other binary probabilities and by grouping terms obtain:

$$2\alpha_{0j}=P_{0j}^{AA}+P_{0j}^{BB}-P_{0j}^{AB}-P_{0j}^{BA}$$
$$=\beta[f_A'(0)-f_B'(0)][\langle E_O\rangle_{j-A}-\langle E_O\rangle_{j-B}]+\frac{\beta^2}{2!}[f_A''(0)-f_B''(0)][\langle E_O^2\rangle_{j-A}-\langle E_O^2\rangle_{j-B}]+\cdots$$
$$+\frac{\beta^n}{n!}[f_A^{(n)}(0)-f_B^{(n)}(0)][\langle (E_O)^n\rangle_{j-A}-\langle (E_O)^n\rangle_{j-B}]+\cdots. \quad (27)$$

From Eqs. (14) and (15) we have

$$f_A(E_O)-f_B(E_O)=\frac{e^{2m_B(\beta E_O+\lambda)}-e^{-2m_A(\beta E_O+\lambda)}}{e^{2m_B(\beta E_O+\lambda)}+e^{-2m_A(\beta E_O+\lambda)}}$$
$$=\tanh(\beta E_O+\lambda) \quad (28)$$

and so we may write Eq. (27) as

$$2\alpha_{0j}=\sum_{n=1}^{\infty}\frac{\beta^n}{n!}T_n(\lambda)[\langle E_O^n\rangle_{j-A}-\langle E_O^n\rangle_{j-B}], \quad (29)$$

where we define

$$T_n(\lambda)\equiv\left.\frac{\partial^n \tanh(X+\lambda)}{\partial X^n}\right|_{X=0}$$

This again is an exact expression for the correlation

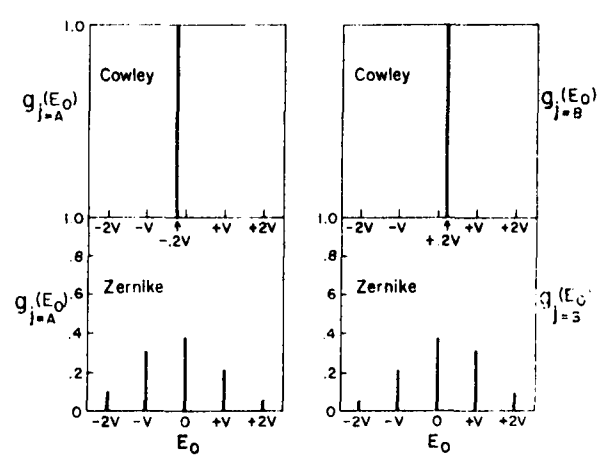

FIG. 2. Probability distribution of the field at the origin site as predicted by the Zernike and Cowley theories for the two cases of an A atom or a B atom at site j. The correlation between j and the neighbors of the origin has been taken as 0.1.

functions, the only unknowns being the moments $\langle E_O^n\rangle_{j=A,B}$ and we can gain some understanding of the theories of Zernike and Cowley by comparing their moment expansion with the exact series. First, it should be realized that since $\langle E_O\rangle_{j=A,B}$ is a sum of two particle correlations, the higher moments $\langle E_O^n\rangle_{j=A,B}$ are, in general, combinations of $n+1$ particle correlations. In order to obtain a closed form solution to the problem these higher moments which occur on the right-hand side of Eq. (29) must be broken up in some approximate way into products of two particle correlations. We have already seen that Cowley accomplished this by the breakup scheme $\langle E_O^n\rangle_{j=A,B}\cong\langle E_O\rangle^n{}_{j=A,B}$. Zernike, on the other hand, allows the individual operators in Eq. (29) to fluctuate about their mean value but assumes they move independently of each other. This leads to the following type of decomposition which is equivalent to Zernike's approximation.

$$\begin{aligned}\langle E_O^n\rangle_{j=A,B}&=\langle(-\tfrac{1}{2}\sum_f^{1..k}V_{Of}\bar\sigma_f)^n\rangle_{j=A,B}\\&=\sum_{p_1\cdots p_k}\frac{n!(-\frac{1}{2})^n}{p_1!p_2!\cdots p_k!}\langle(V_{O1}\bar\sigma_1)^{p_1}\cdots(V_{Ok}\bar\sigma_k)^{p_k}\rangle_{j=A,B}\\&\cong\sum_{p_1\cdots p_k}\frac{n!(-\frac{1}{2})^n}{p_1!\cdots p_k!}\langle(V_{O1}\bar\sigma_1)^{p_1}\rangle_{j=A,B}\cdots\langle(V_{Ok}\bar\sigma_k)^{p_k}\rangle_{j=A,B},\end{aligned}\tag{30}$$

where the sum $\sum_{p_1\cdots p_k}$ is taken over all combinations of the p_i's which satisfy the condition

$$\sum_{i=1}^{k}p_i=n.$$

k is the number of sites which directly interact with O. This is the mathematical statement that the correlations with j of each of the f sites surrounding O are to be retained and the correlations between sites f and f' are to be discarded, which is Zernike's assumption.

It may be seen that both Zernike and Cowley give the first term in Eq. (29) correctly but use different approximations for the second and higher terms. In breaking up a multiparticle correlation function $\langle\bar\sigma_1\cdots\bar\sigma_p\rangle$, it is reasonable to expect that the best approximation would be obtained by retaining the strongest pair correlations. That is, if $\bar\sigma_1$ is strongly coupled to $\bar\sigma_2$, but not to the rest, and $\bar\sigma_3$ is strongly coupled to $\bar\sigma_4$, but not to the rest, etc., then one could guess that a sensible decomposition of the multiparticle correlation would be $\langle\bar\sigma_1\bar\sigma_2\rangle\langle\bar\sigma_3\bar\sigma_4\rangle\cdots\langle\bar\sigma_{p-1}\bar\sigma_p\rangle$. Let us then consider the multiparticle correlation which occurs in the second term of Eq. (29), $\langle(\sum_f V_{Of}\bar\sigma_f)^2\rangle_{j=A,B}$. A particular operator $\bar\sigma_f$ will be most strongly correlated with itself and next most strongly with operators $\bar\sigma_{f'}$ of those sites which are closest to f. Cowley ignores all these correlations and effectively writes $\langle(\bar\sigma_f)^2\rangle_{j=A,B}\cong\langle\bar\sigma_f\rangle_{j=A,B}\langle\bar\sigma_f\rangle_{j=A,B}$ and $\langle\bar\sigma_f\bar\sigma_{f'}\rangle\cong\langle\bar\sigma_f\rangle_{j=A,B}\langle\bar\sigma_{f'}\rangle_{j=A,B}$. Zernike also ignores the second type of correlation (i.e., $\langle\bar\sigma_f\bar\sigma_{f'}\rangle-\langle\bar\sigma_f\rangle\langle\bar\sigma_{f'}\rangle$) but does keep the self-correlation so that $\langle(\bar\sigma_f)^2\rangle$ is retained intact. Similar comparisons can be made between these two theories for higher moments as well.

We may now draw some qualitative conclusions about the usefulness of Zernike's and Cowley's approximations and the possibilities for improved closed form calculations. At first glance it would appear that since Zernike retains the self-correlation and so is able to include a rough estimate of the fluctuations of the distribution function $g(E_O)$ about its mean value, it should be superior to Cowley's theory in all cases. This conclusion is true when the number of operators in E_O is small, the most striking case being the linear chain with nearest-neighbor interactions. For this problem, Zernike's result is very close to the exact expression for the correlation functions and Zernike correctly predicts no cooperative transition. Cowley's theory, on the other hand, is significantly poorer and incorrectly predicts a finite-ordering temperature. This defect may be traced directly to the fact that fluctuations have been ignored. However, as the dimension of the lattice increases, Ashkin and Lamb[11] have pointed out that Zernike's result becomes steadily poorer. This can be understood from the fact that the neighbors of the central site O are becoming more and more correlated with each other via the increased number of coupling paths present in lattices of higher coordination. Increasing the range of interaction has the same effect, and this undoubtedly places Zernike's independent neighbor calculation of $g(E_O)$ in increasingly greater error. On the other hand, the increased correlation between neighbors and the inclusion of more neighbors with a longer range of interaction tends to narrow $g(E_O)$ and so Cowley's estimate of $g(E_O)$ becomes more accurate.

In addition, there is the pragmatic feature that Zernike's calculation becomes extremely difficult to carry out as the coordination number increases and to our knowledge has never been attempted for more than nearest-neighbor interactions. This places it in the same

[11] J. Ashkin and W. E. Lamb, Phys. Rev. 64, 159 (1943).

area of problems which it is feasible to treat with exact high- and low-temperature expansions. If one could give a good fit at the ordering temperature, it would still have an advantage over exact expansions, but it is clear that this is just the region in which the independent neighbor assumption will be worst since short-range order builds up quite rapidly in the neighborhood of the transition point.

Cowley's theory is best, however, for those problems for which exact expansions become increasingly tedious, if not impossible to do with any accuracy (i.e., increasing coordination of the lattice and increasing range of interaction). In addition, the mathematical difficulty in solving Cowley's infinite set of nonlinear equations to some approximation does not increase appreciably for these more complex cases, so that it is likely that such a theory will continue to remain useful for some time. Fortunately, it is possible to find a set of simultaneous linear equations for the correlation functions which have the same order of accuracy as Cowley's nonlinear set *above* the ordering temperature and are capable of being solved exactly for an arbitrary range of interaction and arbitrary coordination.

IV. LINEAR EQUATIONS FOR THE CORRELATION FUNCTIONS ABOVE THE ORDERING TEMPERATURE

Both Zernike and Cowley obtain an infinite set of coupled nonlinear equations in the α_{0j}'s which must be solved in some approximate way to obtain values for the separate α_{0j}'s. It will be the purpose of this section to show that at temperatures above the ordering temperature a much more practical set of linear equations for the α_{0j}'s may be used which have the same degree of accuracy as either of the nonlinear forms of Zernike and Cowley. Moreover, this linear set of equations may be solved exactly for each of the α_{0j}'s and for any range of interaction. The solution is such that the pairwise interaction energy can be derived as a function of interatomic distance directly from the experimental data.

Returning to the exact expansion for α_{0j} [Eq. (29)], we have already seen that Cowley and Zernike have accounted for the first term on the right-hand side exactly but their expressions correspond to some approximation for the higher terms. Cowley's approximation for these higher terms is probably quite bad since the dominant contributions in these higher order correlations can be expected to come from self-correlations of site f, and correlations of site f with sites near to f. These terms are ignored by Cowley's theory and only the correlation between f and j (which is usually distant from f) is retained. However, Cowley's theory does give quite good results for the α_{0j}'s when compared with experiment[12,13] from which it can probably be concluded

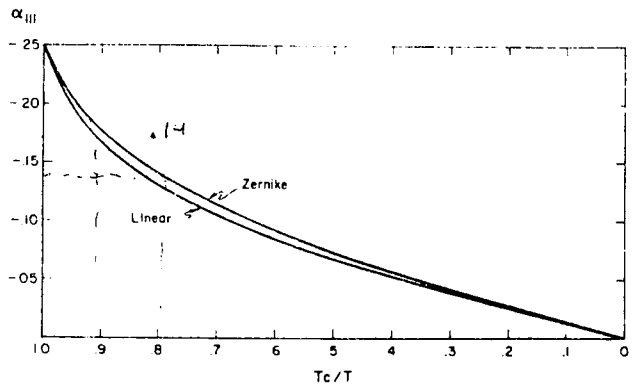

FIG. 3. First-neighbor order parameters as a function of temperature above the transition point, computed by the linear approximation and by Zernike's approximation for an AB alloy on a body centered cubic lattice (Cu-Zn). Only nearest-neighbor interactions are assumed to be nonzero.

that the higher order terms in the expansion are negligible at most temperatures above the ordering temperature. Consequently, the particular approximation used for these higher terms will likely have little effect on the final result. It is then reasonable to suggest that the higher order terms be entirely neglected and Eq. (29) be approximated as follows

$$2\alpha_{0j}=\beta T_1(\lambda)[\langle E_0\rangle_{j=A}-\langle E_0\rangle_{j=B}]. \tag{31}$$

Using Eq. (18) and the definition of $\lambda\equiv\frac{1}{2}\ln(m_A/m_B)$ gives

$$\alpha_{0j}=-2m_Am_B\beta\sum_f V_{0f}\alpha_{fj}. \tag{32}$$

A particular case of this general formula has previously been used by Walker and Keating[14] and Paskin[12] in a calculation for β Cu-Zn, and Clapp[15] has indicated the justification of this linear approximation for A-B alloys generally, using arguments similar to those presented here. Walker and Keating found that a calculation of the nearest-neighbor correlation in β Cu-Zn at 10% above T_c gave -0.182, -0.180, and -0.171 using the Elliott-Marshall theory, the Zernike theory, and the linear approximation, respectively.

For a more detailed quantitative comparison of the linear approximation, Fig. 3 gives the nearest-neighbor correlation in β Cu-Zn above the ordering temperature as calculated by the Zernike and linear formulas. It may be noted that the two calculations differ at most by about 8% at $T_c/T\simeq 0.8$. They are in perfect agreement at $T=T_c$ and have the same asymptotic behavior as $T\to\infty$.

As a test of an A_3B alloy we have compared the linear theory with the Monte Carlo calculations of Fosdick[16] for two choices of the second-neighbor interaction in Fig. 4. The Monte Carlo calculations were performed on a lattice containing $5\times5\times5$ unit cells and periodic

[12] A. Paskin, Phys. Rev. 134, A246 (1964).
[13] S. C. Moss, J. Appl. Phys. 35, 3547 (1964).
[14] C. B. Walker and D. T. Keating, Phys. Rev. 130, 1726 (1963).
[15] P. C. Clapp, Phys. Letters 13, 305 (1964).
[16] L. D. Fosdick, Phys. Rev. 116, 565 (1959).

boundary conditions were assumed. At temperatures well above the critical point, Fosdick's results are probably quite close to the exact correlations of an infinite lattice, but at temperatures near the critical point (say T_c, $T>0.9$) his values will be a much cruder approximation because of the long-range cooperative effects which are now becoming important in an infinite lattice. Since this is also the region of greatest inaccuracy for the linear theory it is a moot point as to which calculation is closer to the truth here. For T_c, $T<0.9$, the two calculations do not differ seriously.

We have not made a quantitative comparison between the Cowley and linear approximations because of the inherent difficulty in solving Cowley's nonlinear equations to sufficient accuracy to make a close numerical comparison meaningful.

The set of equations (32) can be diagonalized by introducing the Fourier transforms of α_{0j} and V_{0f}, i.e.,

$$\alpha_{0j}=\frac{1}{v_k}\int d^3k\,\alpha(k)e^{-i2\pi\mathbf{k}\cdot\mathbf{r}_j} \tag{33a}$$

$$V_{0f}=\frac{1}{v_k}\int d^3k\,V(k)e^{i2\pi\mathbf{k}\cdot\mathbf{r}_f}, \tag{33b}$$

where $\mathbf{r}_j$ is the vector from the origin to site j.

The integration is taken over one unit cell of the reciprocal lattice, the volume of which is v_k. Inserting (33) in (32) yields equations in terms of $\alpha(k)$ and $V(k)$ which give the following solution for any value of k:

$$\alpha(k)=\frac{C}{1+2m_Am_B\beta V(k)}, \tag{34a}$$

$$C=\left[\frac{1}{v_k}\int d^3k\,\frac{1}{1+2m_Am_B\beta V(k)}\right]^{-1}, \tag{34b}$$

where C has been chosen to satisfy the condition

$$\alpha_{00}=\frac{1}{v_k}\int d^3k\,\alpha(k)=1.$$

Finally, one has as the general solution for α_{0j}:

$$\alpha_{0j}=\frac{C}{v_k}\int d^3k\left(\frac{e^{-i2\pi\mathbf{k}\cdot\mathbf{r}_j}}{1+2m_Am_B\beta V(k)}\right). \tag{35}$$

Equations (34) and (35) can be used for experimental analyses in a number of ways. The most direct way in principle, since $\alpha(k)$ (which is actually the appropriately reduced x ray intensity) rather than α_{0j} is the quantity directly measured in the x ray diffuse scattering by the sample (see Moss[13]), would be to insert the experimental values of $\alpha(k)$ in Eq. (34) and thus calculate $V(k)$. The nature of $V(r)$ would then be obtained by Fourier inversion. This inversion, however, requires a complete map of $\alpha(k)$ in k space which, in general, is not possible since strong Bragg reflections completely obscure the x-ray diffuse scattering in certain regions of k space. To make matters worse these regions usually occur where $\alpha(k)$ has its minima and hence where the maximum values of $V(k)$ would lie [v.i. Eq. (34)].

One can proceed in another direction by making some specific guess as to the form of $V(r)$, either assuming that $V(r)$ is essentially short range and has a finite value only for the first few neighbors or assuming a particular long-range form such as the $V(r)$ proposed by Harrison and Paskin[12] for Cu–Zn. The undetermined constants and the validity of the assumed form of $V(r)$ are then determined by fitting Eq. (34) to the data.

Some preliminary restrictions on the form of $V(r)$ can be deduced from the observed distribution of $\alpha(k)$ because of the relation between the symmetry of $V(k)$ and $\alpha(k)$ implied by Eq. (34). This restriction gives a minimum range which $V(r)$ must have to account for the shape and symmetry of $\alpha(k)$ and it is possible to conclude for instance that current data on Cu_3Au[13] imply an interaction at least as far out as third nearest neighbors, so that the agreement which Moss obtained with the Cowley theory using V_1 and V_2 alone represented something more of a forced fit than had originally been thought. This is not a reflection on the accuracy or inaccuracy of the Cowley theory but means that V_3 is not negligible in Cu_3Au and should be included in any theoretical fit to the Cu_3Au data.

A second restriction on $V(r)$ may be obtained from a knowledge of the ordered state of the alloy since the maxima of $\alpha(k)$ fall at those points in k space which correspond to the wave vector of the ordered state even at temperatures above the critical temperature. This implies [via Eq. (34)] that $V(k)$ *must* have absolute minima at these points. For example, Cowley[5] fitted his data on Cu_3Au with values for the first three nearest-neighbor interactions of $V_1=358k$, $V_2=-34k$, and $V_3=-19k$. These values yield minima for $V(k)$ at positions in k space which are incompatible with the ordered structure of Cu_3Au by the above criterion.

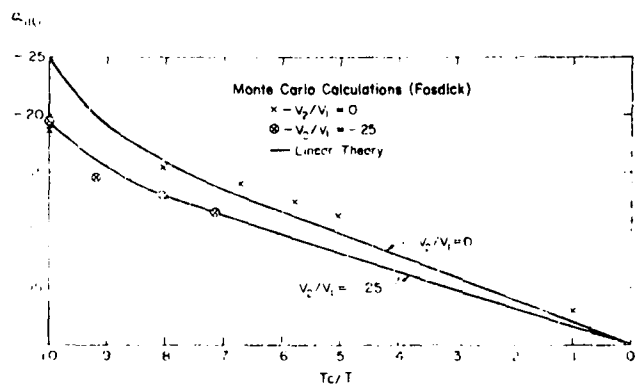

FIG. 4. The linear approximation compared with Fosdick's Monte Carlo calculations for the first-neighbor order parameter in Cu_3Au. The second-neighbor interaction V_2 was given the two values $-0.25\,V_1$ and zero.

In conclusion it may be said that the linear theory should prove useful in determining the strength and range of the pairwise interactions in alloys from the high-temperature data on short-range correlations, since the mathematics involved in making such a determination is quite tractable regardless of crystal symmetry, alloy composition, or range of the pairwise interaction. The theory should be particularly useful for testing the validity of long-range interaction models.

It should be remembered that the linear theory is valid only above the ordering temperature and that its accuracy improves as the temperature increases. A rough guess based on the few comparisons made with three dimensional alloys (to be reported upon in Part II) is that the linear theory probably is accurate enough for most purposes to within 10% of the ordering temperature. The range of validity for a particular system can be crudely estimated by comparing the temperature variation of the measured values of $\alpha(k)$ with the temperature behavior predicted by Eq. (34) [assuming $V(k)$ temperature-independent].

ACKNOWLEDGMENTS

One of us (S. C. M.) would like to express his appreciation to the U. S. Atomic Energy Commission for support of this general program of work.

APPENDIX

The theorem to be proven is that the operator $\sigma_O{}^B$ occurring in Eq. (9) of the text may be replaced by the conditional average, i.e., Eq. (A1) below is exact.

$$\sum_{\bar{\sigma}_k=\pm} \sigma_O{}^B \sigma_j{}^A \rho \Big/ \sum_{\bar{\sigma}_k=\pm} \sigma_j{}^A \rho = \sum_{\bar{\sigma}_k=\pm} \langle \sigma_O{}^B \rangle_{\text{cond}} \sigma_j{}^A \rho \Big/ \sum_{\bar{\sigma}_k=\pm} \sigma_j{}^A \rho, \quad \text{(A1)}$$

where

$$\langle \sigma_O{}^B \rangle_{\text{cond}} \equiv \sum_{\bar{\sigma}_O=\pm} \sigma_O{}^B \sigma_j{}^A \rho \Big/ \sum_{\bar{\sigma}_O=\pm} \sigma_j{}^A \rho$$

and $\rho = e^{-\beta(\frac{1}{2}\sum V_{ij}\bar{\sigma}_i\bar{\sigma}_j)} e^{\lambda \sum \bar{\sigma}_i}$.

The sum $\sum_{\bar{\sigma}_k=\pm}$ implies summing each of the $N\bar{\sigma}$ operators in the lattice (including $\bar{\sigma}_O$) over its two allowed values $+2m_B$ and $-2m_A$. We proceed by first imagining the sum over $\bar{\sigma}_O$ to be performed first in the numerator on the r h.s. of Eq. (A1), i.e.,

$$\sum_{\bar{\sigma}_k=\pm} \langle \sigma_O{}^B \rangle_{\text{cond}} \sigma_j{}^A \rho = \sum_{\bar{\sigma}_k=\pm}{}' \langle \sigma_O{}^B \rangle_{\text{cond}} \sigma_j{}^A \rho, \quad \text{(A2)}$$

where $\sum_{\bar{\sigma}_k=\pm}{}'$ implies a summation for all operators other than $\bar{\sigma}_O$. It will be noticed from the definition of $\langle \sigma_O{}^B \rangle_{\text{cond}}$ above or Eq. (14) of the text that it contains no dependence on the operator $\bar{\sigma}_O$ since a summation over $\bar{\sigma}_O$ has removed this dependence. Therefore the order of $\sum_{\bar{\sigma}_O=\pm}$ and $\langle \sigma_O{}^B \rangle_{\text{cond}}$ in Eq. (A2) can be interchanged. This gives (putting in the definition of $\langle \sigma_O{}^B \rangle_{\text{cond}}$):

$$\sum_{\bar{\sigma}_k=\pm} \langle \sigma_O{}^B \rangle_{\text{cond}} \sigma_j{}^A \rho = \sum_{\bar{\sigma}_k=\pm}{}' \Big(\sum_{\bar{\sigma}_O=\pm} \sigma_O{}^B \sigma_j{}^A \rho \Big/ \sum_{\bar{\sigma}_O=\pm} \sigma_j{}^A \rho \Big) \sum_{\bar{\sigma}_O=\pm} \sigma_j{}^A \rho \quad \text{(A3)}$$

and now the factors $\sum_{\bar{\sigma}_O=\pm} \sigma_j{}^A \rho$ can be cancelled

$$\sum_{\bar{\sigma}_k=\pm} \langle \sigma_O{}^B \rangle_{\text{cond}} \sigma_j{}^A \rho = \sum_{\bar{\sigma}_k=\pm}{}' \Big(\sum_{\bar{\sigma}_O=\pm} \sigma_O{}^B \sigma_j{}^A \rho \Big) = \sum_{\bar{\sigma}_k=\pm} \sigma_O{}^B \sigma_j{}^A \rho \quad \text{(A4)}$$

which is the required equality.

The proof depends upon the use of a grand canonical ensemble and the property that the $\bar{\sigma}$ operators commute.

Reprinted from THE PHYSICAL REVIEW, Vol. 171, No. 3, 754-763, 15 July 1968
Printed in U. S. A.

Correlation Functions of Disordered Binary Alloys. II

PHILIP C. CLAPP
Ledgemont Laboratory, Kennecott Copper Corporation, Lexington, Massachusetts 02173
AND
S. C. MOSS
Department of Metallurgy and Materials Science, Center for Materials Science and Engineering, Massachusetts Institute of Technology, Cambridge, Massachusetts 02139

(Received 3 November 1967; revised manuscript received 16 February 1968)

It has been previously established on the basis of an Ising model of alloy ordering (part I of this series) that the observed maxima of short-range-order diffuse scattering in disordered alloys mark the positions of the minima of $V(\mathbf{k})$, the Fourier transform of the pairwise interatomic potential $V(r)$. It was suggested in I that the superlattice spots of the ordered state should occur at these same positions. This would establish a consistency requirement connecting the ordered and disordered configurations. We prove here that this is a sufficient but not a necessary condition, and we derive the full set of necessary conditions. We also show that for most of the diffuse maxima locations observed in bcc and fcc alloys, it is possible to establish the ordered configuration required by the disordered phase, or conversely to use a knowledge of the ordered configuration to restrict the possible choices of $V(r)$ in fitting the disordered-phase scattering data. The linear approximation for correlation functions in binary alloys presented by the authors in I is compared quantitatively with the more exact but less general formula of Fisher and Burford. Except at temperatures very close to T_c, it is found that the theoretical shape of the short-range order diffuse scattering is in agreement but the temperature dependencies differ. We note also that all the currently known approximate calculations of $\alpha(\mathbf{k})$ for arbitrary $V(r)$ can be represented in the same functional form, $\alpha(\mathbf{k})=G_2(T)/[1+G_1(T)V(\mathbf{k})]$, where the temperature-dependent factors G_1 and G_2 vary according to the method of calculation used, but that $V(\mathbf{k})$, the Fourier transform of $V(r)$, is the same for all. This leads to the conclusion that the ratios $V(r_{n+1})/V(r_n)$ determined by fitting the theoretical form to experimental data are insensitive to the particular choice of G_1 and G_2, but that the magnitudes of the $V(r_n)$ so determined vary according to this choice. As a consequence, the values obtained for $V(r_{n+1})/V(r_n)$ are to be regarded as more accurate than those for $V(r_n)$.

1. INTRODUCTION

IN a previous paper[1] (hereafter referred to as I), the authors derived an expression for the diffuse x-ray or neutron scattering intensity produced by the short-range order present in an alloy above its ordering temperature T_c. The equation [Eq. (34) of I] relates the scattering intensity $\alpha(\mathbf{k})$ to the Fourier transform of the pairwise interatomic potential $V(\mathbf{k})$, the fraction of A and B atoms in the alloy m_A, m_B and the Boltzmann temperature factor β (or $1/kT$). It is written as

$$\alpha(\mathbf{k})=C/[1+2m_Am_B\beta V(\mathbf{k})], \qquad (1.1)$$

where C is a normalization constant whose value is determined by the condition that the integral of $\alpha(\mathbf{k})$ over a unit cell of the reciprocal lattice be unity. An explicit expression for C is given by Eq. (34b) of I.

This part has been written to supplement the theoretical exposition of I in two principal areas. Section 2 is devoted to a more quantitative analysis of the approximations inherent in Eq. (1.1). Section 3 offers a partial analysis of the problem of predicting the ordered configuration of an alloy from a knowledge of the pairwise interatomic potential, and defines the region of values of the interatomic potential in which a given ordered configuration is the ground state of the system.

Since writing I, we have become aware of several derivations by other authors of equations closely related to our Eq. (1.1). deGennes and Friedel[2] and Brout[3] derive equations for magnetic spin-spin correlations (which are analogous to atomic pair correlations in AB alloys) that differ from our equation in the choice of C and the restriction that $m_A=m_B=\frac{1}{2}$. Brout's derivation is particularly informative, since it shows that the expression can be derived by either a random-phase approximation (RPA) or an extension of the molecular-field concept to correlations. Krivoglaz's[4] derivation is for alloy systems and is not restricted to the case $m_A=m_B$. He obtains a different value for C, however, which is the infinite-temperature limit, namely, 1.0.

Equation (1.1) has several advantages as a tool for analyzing diffuse scattering data. It can be used to fit the corrected data directly, rather than fitting to Fourier coefficients of the scattering intensity (as is necessary with Cowley's[5] equations) so that no experimental information is wasted. Furthermore, fits can be made to data that do not cover all three directions in reciprocal space, although it is necessary to have measurements in the regions of reciprocal space that are most sensitive to variations of $V(\mathbf{k})$ in order to establish $V(\mathbf{k})$ within reasonably narrow limits.

One of the most useful aspects of Eq. (1.1) is that it is easy to obtain a graphic picture of the effect that inclusion of second, third, or even higher-neighbor interactions have on the shape of the diffuse intensity.

[1] P. C. Clapp and S. C. Moss, Phys. Rev. 142, 418 (1966).
[2] P. G. DeGennes and J. Friedel, J. Phys. Chem. Solids 4, 71 (1958).
[3] R. Brout, *Phase Transitions* (W. A. Benjamin, Inc., New York, 1965), p. 15.
[4] M. A. Krivoglas and A. A. Smirnov, *The Theory of Order-Disorder in Alloys* (MacDonald & Co., Ltd., London, 1964), p. 345.
[5] J. M. Cowley, Phys. Rev. 77, 669 (1950).

For instance, the disklike intensities observed in Cu_3Au by Cowley[5] and Moss,[6] the almost-spherical peak shapes observed by Roberts[7] in CuAu, and the egglike contours seen by Batterman[8] for $CuAu_3$ can all be obtained by suitably adjusting the strengths of V_2 and V_3 relative to V_1, so that it is possible to get a rough idea of the importance of higher-neighbor interactions by looking at contour plots of the diffuse intensity. These points will be covered in detail in the following paper (paper III).

Another quite useful aspect of Eq. (1.1) is that it is possible to put sharp limits on the range of values for V_2/V_1, V_3/V_1, etc., that will produce maxima of the diffuse intensity at the correct locations in reciprocal space. This may be seen from the fact that the maxima of $\alpha(\mathbf{k})$ occur at the minima of $V(\mathbf{k})$, and so the values of the V_n's must be chosen to locate correctly the minima of $V(\mathbf{k})$. This statement will be expanded upon in Sec. 3.

2. THEORY AND NATURE OF THE APPROXIMATIONS

In this section, two essentially different aspects of the theoretical background of Eq. (1.1) are discussed. The first concerns the validity of the Ising model itself in describing the configuration energy of a real alloy system. The second deals with the mathematical accuracy of the approximations used to derive Eq. (1.1) from an Ising model formulation.

In I it was assumed that the configurational energy of an alloy could be written as a standard Ising model Hamiltonian modified for unequal atom fractions:

$$H=\tfrac{1}{2}\sum_{i,j}^{N} V_{ij}\sigma_i\sigma_j, \tag{2.1}$$

where $\sigma_i=(2m_B, -2m_A)$ if an (A,B) atom is at site i and (m_A,m_B) are the fractions of (A,B) atoms in the alloy. V_{ij} is the familiar combination $\frac{1}{4}(V_{ij}^{AA}+V_{ij}^{BB}-2V_{ij}^{AB})$, which is assumed to depend only on the neighbor distance between i and j and not on direction or location in the crystal. The V_{ij}'s may be assumed to be nonzero for an arbitrary range of neighbor distances, and they are the adjustable parameters of the theory. Very little success has been achieved in attempting to calculate the V_{ij}'s from first principles, and a basic motivation of this work is to establish their values for a number of real-alloy systems from available experimental data.

The pairwise interactions are thought to arise from the overlap of neighboring atomic-core orbitals (which would not be expected to have much effect beyond nearest neighbors) and in some cases from the interaction of incompletely screened ion cores (leading to a long-range oscillatory potential decaying as $1/r^3$).

Historically, two other major ideas have competed with the pairwise interaction model to describe ordering. The first is the well-known Brillouin-zone–Fermi-surface interaction model originally proposed by Jones to explain the Hume-Rothery phases and most recently applied by Sato and Toth[9] to long-period superlattices. This model provides a mechanism for lowering the energy of a particular ordered state, relative to the ensemble of disordered states, but it does not cause different disordered states to have different energies. Consequently, it cannot be used to explain changes in the short-range order of the disordered phase, nor the configuration of the short-range order, which is the principal concern here.

If it is correct to say that the short-range forces postulated for the Ising model are responsible for the local order in the disordered phase, these forces will produce an ordered phase at some lower temperature. It is possible that this process will be interrupted by the appearance of a different ordered phase caused by the Jones mechanism, and Sato and Toth suggest that this explains the interruption in the ordering of the CuAu I phase by the onset of the CuAu II long-period ordered phase. The disappearance of the CuAu II phase at a lower temperature remains paradoxical.

The second concept of ordering, which has more relevance to the disordered phase, is that of strain ordering. Ordering in this model is caused by a reduction in the strain energy of an alloy composed of atoms of different size. A recent calculation based on this model is that of Rudman.[10] Apart from providing a basis for rough estimates of the nearest-neighbor ordering forces, the strain-ordering theories suggest that the energy per atom is not simply a sum of pairwise interactions, but is an n-body interaction, where n is the nearest-neighbor coordination number. Rudman could rewrite his elastic strain energy in terms of a pairwise nearest-neighbor interaction that was dependent on the nearest-neighbor short-range-order parameter α. Rudman states that this dependence on α was very weak, causing the interaction to change by less than 5% as α varied from 0 to -0.2 (roughly the range of α for the disordered phase). These approximations, however, appear to be less valid as the size disparity between atoms increases, and for cases where large shifts of atoms off the regular lattice sites occur, Rudman's theory predicts irreducible n-body forces.

Given then that we expect the Ising Hamiltonian to describe properly the configurational energy of an alloy (with the possible exception of the long-period superlattices and large size-effect alloys noted above), Eq. (1.1) is still limited by the fact that it is not an exact solution of the Ising model. The details of its derivation and a comparison with the approximations

[6] S. C. Moss, J. Appl. Phys. 35, 3547 (1964).
[7] B. W. Roberts, Acta Met. 2, 597 (1954).
[8] B. W. Batterman, J. Appl. Phys. 28, 556 (1957).
[9] H. Sato and R. S. Toth, in *Alloying Behavior and Effects in Concentrated Solid Solutions*, edited by T. B. Massalski (Gordon and Breach Science Publishers, Inc., New York, 1965), p. 295.
[10] P. S. Rudman, Acta Met. 13, 387 (1965).

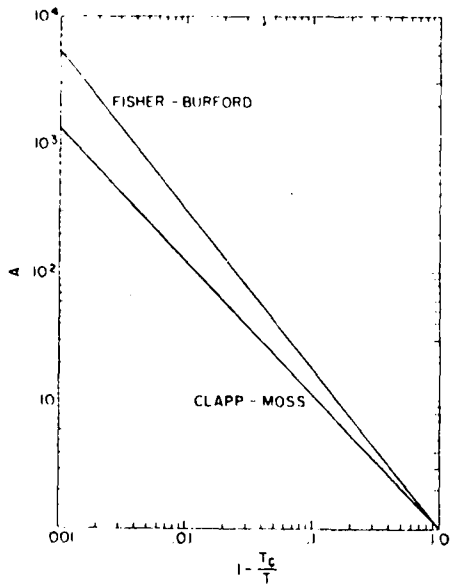

FIG. 1. Comparison of the maximum value of $\alpha(\mathbf{k})$ as predicted by Fisher and Burford (Ref. 11) and by our linear approximation for a fcc AB alloy with a negative nearest-neighbor interaction.

of Cowley and Zernike are the substance of I, and will not be repeated here. A rough estimate was made in I that Eq. (1.1) would be reasonably close to the exact Ising solution at temperatures greater than 10% above T_c, for bcc and fcc alloys. This estimate is in accordance with an estimate of Brout's[3] that the expression is accurate at temperatures above $(1+1/z)T_c$, where z is the nearest-neighbor coordination number of the lattice.

Fisher and Burford[11] have recently obtained a more accurate expression for $\alpha(\mathbf{k})$ in the case of nearest-neighbor interactions and an equiatomic alloy by applying the method of Padé approximants to exact high-temperature expansions. It is thus possible to compare Eq. (1.1) with a more accurate approximation for this special case.

With the exception of temperatures very close to T_c ($T/T_c<1.03$) our equation for $\alpha(\mathbf{k})$ and that of FB can be put in the same functional form[12]:

$$\alpha(\mathbf{k})=A(t)/[1+K^2(\mathbf{k})/K_1^2(t)], \qquad (2.2)$$

[11] M. E. Fisher and R. J. Burford, Phys. Rev. 156, 583 (1967), referred to as FB.

[12] The complete FB expression for three dimensions is

$$\alpha(\mathbf{k})=\frac{A(t)}{1+\psi K^2(\mathbf{k})/K_1^2(t)}\left[\frac{1+\phi^2K^2(\mathbf{k})}{K_1^2(t)}\right]^{1/88}.$$

Here ψ and ϕ are essentially temperature-independent factors. ψ differs from unity by a negligible amount (less than three parts in 10 000). For values of $\mathbf{k}$ inside the half-width, $K^2(\mathbf{k})/K_1^2(t)<1$, the factor containing ϕ^2 is negligible at all temperatures, because it differs from unity by two parts in 10 000 at most. This factor is also insignificant for $T/T_c>1.03$ for all positions in k space (it differs from unity by less than 2%). However, in the temperature region $T/T_c<1.03$, and for values of k outside the half-width, this term does become appreciable and, as FB point out, this causes $\alpha(\mathbf{k})$ to fall off as $k^{-(2+\eta)}$ (rather than k^{-2}) at temperatures close to the critical point.

where $t=T/T_c$ and the nearest-neighbor lattice separation is taken as unity. The temperature-dependent functions $A(t)$ and $K_1(t)$ in our case differ from that of the FB approximation but the k dependence of $\alpha(\mathbf{k})$ [contained in $K(\mathbf{k})$] is identical in the two cases, and has the form

$$K^2(\mathbf{k})=2d[1-V(\mathbf{k})/V(\mathbf{k}_M)],$$

where d is the dimension of the lattice and $\mathbf{k}_M$ is the position of minimum $V(\mathbf{k})$. For small departures of $\mathbf{k}$ from $\mathbf{k}_M$, $K^2(\mathbf{k})\cong(\mathbf{k}-\mathbf{k}_M)^2$, so that Eq. (2.2) represents a Lorentzian of amplitude $A(t)$ and half-width $K_1(t)$ in the neighborhood of the diffuse peak.

In Fig. 1, $A(t)$ is plotted for the two approximations for an fcc lattice with negative nearest-neighbor interactions (i.e., a clustering alloy). In our theory, $A(t)$ is given by $C(t)/(1-t^{-1})$, where $C(t)$ is the normalization constant previously defined. We have approximated the $A(t)$ of FB by $1/[r_1(t)K_1(t)]^{2-1/18}$, where $r_1(t)$ is a parameter plotted by FB in Ref. 11. Note that at a temperature 10% above T_c the peak height $A(t)$ given by our approximation is roughly $\frac{2}{3}$ that predicted by FB. Figure 2 has been taken directly from Fig. 5 of Ref. 11, and indicates that at 10% above T_c, the K_1 of FB is roughly $\frac{2}{3}$ smaller than our K_1 (the mean-field value).

Although this comparison indicates that Eq. (1.1) is not as accurate as might have been hoped, it does show that the k dependence of Eq. (1.1) for $T/T_c>1.03$ is essentially correct, and that it is the temperature-dependent parts of Eq. (1.1) that are in error. In fact, our expression for $\alpha(\mathbf{k})$ can very nearly be brought into

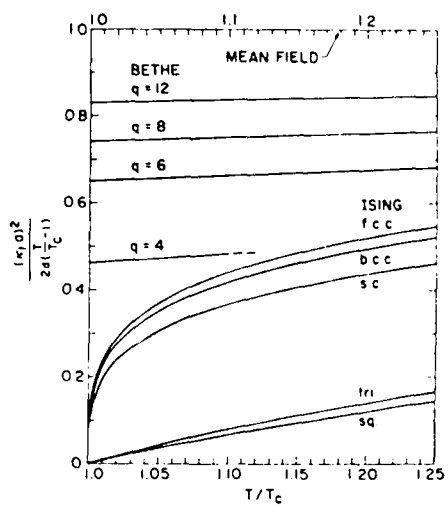

FIG. 2. Variation of the correlation-range parameter $K_1(t)$ for two- and three-dimensional AB alloys as given by the Bethe approximation (the curves labeled with coordination numbers q) the Fisher-Burford calculation (curves labeled by lattice type), and our approximation, which gives the same results for $K_1(t)$ as the mean-field approximation. Either positive or negative nearest-neighbor interactions may be assumed, except for the fcc lattice, where the positive case is special and must be considered separately. This figure is taken directly from Ref. 11.

coincidence with FB by choosing a different value for T/T_c (i.e., for $T/T_c=1.10$, we find that an effective value of 1.05 is necessary in our expression to achieve agreement). This points up a general characteristic of all the approximate theoretical expressions for $\alpha(\mathbf{k})$ for arbitrary $V(r)$ known to us. These include the equations of deGennes and Friedel,[2] of Krivoglas,[4] the RPA,[3] our linear approximation, the spherical-model approximation,[3] the linked-cluster-expansion calculations of Brout[3] and of Horwitz and Callen,[13] and the Green's function calculation of Bell.[14] The results of all of these treatments can be written in the form given by Eq. (2.2) or, equivalently,

$$\alpha(\mathbf{k})=G_2(t)\,[1+G_1(t)V(\mathbf{k})],$$

where the functions of temperature G_1 and G_2 depend upon the particular approximation employed. If this expression is normalized to satisfy the sum rule $\int\alpha(\mathbf{k})d^3k=1$, then $\alpha(\mathbf{k})$ can be written in terms of $G_1(t)$ and $V(\mathbf{k})$ alone, i.e.,

$$\alpha(\mathbf{k})=\frac{1}{1+G_1(t)V(\mathbf{k})}\Big/\int\frac{1}{1+G_1(t)V(\mathbf{k})}d^3k.$$

In fitting this theoretical formula to experiment, the adjustable parameters are seen to be G_1V_1, G_1V_2, G_1V_3, etc., and as a consequence the absolute values of the V_i's will depend upon which theoretical method is used to provide the value of $G_1(t)$. However, the ratios of the V_i's will be model-independent and once they are determined for a particular system, the estimate of the absolute values of the V_i's can be improved as more accurate theoretical calculations of $G_1(t)$ become available. This, of course, assumes that higher-order calculations of $\alpha(\mathbf{k})$ will have the same functional dependence on $V(\mathbf{k})$. We have used our estimate of $G_1(t)$, namely, $2m_Am_B\beta$, to evaluate the V_i's for various alloys in III, because our principal interest here is to determine the range and relative importance of higher-neighbor interactions in real-alloy systems, and because most of the other estimates of G_1 are difficult to evaluate for $m_A\neq m_B$. To summarize then, we believe that the ratios of the V_i's determined in III can be accorded a reasonable degree of reliability, but that the values given for the magnitude of the V_i's should be taken with a grain of salt.

3. ORDERED STRUCTURES

We discuss here the theoretical problem of inferring the ground state configuration of an alloy from $V(r)$, and the converse problem of obtaining restrictions on the possible form of $V(r)$ from a knowledge of the ordered alloy configuration. The diffraction pattern of a disordered alloy is characterized by one or more diffuse peaks. Upon ordering, sharp peaks (or superlattice spots) appear which may or may not be located at the position of the former diffuse peaks. We have shown in I that Eq. (1.1) predicts that the location of the diffuse peaks should coincide with the minima of $V(\mathbf{k})$. We now consider the question of the relationship between $V(\mathbf{k})$ and the superlattice-diffraction spots, assuming that $V(r)$ does not change appreciably on passing through T_c, and that no radical distortions of the lattice occur. We assume also that the ordered phase appearing at T_c remains the stable phase down to zero temperature.[15] Under these circumstances, the ordered structure will be the atomic arrangement that minimizes the configuration energy.

The configurational energy of the lattice can be written directly in terms of the scattering intensity and $V(\mathbf{k})$, by Fourier transforming Eq. (2.1):

$$H=D\int d^3k\,V(\mathbf{k})\alpha(\mathbf{k}),\tag{3.1}$$

where $D=Nm_Am_B/(2\pi)^3$ and the integration is over the first Brillouin zone of the disordered lattice. As we show in the Appendix, $\alpha(\mathbf{k})$ for a perfectly ordered structure is a linear combination of δ functions, i.e.,

$$\alpha(\mathbf{k})=\sum_{\{\mathbf{K}_j\}}^{n}A_j\delta(\mathbf{k}-\mathbf{K}_j),\tag{3.2}$$

where the $\mathbf{K}_j$ are the positions of the superlattice spots. For convenience, we shall include the origin (000) as a superlattice point, although the weight factor A_0 will always turn out to be zero. There are n $\mathbf{K}_j$'s per unit cell of the disordered reciprocal lattice of volume v, and n is the ratio of the number of atoms per unit cell in the ordered and disordered phases. The weight factors A_j are proportional to the square of the structure factor for that reflection of the ordered lattice. They are never negative but may be zero, and they must satisfy the sum rule $\sum A_j=1$, in order that the condition $\alpha(r=0)=(1/v)\int d^3k\,\alpha(\mathbf{k})=1$ be satisfied. Inserting Eq. (3.2) in Eq. (3.1) yields

$$H=D\sum_{\{\mathbf{K}_j\}}^{n}A_jV(\mathbf{K}_j),\tag{3.3}$$

and it is clear that Eq. (3.3) is minimized by that ordered structure for which the $\mathbf{K}_j$ are located only at minima of $V(\mathbf{k})$. If there were no other conditions on the A_j's, the prediction could be made that the superlattice spots of the ordered phase should occur precisely at the maxima of the diffuse peaks of the disordered phase (although not necessarily at all such positions).

[13] G. Horwitz and H. B. Callen, Phys. Rev. 124, 1757 (1961).
[14] R. L. Bell, Phys. Rev. 143, 215 (1966).

[15] For the idealized case of $V(r)$ independent of temperature, Tahir Kheli, Callen, and Jarrett (Ref. 20) have shown for the closely related problem of a Heisenberg antiferromagnet with second-neighbor interactions, that at all points in the phase diagram for the three cubic lattices the ordered phase that minimizes the configurational free energy at T_c does so at all lower temperatures, and thus minimizes the configurational energy at 0°K. They computed the configurational free energy at finite temperatures by the method of two-time Green's functions.

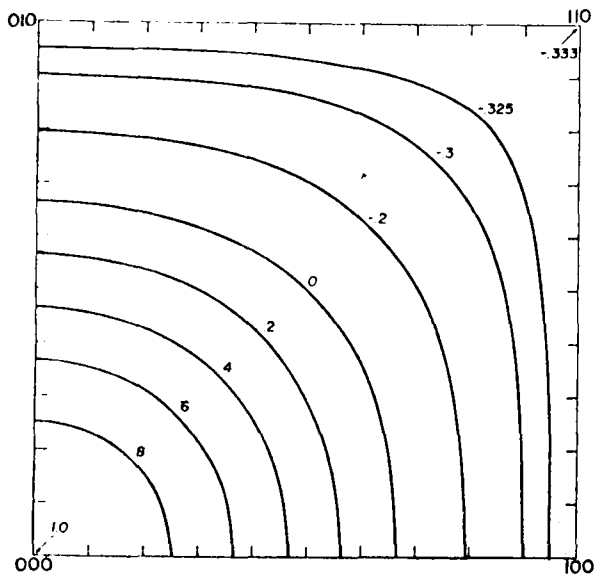

FIG. 3. $C_1(h_1h_20)$ for the fcc lattice.

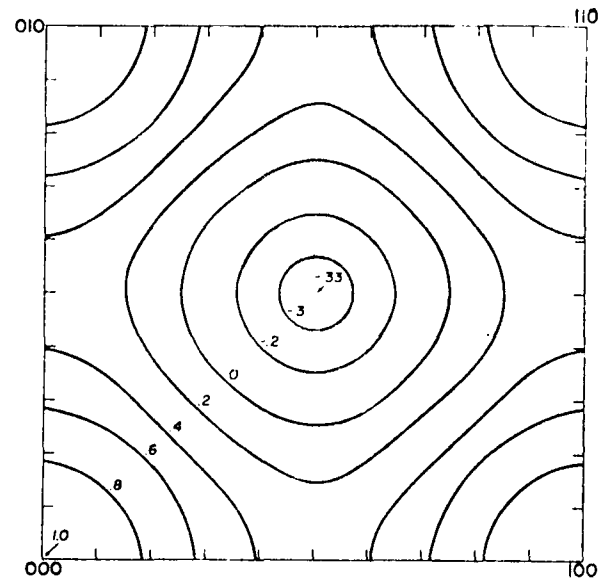

FIG. 4. $C_2(h_1h_20)$ for the fcc lattice.

This, then, is the proper theoretical basis for our suggestion in I that the superlattice spots of the ordered phase should occur at $V(\mathbf{k})$ minima, and it is clear that this conclusion is based entirely on the fundamental Ising Hamiltonian, and is independent of statistical approximations. It is, however, only a sufficient condition, and not a necessary one, because it is not always possible to find an ordered structure of the correct composition that satisfies this simple condition. This is so because there are additional restrictions on the A_j's that stem from the fact that each site of the ordered lattice must be occupied by either an A or a B atom, with fractional occupation prohibited. These necessary conditions are derived in the Appendix and are contained in Eqs. (A10) and (A12).

Luttinger[16] was apparently the first to consider this problem of finding the ground state configuration of an antiferromagnetic Ising system for arbitrary $V(r)$. He could find no general solution, but suggested a procedure that is equivalent to initially relaxing the subsidiary conditions on the A_j's. This has come to be known as Luttinger's "weak condition," and the procedure is then to check whether any of the solutions generated with the weak condition also satisfy the necessary conditions. If one is lucky, at least one solution will, and the search is over.

This development has been continued by a number of other workers,[17-20] so that we now know the ground-state configurations for an AB alloy with first- and second neighbor interactions in the three cubic lattices.

Our approach here is different from that just cited, in that we treat compositions other than AB and use conditions based on the Fourier transform of the Ising Hamiltonian [i.e., Eq. (3.3)], which enables us to consider $V(r)$ of arbitrary range as long as the positions of $V(\mathbf{k})$ minima or, equivalently, the positions of diffuse maxima of $\alpha(\mathbf{k})$ are known.

Philhours and Hall[21] have recently published several investigations based upon our suggestion in I that the wave vectors (or superlattice spots) of the ordered phase should lie at the positions of $V(\mathbf{k})$ minima. They found independently that this is a sufficient but not a necessary condition for the ground state, and that it is dependent only upon the fundamental Ising Hamiltonian and not upon any statistical approximation.

The sufficient condition is satisfied for many of the familiar ordering systems, such as CuAu, Cu_3Au, CuPt, CuZn, etc., but there are also exceptions, such as Au_3Mn [22] which are explicable only by including the subsidiary conditions on the A_j's. Before proceeding to a discussion of the full set of conditions, we shall examine the possible locations of the minima in $V(\mathbf{k})$ as determined by the strengths of near-neighbor interactions.

We first take the case of a fcc lattice. The vector from an atom to its (lmn) neighbor is expressed by

$$\mathbf{r}(lmn)=\tfrac{1}{2}l\,\mathbf{a}_1+\tfrac{1}{2}m\,\mathbf{a}_2+\tfrac{1}{2}n\,\mathbf{a}_3,$$

where $\mathbf{a}_1$, $\mathbf{a}_2$, $\mathbf{a}_3$ are the three cubic axes; l, m, n are integers, and $l+m+n$ is even. The continuous vector $\mathbf{k}$ in reciprocal space is represented by the continuous variables h_1, h_2, h_3 and the three vectors $\mathbf{b}_1$, $\mathbf{b}_2$, $\mathbf{b}_3$

[16] J. M. Luttinger, Phys. Rev. 81, 1015 (1951).
[17] J. S. Smart, Phys. Rev. 86, 968 (1952).
[18] D. ter Haar and M. E. Lines, Phil. Trans. Roy. Soc. London A254, 521 (1962).
[19] D. H. Lyons and T. A. Kaplan, Phys. Rev. 120, 1580 (1960).
[20] R. A. Tahir Kheli, H. B. Callen, and H. Jarrett, J. Phys. Chem. Solids 27, 23 (1966).
[21] J. Philhours and G. L. Hall, Phys. Rev. 163, 460 (1967).
[22] L. E. Tanner, Ledgemont Laboratory Internal Report No. TN 33, 1967 (unpublished).

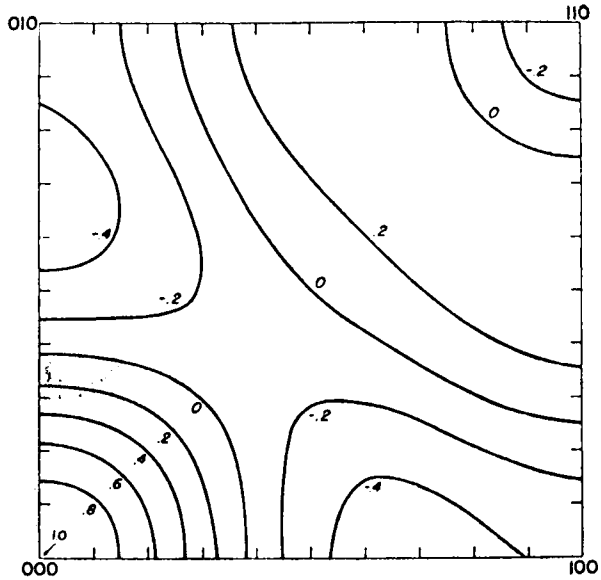

FIG. 5. $C_3(h_1h_20)$ for the fcc lattice.

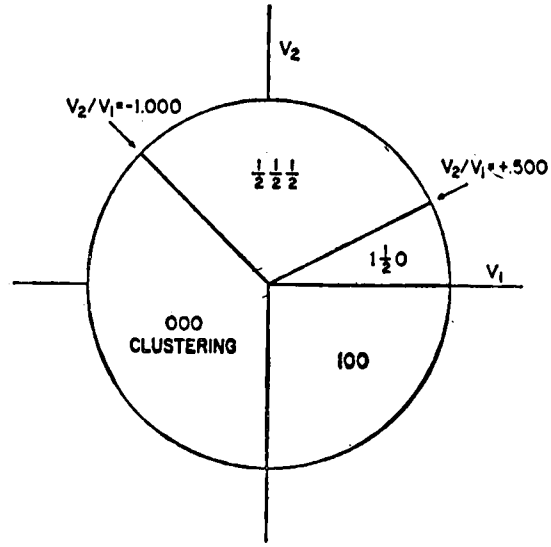

FIG. 6. Locations of the minima of $V(\mathbf{k})$ as a function of the ratio V_2/V_1 for the fcc lattice.

reciprocal to the a_i's,

$$\mathbf{k}=h_1\mathbf{b}_1+h_2\mathbf{b}_2+h_3\mathbf{b}_3.$$

In this notation, the Bragg reflections occur at $(h_1h_2h_3)$ all odd or all even integers, i.e., (111), (200), etc. Writing out $V(\mathbf{k})$ explicitly for up to third-neighbor interactions, we have

$$\begin{aligned}V(\mathbf{k}) &\equiv \sum_{lmn} V_{lmn}\cos\pi lh_1\cos\pi mh_2\cos\pi nh_3,\\ &=\sum_i Z_iV_iC_i(h_1h_2h_3),\\ &=12V_1[\tfrac{1}{3}(\cos\pi h_1\cos\pi h_2+\cos\pi h_2\cos\pi h_3\\ &\quad+\cos\pi h_1\cos\pi h_3)]+6V_2[\tfrac{1}{3}(\cos2\pi h_1+\cos2\pi h_2\\ &\quad+\cos2\pi h_3)]+24V_3[\tfrac{1}{3}(\cos2\pi h_1\cos\pi h_2\cos\pi h_3\\ &\quad+\cos\pi h_1\cos2\pi h_2\cos\pi h_3\\ &\quad+\cos\pi h_1\cos\pi h_2\cos2\pi h_3)], \quad (3.4)\end{aligned}$$

where Z_i is the coordination number of the i shell, V_i is the ith-neighbor interaction, and $C_i(h_1h_2h_3)$ is the appropriate sum of cosine terms, normalized such that $C_i(000)=1$. C_1, C_2, and C_3 have been plotted in the $h_3=0$ plane in Figs. 3–5. C_1 can never be greater than $+1$, nor less than -1, so that (000) is always a maximal point, but it may not be the only such point. The minimum value of C_1 is $-\frac{1}{3}$ and this occurs at all points of the line between (100) and (1 $\frac{1}{2}$ 0) and all equivalent points (i.e., all points obtainable from these by applying the symmetry operations of the body-centered space group). Henceforth, the mention of a point $(h_1h_2h_3)$ will imply its equivalents as well.

The maxima of C_2 occur at (100) as well as (000) and the minima occur at ($\frac{1}{2}$ $\frac{1}{2}$ $\frac{1}{2}$) having a value of -1. The point ($\frac{1}{2}$ $\frac{1}{2}$ 0) in Fig. 2 where C_2 is $-\frac{1}{3}$ is only a minimax. The maxima of C_3 occur only at (000) and C_3 takes on its lowest value $-\frac{1}{2}$ at ($\frac{2}{3}$ 0 0). (100) is a minimax.

Varying the strength of V_2 and V_3 relative to V_1 will obviously affect the location of the minima of $V(\mathbf{k})$. Figure 6 shows the position of the minima for the case when only V_1 and V_2 are nonzero. Figures 7 and 8 are similar plots for the case when V_3 is also nonzero. Where ordered structures are known that have superlattice spots at the given minima, their *Strukturbericht* symbols have been designated and a few examples indicated. Figure 9 illustrates the structures for AB and A_3B stoichiometric compositions. It is interesting that the AB analog of the DO_{22} structure has not yet been found in any system, and the only alloy known to be a possible candidate for the A_3B analog of the $L1_1$ structure is $CuPt_3$.

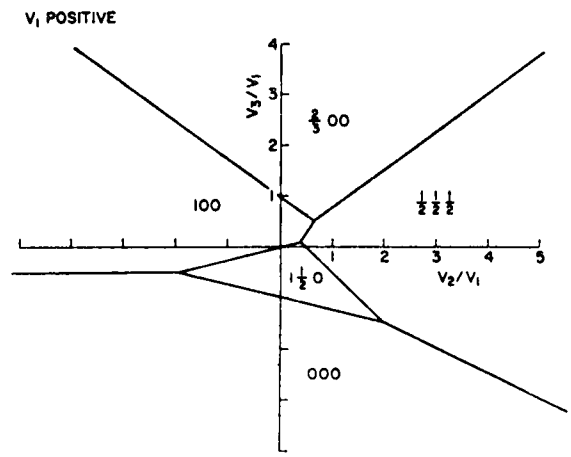

FIG. 7. Locations of the minima of $V(\mathbf{k})$ for V_1, V_2, and V_3 with V_1 positive in an fcc lattice.

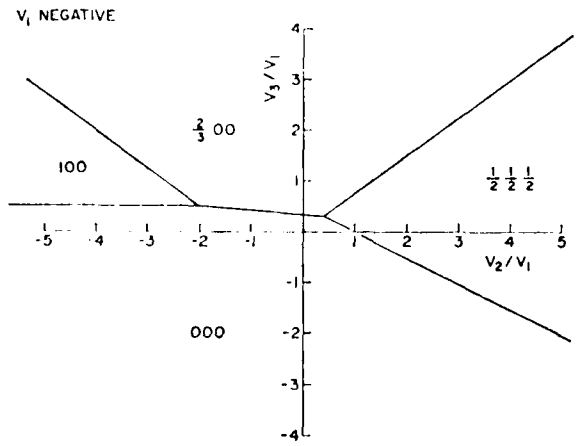

FIG. 8. Location of the minima of $V(\mathbf{k})$ for V_1, V_2, and V_3 with V_1 negative in an fcc lattice.

For a bcc lattice, a similar analysis is easily carried out. The atoms are again separated by the vector

$$\mathbf{r}(lmn)=\tfrac{1}{2}l\mathbf{a}_1+\tfrac{1}{2}m\mathbf{a}_2+\tfrac{1}{2}n\mathbf{a}_3,$$

where now l, m, n are all even or all odd, and the $\mathbf{k}$ vector has the same meaning as above, but with $h_1+h_2+h_3$ even for the Bragg reflections, namely, (110), (200), etc. A plot of the positions of $V(\mathbf{k})$ minima is given in Fig. 10 as a function of V_2 and V_1. $V(\mathbf{k})$ is now

$$V(\mathbf{k})\quad 8V_1[\cos\pi h_1\cos\pi h_2\cos\pi h_3]+6V_2[\tfrac{1}{3}(\cos2\pi h_1+\cos2\pi h_2+\cos2\pi h_3)]+12V_3[\tfrac{1}{3}(\cos2\pi h_1\cos2\pi h_2+\cos2\pi h_2\cos2\pi h_3+\cos2\pi h_1\cos2\pi h_3)]. \qquad (3.5)$$

The two ordered structures of AB composition that have superlattice spots at the $V(\mathbf{k})$ minima are shown in Fig. 11. In both cases the diffuse short-range-order peaks of the disordered phase would be centered about the superlattice positions of the ordered phase.

We now return to the problem of predicting the configuration of the ordered phase from a knowledge of the positions of the $\alpha(\mathbf{k})$ diffuse maxima. As a first example, assume that the disordered lattice is fcc, that the composition is A_3B, and that the diffuse maxima are at (100) and (110) positions. Solving the necessary conditions for the ordered structure [Eqs. (A10)] requires two steps: (a) specifying the location of the superlattice spots (i.e., the set $\{\mathbf{K}_j\}$), and (b) solving Eqs. (A10) for the structure factors $F(\mathbf{K}_j)$, and hence the A_j's via Eqs. (A12). The set $\{\mathbf{K}_j\}$ can only be the four points 000, 100, 110, and 010 if the superlattice spots are to appear only at minima of $V(\mathbf{k})$. Equation (A10) then gives us four equations in the four unknown structure factors $F(000)$, $F(100)$, $F(110)$, and $F(010)$, which will be denoted as F_0, F_1, F_2, and F_3 in that order. The four equations are

$$\begin{aligned}&F_0^2+F_1^2+F_2^2+F_3^2=1,\\&2F_1F_2+2F_3F_4=0,\\&2F_1F_3+2F_2F_4=0,\\&2F_1F_4+2F_2F_3=0.\end{aligned} \qquad (3.6)$$

The composition A_3B immediately fixes F_0 to be $\frac{1}{2}$ and by a process of eliminating variables the only solution is found to be

$$F_0^2=F_1^2=F_2^2=F_3^2=\tfrac{1}{4}.$$

Equations (A12) then give $A_0=0$, $A_1=A_2=A_3=\frac{1}{3}$. This obviously corresponds to the $L1_2$-ordered structure, and this proves it to be the unique solution for the ordered ground state.

For the composition AB and the diffuse maxima as above, one again obtains Eqs. (3.6), except that now $F_0=0$. This leads to a degeneracy of three solutions ($A_0=0$, $A_1=1$, $A_2=0$, $A_3=0$), ($A_0=0$, $A_1=0$, $A_2=1$, $A_3=0$), or ($A_0=0$, $A_1=0$, $A_2=0$, $A_3=1$), which corre-

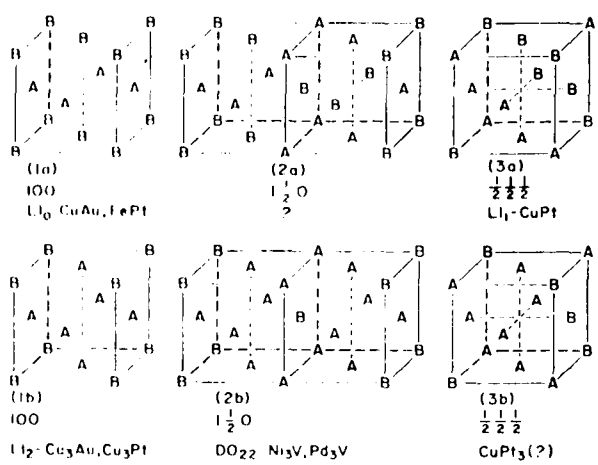

FIG. 9. Ordered structures on an fcc lattice showing location of superlattice spots and *Strukturbericht* symbols. The upper row is AB composition and the lower row is A_3B.

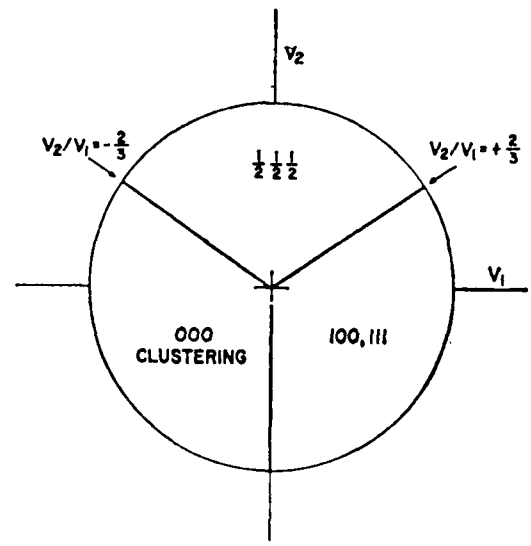

FIG. 10. Location of the minima of $V(\mathbf{k})$ as a function of the ratio V_2/V_1 for the bcc lattice.

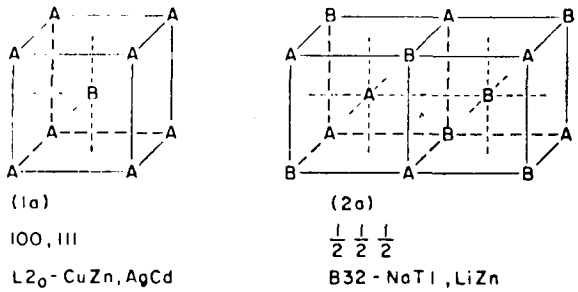

FIG. 11. Ordered structures on a bcc lattice for AB composition.

sponds to the well-known $L1_0$ structure with three possible directions for the tetragonal axis.

Finally we consider an example where all of the superlattice peaks cannot be located at the $V(\mathbf{k})$ minima, namely, when the diffuse peaks are at $(1\ \frac{1}{2}\ 0)$ positions, as in Ni_3V and Au_3Mn. We begin with the AB case. The simplest starting assumption is that $\{\mathbf{K}_j\}$ consists of the two points (000) and $(1\ \frac{1}{2}\ 0)$, implying an ordered structure with two atoms per unit cell. However, the set $\{\mathbf{K}_j\}$ must have the property that any integral multiple of a member also be a member of the set, since they form a lattice, and that any two points separated by a lattice spacing of the disordered reciprocal lattice are equivalent. These requirements make it necessary to include the point $(1\ \frac{3}{2}\ 0)$, which is located at a minimum of $V(\mathbf{k})$, and the point (010), which is not. Figure 12 shows the proposed location of superlattice spots.

The second step of determining the A_j's may be done either by generating all possible values of the $F(\mathbf{K}_j)$'s from Eq. (A4b) by trying the various arrangements of atoms in a four-atom unit cell, or by finding the possible solutions to Eqs. (A10) by successively eliminating variables. By either method one finds a unique solution for both the AB and A_3B compositions as follows:

$$AB: A(000)=0,$$
$$A(1\ \tfrac{1}{2}\ 0)=\tfrac{1}{2},\quad A(1\ \tfrac{3}{2}\ 0)=\tfrac{1}{2},\quad A(010)=0,$$
$$A_3B: A(000)=0,$$
$$A(1\ \tfrac{1}{2}\ 0)=\tfrac{1}{2},\quad A(1\ \tfrac{3}{2}\ 0)=\tfrac{1}{2},\quad A(010)=\tfrac{1}{3}.$$

The AB solution corresponds to the (2a) structure of Fig. 9, and the fact that the A_j's are nonzero only at minima of $V(\mathbf{k})$ implies that this structure has the lowest possible configurational energy for this type of $V(r)$ as in the two cases above. It is perhaps puzzling that such a structure has never been observed in nature. The A_3B solution is the DO_{22} structure illustrated in Fig. 9, and, since $A(010)$ is now nonzero, we see that if this is indeed the arrangement of lowest configurational energy for A_3B composition, the subsidiary conditions for the A_j's force $\frac{1}{3}$ of the superlattice intensity in the ordered phase to appear at locations different from the diffuse maxima positions of the disordered phase.

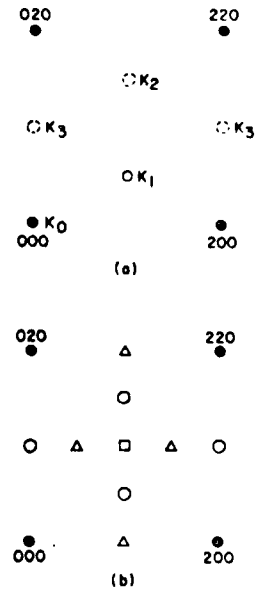

FIG. 12. (a) Minimum set $\{K_j\}$ necessary to locate a superlattice peak at $(1\ \frac{1}{2}\ 0)$. (b) Superlattice spots of the DO_{22} structure. Contributions from the three possible orientations of the tetragonal axis are labeled by separate symbols.

The question naturally arises, whether the diffuse intensity pattern anticipates this "anomalous" superlattice peak before the ordering temperature is actually reached, or if this peak emerges abruptly below T_c, as our theory would suggest. Tanner[22] has found from electron-diffraction measurements on thin films of Au_3Mn that, for this system at least, the latter suggestion fits the observations. Tanner's results will be discussed further in III.

Summarizing this discussion, we can say that we have provided a method for predicting the ordered configuration of an alloy by knowing only the location of the diffuse peaks in the disordered state in a number of simple cases. We do not claim to have completely solved the general problem of determining the ordered structure that is compatible with a given $V(\mathbf{k})$, and we have shown that, in at least one case (Au_3Mn), it is necessary to know more about $V(\mathbf{k})$ than just the location of its minima. It is clear that the stability of the DO_{22} structure, relative to others that may be imagined, will depend critically on the magnitude of $V(\mathbf{k})$ at the nonminimal (010) position.

4. SUMMARY AND CONCLUSION

The primary motivation of our first investigation (I) in this series was to provide a tractable method for determining the pairwise interaction strengths in alloys from an analysis of the short-range order diffuse scattering in the disordered state. In this paper, we have examined the accuracy of our method in greater detail to provide a better understanding of its limitations and its strengths. We have shown, by comparison with the recently published equation of Fisher and Burford for the special case of an AB alloy with nearest-neighbor interactions, that it has the same k dependence as ours but has a different temperature dependence. The two

predictions become nearly identical if $(T-T_c)/T_c$ is reduced by roughly a factor of two in our equation in the neighborhood of $(T-T_c)/T_c=0.1$. For interactions beyond first neighbors, we have shown that the relative values of the V_i's can be determined with greater certainty than can their absolute values.

We have also shown that a study of the ordered state is valuable in determining the pairwise interactions in alloys, because the relative strengths of the pairwise interactions compatible with a given ordered structure are limited to a certain range. This is useful in narrowing down the field of interaction strengths that may be used to fit the diffuse short-range order scattering data of a particular alloy, assuming that the ordered structure is known and that it remains stable at lower temperatures. However, the actual values of the V_i ratios can be determined only from a detailed fit to the diffuse-scattering data. It should be realized that these consistency conditions do not depend in any way on the approximations used in I to derive our diffuse-scattering equation, but rely only upon the basic Ising model formulation of the configurational energy of an alloy.

We now have the theoretical framework necessary to provide a reasonably complete analysis of available diffuse short-range order scattering data in alloy systems. This is the subject of the following paper (III).

ACKNOWLEDGMENTS

One of us (S. C. M.) would like to express his appreciation to the U. S. Atomic Energy Commission for initial support of this work, and to the Advanced Research Projects Agency, under Contract No. SD-90 at the Center for Materials Science and Engineering, for continued support.

APPENDIX

For the purposes of describing ordered alloys, we shall use operators σ_i, which are given the value $(+1, -1)$ for an (A,B) atom at site i. The σ_i operators are related to the $\tilde{\sigma}_i$ operators of I by the relation

$$\sigma_i=\tilde{\sigma}_i+(m_A-m_B), \tag{A1}$$

and, recalling the relation between α_{ij} and $\langle\tilde{\sigma}_i\tilde{\sigma}_j\rangle$ given by Eq. (12) of I, i.e., $\langle\tilde{\sigma}_i\rangle=0$, the result is as follows:

$$\langle\sigma_i\sigma_j\rangle=4m_Am_B\alpha_{ij}+(m_A-m_B)^2. \tag{A2}$$

The N atoms of a disordered alloy are assumed to be on the points of a regular lattice located at endpoints of vectors $\mathbf{r}_j$, where $j=0, N-1$. $\mathbf{r}_0$ is taken to be the null vector; and $\mathbf{r}_1$, $\mathbf{r}_2$, and $\mathbf{r}_3$ are taken as the unit vectors of the unit cell. An analogous convention is to be understood for the other types of lattices which we shall consider. For the sake of simplicity we confine the discussion to disordered lattices having a single atom per unit cell (i.e., the Bravais lattices).

Upon ordering, a larger unit cell is formed containing, say, n atoms. Equivalent positions in the ordered structure form a superlattice whose points are now separated by vectors $\mathbf{R}_j$.

We define a "structure factor" $\sigma_\mathbf{k}$ for the ordered lattice of N sites, where N will ultimately become indefinitely large.

$$\sigma_\mathbf{k}\equiv\sum_{j=0}^{N-1}\sigma_j e^{i\mathbf{k}\cdot\mathbf{r}_j}, \tag{A3}$$

which can be immediately factored into a unit-cell structure factor $F(\mathbf{k})$ and a superlattice structure factor $S(\mathbf{k})$ in the usual manner:

$$\sigma_\mathbf{k}=S(\mathbf{k})\times F(\mathbf{k}), \tag{A4a}$$

with

$$F(\mathbf{k})\equiv\frac{1}{n}\sum_{j=0}^{n-1}\sigma_j e^{i\mathbf{k}\cdot\mathbf{r}_j} \tag{A4b}$$

and

$$S(\mathbf{k})\equiv n\sum_{j=0}^{N'-1}e^{i\mathbf{k}\cdot\mathbf{R}_j}=\sum_{\{\mathbf{K}_j\}}\delta(\mathbf{k}-\mathbf{K}_j), \tag{A4c}$$

where $N'=N/n$ and $\delta(\mathbf{k}-\mathbf{K}_j)=N$ if $\mathbf{k}=\mathbf{K}_j$, and is zero otherwise. The set of points $\{\mathbf{K}_j\}$ are the points of the lattice reciprocal to the superlattice, and there will be n of them contained within a unit cell of the disordered reciprocal lattice. In the limit of N very large, $\delta(\mathbf{k}-\mathbf{k}')$ becomes a Dirac delta function and has the property

$$\frac{1}{v}\int\int\int G(\mathbf{k})\delta(\mathbf{k}-\mathbf{k}')d^3k=G(\mathbf{k}') \tag{A5}$$

if $\mathbf{k}'$ is within the unit volume v of reciprocal space integrated over, and is zero otherwise. $G(\mathbf{k})$ is an arbitrary function of $\mathbf{k}$.

The inverse of Eq. (A3) is

$$\sigma_j=\frac{1}{v}\int\int\int\sigma_\mathbf{k}e^{-i\mathbf{k}\cdot\mathbf{r}_j}d^3k, \tag{A6}$$

which becomes, on using Eq. (A4)

$$\sigma_j=\sum_{\{\mathbf{K}_j\}}F(\mathbf{K}_j)e^{-i\mathbf{K}_j\cdot\mathbf{r}_j}. \tag{A7}$$

Since σ_j can only be $+1$ or -1, we have

$$\sigma_j^2=1=\sum_{\mathbf{K}_j}\sum_{\mathbf{K}_{j'}}F(\mathbf{K}_j)F(\mathbf{K}_{j'})e^{-i(\mathbf{K}_j+\mathbf{K}_{j'})\cdot\mathbf{r}_j}. \tag{A8}$$

Using the variable change

$$\mathbf{K}_i=\mathbf{K}_j+\mathbf{K}_{j'} \quad\text{and}\quad H(\mathbf{K}_i)=\sum_{\mathbf{K}_j}F(\mathbf{K}_j)F(\mathbf{K}_i-\mathbf{K}_j),$$

Eq. (A8) becomes

$$\sigma_f^2 = 1 = \sum_{\mathbf{K}_i} H(\mathbf{K}_i) e^{-i\mathbf{K}_i \cdot \mathbf{r}_f}. \tag{A9}$$

The left hand side of Eq. (A9) is the same regardless of the choice of f, and in order that the right-hand side also be independent of f, the following conditions must hold:

$$H(\mathbf{K}_i) \sum_{\mathbf{K}_j} F(\mathbf{K}_j) F(\mathbf{K}_i - \mathbf{K}_j) = 0, \quad \text{if} \quad \mathbf{K}_i \neq 0 \tag{A10a}$$

and

$$H(0) = \sum_{\mathbf{K}_j} F(\mathbf{K}_j) F(-\mathbf{K}_j) = 1. \tag{A10b}$$

These equations provide n interrelations among the n F's, so that in general there will only be a small limited set of F's that are allowable. In addition, $F(0)$ is fixed by the composition and is given by

$$F(0) \equiv \frac{1}{n} \sum_{f=0}^{n-1} \sigma_f = m_A - m_B. \tag{A11}$$

We shall now show that the A_j's of Eq. (3.2) are related to the $F(\mathbf{K}_j)$'s as follows:

$$A_0 = F^2(0) - (m_A - m_B)^2 = 0, \tag{A12a}$$

$$A_j = F(\mathbf{K}_j) F(-\mathbf{K}_j) / 4 m_A m_B, \quad j \neq 0. \tag{A12b}$$

We have

$$\alpha(\mathbf{k}) \equiv \frac{1}{N} \sum_{f,g}^{N} \alpha_{fg} e^{i\mathbf{k} \cdot (\mathbf{r}_f - \mathbf{r}_g)},$$

and from (A2) and (A7) we get

$$\alpha(\mathbf{k}) = \frac{1}{4 m_A m_B N} \sum_{f,g}^{N} \sum_{\{\mathbf{K}_j\}} \sum_{\{\mathbf{K}_{j'}\}}^{*} F(\mathbf{K}_j) F(\mathbf{K}_{j'}) e^{i(\mathbf{k} - \mathbf{K}_j) \cdot \mathbf{r}_f} \times e^{-i(\mathbf{k} + \mathbf{K}_j) \cdot \mathbf{r}_g} - \frac{(m_A - m_B)^2}{4 m_A m_B N} \sum_{f,g}^{N} e^{i\mathbf{k} \cdot (\mathbf{r}_f - \mathbf{r}_g)},$$

which becomes

$$\alpha(\mathbf{k}) = \frac{1}{4 m_A m_B} \sum_{\{\mathbf{K}_j\}} F(\mathbf{K}_j) F(-\mathbf{K}_j) \delta(\mathbf{k} - \mathbf{K}_j) - \frac{(m_A - m_B)^2}{4 m_A m_B} \delta(\mathbf{k}). \tag{A13}$$

By comparing (A13) with Eq. (3.2), i.e.,

$$\alpha(\mathbf{k}) = \sum_{\{\mathbf{K}_j\}}^{n} A_j \delta(\mathbf{k} - \mathbf{K}_j), \tag{3.2}$$

it is apparent that Eqs. (A12) are recovered when the relation given by (A11) is included.

In conclusion, the $F(\mathbf{K}_j)$'s are restricted by the n equations given above and the A_j's in turn are determined by the $F(\mathbf{K}_j)$'s. The n conditions (A10) cannot be written in terms of the A_j's directly, with the exception of (A10b), which converts to

$$\sum_{\{\mathbf{K}_j\}} A_j = 1.$$

This was mentioned in Sec. 3 as the condition necessary to ensure that $\alpha(r=0) = 1$.

Reprinted from THE PHYSICAL REVIEW, Vol. 171, No. 3, 764–777, 15 July 1968
Printed in U. S. A.

Correlation Functions of Disordered Binary Alloys. III

S. C. MOSS*
Department of Metallurgy and Materials Science, Center for Materials Science and Engineering, Massachusetts Institute of Technology, Cambridge, Massachusetts 02139

AND

PHILIP C. CLAPP
Ledgemont Laboratory, Kennecott Copper Corporation, Lexington, Massachusetts 02173

(Received 3 November 1967; revised manuscript received 16 February 1968)

The linearized approximation for the correlation functions of a binary alloy, developed in parts I and II by the authors, is here applied to the experimental measurement of the diffuse scattering of x rays, thermal neutrons, and electrons. Information on the magnitude, sign, and range of the pairwise interactions has been extracted from the data on several alloys and alloy systems. The copper-gold system seems to be characterized by an oscillatory interaction out to at least third neighbors. The data on CuPt can be explained in terms of first- and second-neighbor energies, as can the results on Au_3Mn, Ni_4Mo, and CuNi, the latter being a clustering alloy. The results for β-CuZn are discussed in terms of a possible long-range oscillatory interaction, and an experiment is suggested for this alloy which would help to determine the presence of such an interaction.

1. INTRODUCTION

WITH the theoretical framework of parts I and II in hand we are now in a position to examine the existing data on short-range order in alloys and to apply Eq. (II, 1.1) to these data. The ultimate object is to extract information on the magnitude and range of the pairwise interactions in these alloys. We shall also indicate how the discussion of ordered structures in II is intimately related to our evaluation of the diffuse scattering of x rays or thermal neutrons and to the interaction energies that may be calculated from the diffraction data via Eq. (II, 1.1).

2. fcc ALLOYS

A. Cu-Au System

The Cu-Au system is characterized by complete solubility of the two fcc metals at high temperatures with various ordered structures that appear at lower temperatures. The major structures occur at the stoichiometric compositions Cu_3Au, CuAu, and $CuAu_3$ with critical temperatures T_c, respectively, of 390, 410, and $\sim 200°C$. While T_c for Cu_3Au and CuAu is a maximum exactly at stoichiometry, T_c for $CuAu_3$ increases continuously from the gold-rich side to CuAu. All of these transitions are first order in character, showing a discontinuous drop in the Bragg-Williams order parameter S at T_c. As mentioned in II, in the case of CuAu the fully ordered structure is interrupted by the appearance, below T_c, of an equilibrium long-period superlattice. With reference to Fig. 9(II), both Cu_3Au and $CuAu_3$ have the $L1_2$ structure while the low-temperature form of CuAu, consisting of alternating (100) planes of copper and gold atoms, has the $L1_0$ structure.

All of these ordered structures exhibit short-range order above T_c,[1–4] and it will be our purpose to relate the measured short-range order parameters to the interaction energies in the alloy system via Eq. (II, 1.1). Both the order parameters and the corresponding diffuse intensity from which they are obtained show certain distinct features that we shall try to interpret in terms of the pair interactions. Two points should be noted at the outset. In the first place, no correction for atomic size-effect displacements[5] has been applied to the theory. This means that the predicted diffuse intensity will differ more or less from the measured intensity, depending upon the magnitude of the size effect. The size-effect scattering generally will increase as the atomic fraction of the larger atom increases,[6] so that the $CuAu_3$ intensity will be severely affected, the Cu_3Au data less so. There have been attempts to incorporate the size-effect contribution into a purely thermodynamic expression, such as Eq. (II, 1.1) in order to predict the disorder-diffuse intensity more accurately.[6] Our belief is that given the approximate nature of both types of calculations—the thermodynamic one for pair correlations and the elasticity calculation for the size-effect scattering—it is better to remove the size-effect scattering from the data if one is primarily interested in pair correlations, and to study it separately if one wishes to extract information about atomic displacements in binary alloys. Such a technique for data separation

* Supported in part by the U. S. Atomic Energy Commission and by the Advanced Research Projects Agency under Contract No. SD-90.

[1] J. M. Cowley, J. Appl. Phys. **21**, 24 (1950).
[2] S. C. Moss, J. Appl. Phys. **35**, 3547 (1964).
[3] B. W. Roberts, Acta Met. **2**, 597 (1954).
[4] B. W. Batterman, J. Appl. Phys. **28**, 556 (1957).
[5] B. E. Warren, B. L. Averbach, and B. W. Roberts, J. Appl. Phys. **22**, 1493 (1951); for the most recent survey of the diffraction effects arising from local-order and size-effect displacements, see C. J. Sparks and B. Borie, in *Local Atomic Arrangements Studied by X-Ray Diffraction*, edited by J. B. Cohen and J. Hilliard (Gordon and Breach Science Publishers, Inc., New York, 1966), p. 5.
[6] S. V. Semenovskaya, Fiz. Tverd. Tela **8**, 2841 (1966) [English transl.: Soviet Phys.—Solid State **8**, 2273 (1967)].

has been developed by Borie[7] and, more recently, has been extended by Borie and Sparks.[8]

The second point which we would stress is that, while Eq. (II, 1.1) is certainly a high-temperature approximate expression, valuable information can be extracted through its application to alloy-diffuse scattering. The validity of the information obtained depends greatly not only upon the use to which it is put, but also upon which features of the theory are being emphasized.

Both the ordered and disordered structures of Cu_3Au and $CuAu_3$ have cubic symmetry and the diffuse x-ray scattering above T_c peaks at all of the equivalent superlattice reflection points that the ordered structure exhibits below T_c. The diffuse intensity will therefore have absolute maxima at values of $(h_1h_2h_3)$ equal to 100, 110, etc. The ordered structure of CuAu is tetragonal but its diffraction pattern invariably shows pseudocubic symmetry, because the c axis can assume with equal probability the $\mathbf{a}_1$, $\mathbf{a}_2$, or $\mathbf{a}_3$ axes of the disordered structure. For this reason, the collection of allowed superlattice positions and the positions of the diffuse maxima above T_c are equivalent to those for the other two alloys. Via Eq. (II, 1.1), absolute minima in $V(\mathbf{k})$ must also occur at the reciprocal lattice points where $\alpha(\mathbf{k})$ is a maximum in the disordered phase. The critical point can thus be defined as that temperature for which the denominator in Eq. (II, 1.1) goes to zero at the appropriate place in reciprocal space, namely, 100 and equivalent points. Given the expressions for $V(\mathbf{k})$ in Eq. (II, 3.4) and the definition of T_c,

$$1=-2m_Am_B(1/kT_c)V(\mathbf{k}_M),$$

the critical temperatures can be written as

$$T_c=(3V_1/2k)(1-\tfrac{3}{2}V_2/V_1+2V_3/V_1) \qquad (2.1)$$

for Cu_3Au and $CuAu_3$, and as

$$T_c=(2V_1/k)(1-\tfrac{3}{2}V_2/V_1+2V_3/V_1) \qquad (2.2)$$

for CuAu. $V(\mathbf{k}_M)$ is the value of $V(\mathbf{k})$ at the reciprocal lattice point where it assumes an absolute minimum. The first of these two expressions is identical to the critical temperature derived in a different way by Cowley[9] for the same structure.

All of our critical temperatures are essentially the mean-field prediction for T_c which, given a fixed value for V_1, V_2, V_3, etc., may be as much as 15–20% too high for face-centered alloys. This rough estimate is derived from the fact that the mean field value of T_c is 22% higher than the exact high-temperature Padé-approximant result for fcc lattices with negative nearest-neighbor interaction.[10] In order that the mathematical singularity of Eq. (II, 1.1) coincide with the experimentally observed critical temperature, the equation is rewritten in terms of T_c/T by inserting $kT_c/V(\mathbf{k}_M)$ in place of $-2m_Am_B$. The dependence of $\alpha(\mathbf{k})$ on composition and on V_1 is thereby absorbed into the expression for T_c. The resulting diffuse intensity, in Laue monotonic units, is

$$\alpha(\mathbf{k})=C/[1-(T_c/T)V(\mathbf{k})/V(\mathbf{k}_M)]. \qquad (2.3)$$

Since V_1 may be factored out of both $V(\mathbf{k})$ and $V(\mathbf{k}_M)$, we are left with an expression in which the variables are the ratios T_c/T, V_2/V_1, and V_3/V_1, if we arbitrarily decide that all $V_i(i>3)$ are negligible.

Once $\alpha(\mathbf{k})$ is computed, the short-range order parameters α_i can be obtained through a Fourier inversion, which is most easily done by computer. The transforms were taken using a summation over 1000 points of a symmetry cube of the reciprocal lattice extending on a side from the origin 000 to the 100 position. Taking a limited number of points means that $\alpha(\mathbf{k})$ near T_c will be in error because of the contribution of harmonics whose wave vector is smaller than, or comparable to, the interval between points. Since the region very near T_c is generally not of interest to us anyway, this is not a serious difficulty.

The fit of theory to experiment in the Cu-Au system was was begun with the measured short-range order parameters of Moss[2] on Cu_3Au. These are probably an improvement over the earlier Cowley values because the measured intensities were greater and were standarized independently using polystyrene, and because a nearest-neighbor size-effect correction was made. Theoretical values of the first ten α_i were calculated for Cu_3Au corresponding to both temperatures of measurement, 405 and 450°C, for which T_c/T is, respectively, 0.98 and 0.92. It was decided to allow V_2/V_1 and V_3/V_1 to vary over a wide range of the (100) portion of Fig. 7 (II) and to use as the criterion of best fit to the data that set of α_i's which gave the minimum square deviation $\langle\Delta^2\rangle_{\min}$ from the measured values. Figures 1 and 2 show these results with the contours labelled in units of

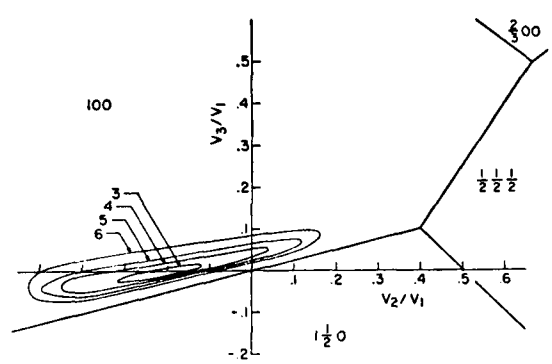

FIG. 1. Comparison of theory with the experimental short-range order parameters of Moss (Ref. 2) for Cu_3Au at 405°C. The contours are labelled in units of $10^3\ \langle\Delta^2\rangle_{\min}$.

[7] B. Borie, Acta Cryst. 14, 472 (1961).
[8] B. Borie and C. J. Sparks, Acta Cryst. (to be published).
[9] J. M. Cowley, Phys. Rev. 77, 669 (1950).
[10] M. E. Fisher and R. J. Burford, Phys. Rev. 156, 583 (1967).

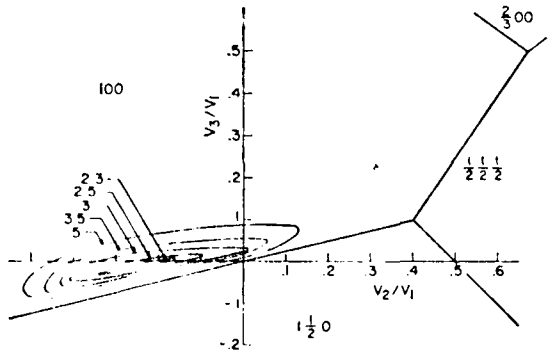

FIG. 2. Comparison of theory with the data of Moss at 450°C. In both Figs. 1 and 2 the fit rapidly becomes poor as the boundary line between the 100 and $1\frac{1}{2}0$ structures is approached.

$10^3\langle\Delta^2\rangle_{\min}$, where

$$\langle\Delta^2\rangle_{\min}=10^{-1}\sum_{i=1}^{10}[\alpha_i(\text{theory})-\alpha_i(\text{expt})]^2.$$

In both cases, the region of best agreement centers around the values $V_2/V_1=-0.20$, $V_3/V_1\approx 0$. These results are in complete disagreement with an earlier trial-and-error fit[2] of the same data to the Cowley theory,[9] and it must be concluded that, however enticing the success of the earlier fit seemed to be ($V_2/V_1=+0.10$, $V_3=0$), it was not an exact solution to the Cowley equations and was, in fact, wrong. The result $V_2/V_1=+0.10$, $V_3/V_1=0$ also violates the stability criterion for the Cu_3Au ordered structure, producing a peak at $1\frac{1}{2}0$ and not at 100. In this connection, it should be noted that Cowley's original fit of his theory to his Cu_3Au data, although much closer to our present values of $V_2/V_1=-0.20$, $V_3/V_1\approx 0.0$, was in violation of the same stability criterion, in that he found $V_2/V_1\cong-0.10$, $V_3/V_1\cong-0.05$. Since the agreement at $T_c/T=0.92$ is more to be trusted because of both the nature of the theory and the aforementioned calculation problems, the comparison at that temperature (450°C) was chosen for Table I.

The agreement can be considered quite good, although the calculated α_1 is somewhat smaller than the measured value. All of the main features of the measured α_i's are reproduced, including the very small value of α_3 and the signs and magnitudes of the other coefficients. Although the best fit seems to center around the ratios $V_2/V_1=-0.20$, $V_3/V_1=0.0$, we chose $V_2/V_1=-0.230$, $V_3/V_1=-0.015$ for Table I. The values of the α_i's do not change to the accuracy given in Table I and the reason for using these slightly different ratios will be discussed after we have presented the comparisons with CuAu and $CuAu_3$.

The other aspect of the Cu_3Au data that is most noteworthy is the pronounced disklike character of the diffuse intensity,[1] and it seemed worthwhile to see if this disk shape would be reproduced by Eq. (2.3) using the values $T_c/T=0.92$, $V_2/V_1=-0.20$, $V_3/V_1=0.0$. This direct comparison can help us decide if our neglect of higher-neighbor interactions ($V_i\cong 0$, $i>2$) is very serious. We shall also be comparing the shapes of the diffuse scattering for CuAu and $CuAu_3$, as well as for other alloys, and in all cases what we are mainly interested in is the reproduction, using a limited set of V_i, of the *major* topological features of the scattering. In many cases the comparisons will be actually with data from quenched crystals for which no fit to an equilibrium calculation is possible. Even in these instances, the major features of the diffuse intensity—where it peaks, what shape it has—can be given by the theory, the discrepancy lying mostly in the degree of sharpness in the experimental data. By making calculations of the intensity for constant values of the interaction energy ratios, but varying T_c/T, we have in fact satisfied outselves that it is indeed the sharpness, and not the characteristic shape, that changes with temperature. This fact has also been experimentally verified for rapidly quenched crystals. For example, in the case of Cu_3Au[2] the disklike intensity and the corresponding correlation functions are very similar in all particulars in the quenched and equilibrium ($T>T_c$) states. The intensity seems merely to be enhanced in the quenched state, due to a small amount of vacancy-enhanced ordering on quenching. This would indicate that the ratios V_{n+1}/V_1 are nearly constant over wide ranges of temperature in these systems.

Figures 3(a) and 3(b) show the diffuse-scattering

TABLE I. Calculated and measured short-range order parameters in the Cu-Au system.

		Cu_3Au ($T_c=390$°C) Theory: $V_2/V_1=-0.230$, $V_3/V_1=-0.015$		CuAu ($T_c=410$°C) Theory: $V_2/V_1=-0.500$, $V_3/V_1=0.200$		$CuAu_3$ ($T_c=200$°C) Theory: $V_2/V_1=-1.200$, $V_3/V_1=0.900$	
		α_i—450°C:	$T_c/T=0.92$	α_i—525°C:	$T_c/T=0.87$	α_i—250°C:	$T_c/T=0.90$
i	lmn	meas. (Moss)	Theory	meas. (Roberts)	Theory	meas. (Batterman)	Theory
1	110	−0.19	−0.17	−0.12	−0.10	−0.06	−0.06
2	200	0.21	0.20	0.00	0.13	0.20	0.16
3	211	0.00	0.01	0.00	−0.03	−0.08	−0.07
4	220	0.08	0.07	0.05	0.06	0.14	0.08
5	310	−0.05	−0.06	−0.03	−0.02	0.01	0.00
6	222	0.03	0.01	0.03	0.03	0.03	0.05
7	321	−0.01	−0.01	−0.02	−0.01	−0.04	−0.01
8	400	0.04	0.06	0.00	0.02	0.02	0.04

maps for Cu_3Au obtained by Cowley[1] at 405°C [Fig. 3(a)] and from theory [Fig. 3(b)] with $T_c/T=0.92$ (150°C), $V_2/V_1=-0.20$ and $V_3/V_1=0.0$. In a sense it is not surprising that the interaction energies that gave the best fit to the correlation functions should also fit the Fourier transform of these data, namely, the diffuse-intensity distribution. What is pleasing about the agreement in Figs. 3(a) and 3(b) is the reproduction of the disk shape with only V_1 and V_2. That this might be so could be gathered from a closer look at the plots in II (Figs. 3 and 4), but that it should in detail actually be so is gratifying. Cowley's original data were not corrected for size effect because the effect had not yet been discovered. He did, however, notice a shifting of the 300 diffuse peak off the position determined by the 200 and 400 reflections, and, attributing this to instrumental errors, he obtained Fig. 3(a) by averaging the data across the appropriate symmetry planes in reciprocal space.[11] We now know that such an averaging removes much of the size effect distortion. It was indeed fortunate that these early data were collected on a system for which the size-effect scattering, while significant, is far less important a correction than it is for CuAu or $CuAu_3$.

Note also that the diffuse intensity in Fig. 3(b) never achieves a value of zero. A plot along a ⟨100⟩ axis would make this more apparent but it is true that at any fundamental reflection including, of course, 000, the predicted diffuse scattering is never zero, nor does it reveal any discontinuities or singularities. Rather it extrapolates smoothly to some nonzero value between zero and unity, in Laue monotonic units, and the higher the temperature the closer will this limiting value be to unity.

This behavior seems to violate the known fact that for a system of fixed composition $\alpha(\mathbf{k})$ must be zero at $\mathbf{k}=0$ (or at any other Bragg position) at all temperatures. Any calculation based on a grand-canonical ensemble (such as ours) that allows the composition to vary will not reproduce this feature of $\alpha(\mathbf{k})$, and, although at first sight this appears to be a serious discrepancy between canonical and grand-canonical calculations, we shall show by a simple example that the difference is not physically significant. Consider a system of $\frac{1}{2}N$ A atoms and $\frac{1}{2}N$ B atoms. In the perfectly disordered state of the grand canonical ensemble (i.e., the high temperature limit), α_i is exactly zero except for the self correlation α_0 which is 1. Thus,

$$\alpha(\mathbf{k})_{GC}=\sum_{i=0}^{N-1}\alpha_i e^{i\mathbf{k}\cdot\mathbf{r}_i}=1 \quad \text{for all } \mathbf{k}.$$

However, for the canonical ensemble, if an A atom is at the origin, the probability of an A atom being at site i is $\frac{1}{2}[1-1/(N-1)]$ and the probability of a B atom is $\frac{1}{2}[1+1/(N-1)]$. Therefore, $\alpha_i=-1/(N-1)$ for all i except $\alpha_0=1$. Hence,

$$\alpha(\mathbf{k})_C\equiv 1+\sum_{i=1}^{N-1}\frac{-1}{N-1}e^{i\mathbf{k}\cdot\mathbf{r}_i},$$

which is equal to zero if $\mathbf{k}=0$ (or some other Bragg position), and is equal to unity otherwise. This infinitely narrow singularity in $\alpha(\mathbf{k})_C$ could never be observed experimentally and it is clear that $\alpha(\mathbf{k})_C$ differs from $\alpha(\mathbf{k})_{GC}$ only at this isolated point. We can then conjecture that, at lower temperatures, $\alpha(\mathbf{k})_C$ and $\alpha(\mathbf{k})_{GC}$ are also identical except at $\mathbf{k}=0$ because the singularity in the perfectly disordered state cannot be due to any measurable distinction between the correlations given by the grand-canonical and canonical calculations. The use of a grand-canonical ensemble eliminates considering this singularity in $\alpha(\mathbf{k})$ as part of the diffuse intensity. It is therefore apparent that it would be quite wrong to extrapolate low-angle scattering data to the value of zero at $\mathbf{k}=0$ since this result arises solely from including the singularity.

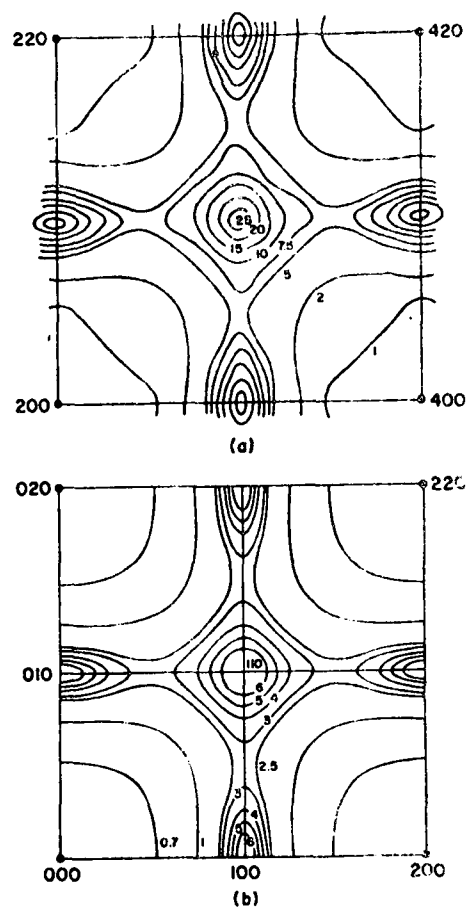

FIG. 3. (a) The Cowley (Ref. 1) diffuse-scattering map for Cu_3Au at 405°C in the h_1h_20 plane of reciprocal space. The equi-intensity contours are in arbitrary units, but are corrected for scattering factor and polarization variation. (b) Theoretical contour plot for Cu_3Au at 450°C ($T_c/T=0.92$) with $V_2/V_1=-0.20$, $V_3/V_1=0$. The intensities are in absolute units.

[11] J. M. Cowley (private communication).

Comparisons with CuAu and $CuAu_3$ are more difficult, both because of the increasing contribution of the size effect scattering and because the associated Fourier inversion will be affected in a not particularly obvious way. Therefore, it is not always clear which order parameters will be most seriously in error when the size effect has not been removed from the data. But the major features of the measured diffuse intensity are still present even in the uncorrected data, and this is certainly a place to start. In the case of CuAu, Borie[7] has shown that applying a rigorous size-effect correction to Roberts's original intensity map for a quenched crystal[3] changes the shape of the diffuse peaks at 100 and 110 from almost completely spherical to slightly disk shaped though the disklike character is not at all as pronounced as in Cowley's Cu_3Au plot [Fig. 3(a)]. We thus began by trying to reproduce Roberts's data on the quenched crystal as corrected by Borie. In the process, we hoped to obtain a set of V_2/V_1 and V_3/V_1, which, when applied to Roberts's at-temperature data, would give good agreement with the measured equilibrium short range-order parameters in this alloy.

It was found that the inclusion of a small positive value of V_3 was necessary in order to provide the slight bulging along the [100] axis that is apparent in the corrected Roberts' data of Figure 4(a). This can be appreciated by looking at Fig. 5(II), where the effect of V_3 alone is to spread the diffuse scattering out along equivalent ⟨100⟩ axes away from the {100} positions. Figure 3(b) is the calculated CuAu diffuse-intensity map for T_c/T somewhat arbitrarily set at 0.95, $V_2/V_1 = -0.400$ and $V_3/V_1 = +0.200$. Actually, V_2/V_1 could range from -0.400 to -0.600, with V_3/V_1 ranging from $+0.200$ to $+0.300$, without much altering the shapes in Fig. 4(b). It is apparent that the real difference in shape between Figs. 4(b) and 3(b) arises from raising V_2 and including an appreciable V_3. A very much wider range of interaction energy ratios around the above values could fit the short-range order parameters measured by Roberts at 525°C ($T_c/T = 0.87$) and for the purposes of comparison in Table I we chose nearly the same values as used to compute Fig. 4(b), again for reasons to be discussed later. Considering that Roberts did not make any size effect correction, and did not use an external standardization to obtain absolute intensity units, the agreement between theory and experiment for CuAu at 525°C is reasonable. Roberts's measured value of $\alpha_2 = 0.00$ is almost certainly incorrect (as he notes in his paper) and probably arises from the inclusion of the leading size effect term in the short-range order scattering. This term has the form $-8\pi h_1 \beta_1 \sin \pi h_1$, where β_1 is the usual first-neighbor size effect coefficient.[5] Its effect is to produce an extremum at the same place as the α_2 term in the short-range-order Fourier cosine series. We do not place too much faith in Roberts's order parameters, and believe that a least-square fit would be meaningless. Nonetheless, it seems clear to us that both V_2/V_1 and V_3/V_1, in the ranges quoted above, are necessary to explain the over-all results.

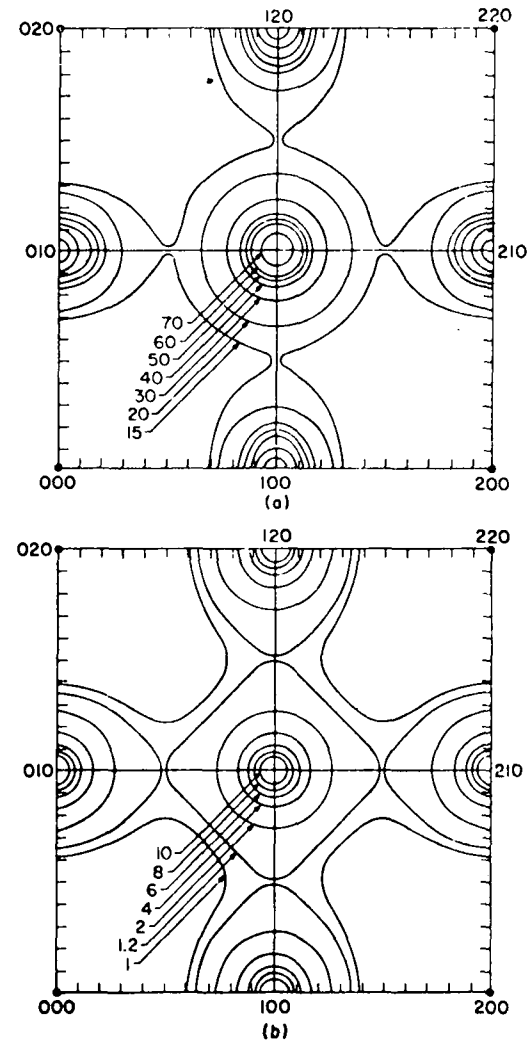

FIG. 4. (a) The experimental diffuse-scattering map for a quenched CuAu crystal. The data were taken by Roberts (Ref. 3) and corrected for the size-effect by Borie (Ref. 7). The intensity units are arbitrary, but are corrected for scattering factor and polarization variation. (b) Theoretical contour plot for CuAu with $T_c/T = 0.95$, $V_2/V_1 = -0.400$, and $V_3/V_1 = +0.200$. The intensities are in absolute units.

The difficulty in matching to the $CuAu_3$ data should, offhand, be even more pronounced, since here the size-effect scattering is the most intense, even though the actual atomic displacements may be smaller than in Cu_3Au. The data of Batterman[4] on quenched $CuAu_3$ are reproduced in Fig. 5(a), and the contribution of the size effect is very noticeable in the shifting of the centers of the diffuse maxima from the actual superlattice positions 100, 210, 300, 310, etc. There is also apparently a large Huang scattering around the 200 and 400 fundamental reflections. Batterman partially eliminated the severe size-effect distortion by calculat-

ing order parameters from intensity data averaged across the boundary plane containing the points 300, 310, and 311.

The most distinct characteristic of Fig. 5(a), other than the atom size-effect, is the egg-shaped intensity distribution. Whereas the profile from Cu_3Au is disklike and that from CuAu is more nearly spherical, $CuAu_3$ shows a disorder diffuse scattering that extends along the ⟨100⟩ axes with a seemingly spherical cross section, as evidenced by the contours around the 310 position. Neither V_1 nor V_2 will produce such a distribution, and it is essential in $CuAu_3$ to use a large positive V_3 to reproduce this feature of Fig. 5(a). By adjusting V_2/V_1 and V_3/V_1 to achieve this purpose and to give reasonable agreement with Batterman's at-temperature short-range-order parameters, we obtained the map of Fig. 5(b), with $T_c/T=0.95$, $V_2/V_1=-1.200$, and $V_3/V_1=+0.900$. Again, since the comparison is with data from a quenched crystal, the choice of $T_c/T=0.95$ is only to enhance the scattering that would be more diffuse, though similar in shape, at a higher temperature. In Table I the experimental and theoretical order parameters are compared, using the same energy ratios for $T_c/T\cong 0.90$. The agreement is fairly good, with α_2 and α_4 being the worst discrepancies; there was no set of parameters that would give any better agreement for different ratios of V_2/V_1 and V_3/V_1. The experimental results were only approximately corrected for size effect and are therefore subject to errors, again in an unknown way.

The trends in the Cu-Au system can now be examined in light of both the diffuse scattering in Figs. 3–5, and its Fourier inversion in Table I. The change in shape from disklike to egg-shaped, we believe is related to the increasing importance of V_3 with a correspondingly diminished V_1. This change is reflected in the order parameters, proceeding from Cu_3Au to CuAu to $CuAu_3$, through a decreasing α_1 and an α_3 that starts out very small, or slightly positive, and increases to a larger negative value at $CuAu_3$. The agreement in Table I is best for Cu_3Au, which is the most accurate data set and the only one for which a least-square fit to theory was possible.

It would seem that all of the grosser trends and changes with composition can be accounted for by the variation of the interaction energies, and this suggests the possibility of obtaining a pair-interaction energy plot versus interatomic distance for the Cu-Au system. Since the critical temperatures are known at all three compositions, knowing the ratios V_2/V_1 and V_3/V_1 enables us, through Eqs. (2.1) and (2.2), to calculate V_1, V_2, and V_3 as a function of composition. We shall assume that each V_i does not depend upon environment, but rather that its major dependence is upon the average interatomic distance, which is known to increase with increasing gold content. We would like the results all to lie on one smooth plot that will be conveniently labelled $V(r)/k$ versus $2r/a_0(Cu_3Au)$, where k is the Boltzmann factor, r is an interatomic distance, and $a_0(Cu_3Au)$ is the lattice parameter for disordered Cu_3Au. For Cu_3Au, V_1/k will be a point at 1.414, V_2/k at 2.000, and V_3/k at 2.450. This plot was first constructed with the same values of V_2/V_1 and V_3/V_1 used in Figs. 3–5. The trend was obvious at once, but the points were a bit scattered off a smooth curve, and a few different trials were made to bring them onto the curve in Fig. 6. The final values, as we have said, do not appreciably affect either the maps of Figs. 3–5 or the order parameters of Table I. The ratios in Table I are therefore the same as those used to draw Fig. 6.

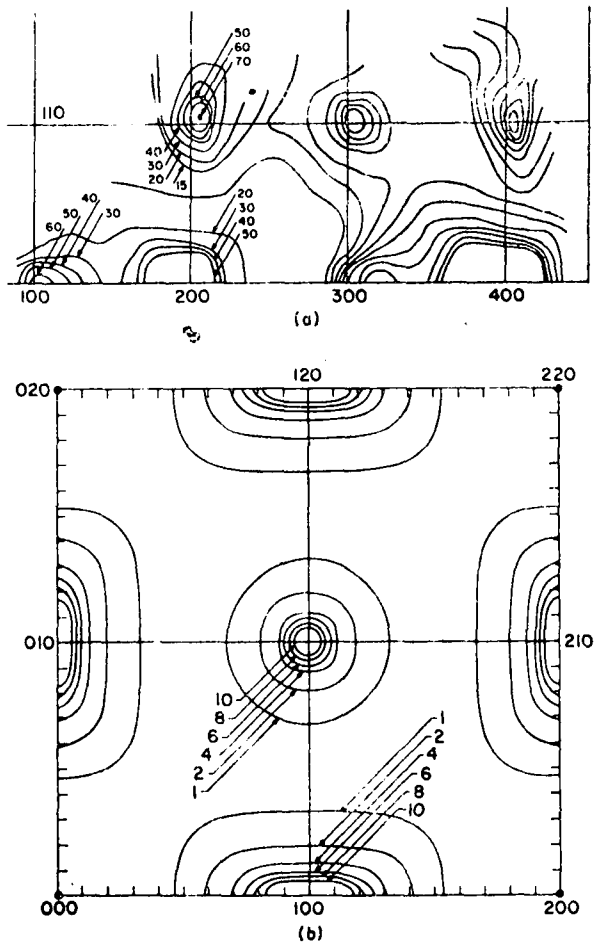

FIG. 5. (a) The experimental diffuse-scattering map for a quenched $CuAu_3$ crystal. The data were collected by Batterman (Ref. 4), and are in arbitrary units corrected for scattering factor and polarization variation. (b) Theoretical contour plot for $CuAu_3$ with $T_c/T=0.95$, $V_2/V_1=-1.200$, and $V_3/V_1=+0.900$. The intensities are in absolute units.

The curve in Fig. 6 is interesting in several ways. The nearest-neighbor portion shows a rapidly increasing V_1 as r_1 decreases with decreasing gold content. We attribute this behavior to the increasing importance of Au-Au ion-core repulsive interactions as the gold ions come closer to each other. The contribution of V_{Au-Au}

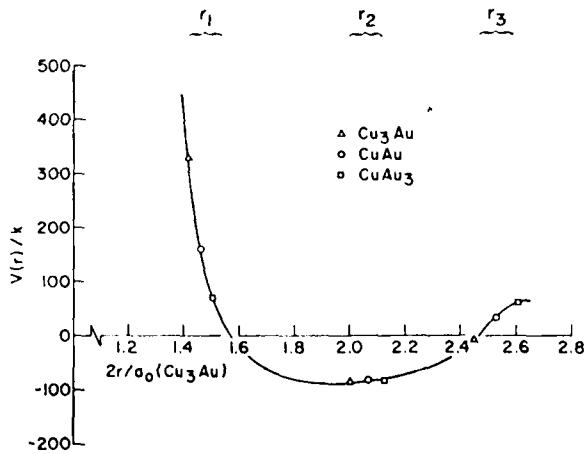

FIG. 6. Pair-interaction energy $V(r)/k$ as a function of interatomic separation $2r/a_0$ (Cu_3Au) in the copper-gold system. The variable r is thereby normalized to the lattice constant for Cu_3Au, $a_0(Cu_3Au)$.

to V_1 becomes rapidly dominant as the lattice constant, and thus the nearest-neighbor separation, decreases. This is essentially the equivalent of a strain-ordering concept, since the large positive V_1 drives the large gold atoms apart and helps to stabilize the ordered structure. As we know, however, V_1 alone will not stabilize any fcc ordered structure[12] and second (and higher) neighbors must be invoked which have little or nothing to do with ion core repulsive interactions. It would seem that the vanishing V_3 in Cu_3Au is more an accident than evidence for the unimportance of longer-range interactions. Merely by increasing slightly the interatomic separation, not only does V_1 quickly decrease, but V_3 becomes important. Without it, as we have seen, the shape of the $CuAu_3$ intensity distribution cannot be explained.

Our plot extends only to V_3 and it is difficult to imagine that all V_i ($i>3$) are negligible. If anything, speculation based on Fig. 6 would suggest that the Cu-Au system might be characterized by a long-range oscillatory interaction potential that dominates the shape of the curve beyond $V_2(r_2)$. Still, the curve was derived using only V_1, V_2, and V_3, and we would have to conclude that if many higher neighbors were included, its shape might change appreciably. In addition, since the critical temperatures of our theory are too high, the corresponding V_i's will also be too high. However, in line with the reasoning presented in II, we would expect the ratios of the interaction energies to be much more reliable.

What finally can be claimed for Fig. 6 is that it is provocative. All of the known major features of the measured diffuse intensity can be accounted for by it, and it does indicate the presence of longer-range interactions. We have certainly convinced ourselves that a quasichemical interaction that is not a function of interatomic separation is an essentially useless quantity. There is, however, one set of experimental results that suggests that the entire statistical approach, at least one such as ours, may be an insufficient description of the disordered state. Cowley[13] has discussed recently the various experimental results on split diffuse peaks in the electron and x-ray diffraction patterns from disordered Cu-Au alloys. These splittings, above T_c, strongly suggest a microdomain model for the disordered state in the vicinity of T_c. The shape and general structure of the diffuse scattering are still the same as discussed here, but our thermodynamic calculations cannot reproduce the diffuse satellites. This need not be paradoxical; it is possible that the dominant features of the scattering are given by the pairwise statistical theory, but that the more detailed atomic arrangements depend perhaps on special electronic or strain-relaxation effects that are not easily incorporated into the pair-interaction theory.

B. Cu-Pt System

The Cu-Pt system should be an especially attractive one to compare with theory. As with Cu-Au alloys, there exists a continuous fcc solid solution at high temperatures, and three prominent ordered structures, Cu_3Pt, CuPt, and $CuPt_3$ at lower temperatures.[14] The Cu_3Pt structure is similar to that of Cu_3Au but with a maximum in T_c displaced off stoichiometry to 20 at.% Pt. CuPt has the $L1_1$ structure consisting of alternating (111) planes of Cu and Pt atoms, which is interesting because each Cu has six nearest Cu neighbors in the (111) plane and six nearest Pt neighbors in the parallel adjacent planes, with three above and three below. $CuPt_3$ is thought to be the same as CuPt but with an ordering of the excess Pt atoms.[15] Whereas in the Cu-Au system all three ordered structures are characterized by superlattice peaks [or $V(\mathbf{k}_M)$] at 100, 110, etc., in the Cu-Pt alloys, as the Pt content increases, the minimum in $V(\mathbf{k})$ shifts from 100 to $\frac{1}{2}\frac{1}{2}\frac{1}{2}$. Actually, CuPt is not a cubic structure, even aside from the rhombohedral contraction that occurs on ordering the (111) planes, because all ⟨111⟩ directions in a unit cell are not equivalent. But, as with CuAu, it invariably shows pseudocubic symmetry because of the presence of the four ⟨111⟩ directions along which it can chose to order with equal probability.

The only existing diffuse scattering data on the Cu-Pt alloys are the studies of Walker[16] on CuPt and Kaplow[17] on a series of other compositions at various temperatures. Both studies were done using powder samples, and there is therefore no reciprocal lattice map of the

[12] P. C. Clapp, Phys. Rev. Letters 16, 687 (1966).

[13] J. M. Cowley, J. Australian Inst. Metals 11, 258 (1966).

[14] M. Hansen, *Constitution of Binary Alloys* (McGraw-Hill Book Co., New York, 1958) 2nd ed.

[15] Y. C. Tang, Acta Cryst. 4, 377 (1951).

[16] C. B. Walker, J. Appl. Phys. 23, 118 (1952).

[17] Roy Kaplow, Ph.D. thesis, Department of Metallurgy, Massachusetts Institute of Technology, 1958 (unpublished).

diffuse intensity distribution. If the powder data were extensive and accurate enough, such a map could be reconstructed from the measured α_i's. But powder data, except under extraordinary circumstances, are never really too accurate, being contaminated by thermal-diffuse, size effect, Huang, and Compton scattering, all of which are averaged over the powder-pattern sphere. We shall thus not attempt an elaborate analysis of the Cu Pt data. We shall largely restrict our attention to CuPt and invoke only V_2/V_1 and the temperature ratio T_c/T. This is not because we have any reason to believe that higher-neighbor interactions are not present, but because we prefer to extract qualitative conclusions using the fewest assumptions. When better single-crystal data are available we would expect that some of these simpler conclusions might be modified.

By requiring that $V(\mathbf{k}_M)$ be at $\frac{1}{2}\frac{1}{2}\frac{1}{2}$, the critical temperature for the CuPt structure can be written as

$$T_c = 3V_2/k, \tag{2.4}$$

which includes interactions out to third neighbors. Neither V_1 nor V_3 has any effect on T_c; rather, they affect only the question of stability of the CuPt structure and the shape of $\alpha(\mathbf{k})$. In the fully ordered condition, the planar structure of CuPt has a set of α_i which oscillate as i proceeds from one in the manner $\alpha_1=0$, $\alpha_2=-1.000$, $\alpha_3=0$, $\alpha_4=+1.000$, etc. All odd shells have zero α_i and the even shells oscillate -1.000, $+1.000$, -1.000, $\cdots$. The vanishings, especially of α_1, have led workers to suspect (i) that V_1 is negligible, (ii) that there is a separate in-plane and out-of-plane interaction. Neither of these considerations seems proper to us although, with regard to the latter, if there is a [111] contraction, nearest neighbors in adjacent planes will be slightly closer than those within the plane. The preference for unlike first neighbors may thereby be enhanced and the energy lowered.

The CuPt structure has an ordering temperature of about 815°C above which it is statistically fcc with local atomic arrangements characteristic of the ordered structure.[16] The powder-diffuse measurements of Walker by necessity gave only rough estimates of the pair correlations, and were conducted at a temperature of 890°C as well as on a quenched sample. Our comparison will be with the 890°C data ($T_c/T\cong 0.94$). We have chosen $T_c/T=0.95$, and have run sets for several different ratios of V_2/V_1 in the positive quadrant of Fig. 6 (II) from $+0.600$ to $+20.000$. The tendency in Table II is quickly to reach limiting values for the even-shell parameters, which are in agreement with Walker's set of measured coefficients. The odd-shell-order parameters are appreciable at $V_2/V_1=+0.600$ and fall off to zero as this ratio increases. Walker's conclusion was that these latter parameters were essentially zero as they are in the ordered state, and that above T_c the local order was very similar [(111) layering] to that below T_c. The theoretical calculations indicate that this becomes truer as V_2 takes on greater values relative to V_1. We would thus suggest that many of the known features of the local order in CuPt can be reproduced using only V_1 and V_2, and that a fairly large relative contribution of V_2 is necessary to yield very small magnitudes of the even-shell parameters.

The data of Kaplow should be more accurate than Walker's although it is restricted to compositions other than CuPt, because a size-effect estimate was included. His results were for alloys ranging from 4 to 43 at.% Pt, and showed anomalies that, if real, cannot easily be explained solely on the basis of V_1 and V_2. At 43 at.% Pt, the first seven α_i's of Kaplow are quite similar to the Walker results on CuPt, namely, very small odd-shell parameters with larger even-shell parameters that oscillate in sign. But the dependence with temperature suggests that neither α_2 nor α_4 changes as the temperature is raised increasingly above T_c. The parameters at 24 at.% Pt cannot really be understood in terms of the Cu_3Au structure (or the $1\frac{1}{2}0$ Ni_3V structure), since the negative α_1 is larger in magnitude than the positive α_2. While α_3 is very small and positive (reminiscent of Cu_3Au, albeit accidentally) the largest measured α_i is $\alpha_4\cong\pm 0.14$ at $T_c/T=0.95$, and this value appears to increase as T_c/T decreases to 0.90. It is quite possible that higher-neighbor interactions are important, and our understanding should probably wait on more accurate single-crystal analyses. In addition, a very recent study of copper activities in Cu-Pt alloys indicates that the ordering reactions around Cu_3Pt are much more

TABLE II. Calculated and measured short-range order parameters in the alloy CuPt.

		α_i		α_i from theory, $T_c/T=0.95$						
i	lmn	perfect order	meas. ($T_c/T=0.94$) by Walker	V_2/V_1 0.60	0.80	1.00	3.00	6.00	10.00	20.00
1	110	0	~0	−0.13	−0.09	−0.07	−0.02	−0.01	−0.01	0.00
2	200	−1.00	−0.20±0.06	−0.18	−0.21	−0.22	−0.24	−0.24	−0.24	−0.24
3	211	0	~0	0.07	0.05	0.03	0.01	0.00	0.00	0.00
4	220	+1.00	+0.12±0.05	0.06	0.09	0.10	0.11	0.11	0.11	0.11
5	310	0	~0	0.03	0.03	0.02	0.01	0.01	0.00	0.00
6	222	−1.00	−0.06±0.03	−0.08	−0.07	−0.07	−0.07	−0.07	−0.07	−0.07
7	321	0	···	−0.04	−0.03	−0.02	−0.01	0.00	0.00	0.00
8	400	+1.00	···	0.03	0.05	0.06	0.07	0.07	0.07	0.07

complex than had been thought.[18] There apparently is a second higher-temperature transformation involving an as yet unknown structure that is tentatively identified by the authors as a possible periodic antiphase domain structure.

It is with a sense of somewhat wanton speculation that we suggest that the Cu-Pt alloy system may be characterized by a longer-range oscillatory interaction. At the larger interatomic separation of CuPt, V_2 may lie near the top of the first positive oscillation (where V_3 is in Fig. 6 for $CuAu_3$) and V_1 may be essentially zero—either very small negative or positive. As the spacing decreases, with decreasing Pt content, it would then be possible to diminish V_2 while V_1 rapidly increases, and the Cu_3Au structure would take over when V_2 becomes negative. This premise demands, if only V_1 and V_2 are included, that the Ni_3V structure be an intermediate phase between CuPt and Cu_3Pt. If higher-neighbor interactions are important this need not be the case.

There have been other studies of the importance of higher-neighbor interactions (other than V_1) in the Cu-Pt system, most notably those of Fournet[19] and of Hirone and Adachi.[20] The former restricted his attention to the composition CuPt and, using a method based on the theory of Yvon,[21] extracted V_1 and V_2 from Walker's measurements of long-range order in this alloy. Fournet obtained a ratio of 1.67 for V_2/V_1 and, from Table II, we can see that at this ratio the odd-shell parameters are small and the even-shell parameters are close to their limiting values. Using this ratio, Fournet was also able to calculate $\alpha(\mathbf{k})$ for a powder sample, and he obtained fair agreement with Walker's measured powder-diffuse scattering. Hirone and Adachi use a Bragg-Williams method, but incorporate both V_1 and V_2 and allow for the composition dependence of the interaction energies. From observations based on the structures and critical temperatures of the various ordered phases, these authors solved for the ratio V_2/V_1 at CuPt, estimating a value of about 3.00, again consistent with the results in Table II. There was no treatment of correlations in the disordered phase, but there was an interesting discussion of the possible origination of a longer range electronic interaction in the Cu-Pt alloys. This was based on Mott's polar model for alloys[22] and predates, in a qualitative way, the more recent calculations of Harrison and Paskin,[23] to be discussed later in Sec. 3.

[18] L. R. Bidwell, W. J. Schulz, and R. K. Saxer, Acta Met. 15, 1143 (1967).
[19] G. Fournet, Compt. Rend. 235, 1377 (1952).
[20] T. Hirone and K. Adachi, Sci. Rep. Res. Inst. Tohoku Univ. Ser. A, 7, 282 (1955).
[21] J. Yvon, Cahiers Phys. 28, 1 (1945).
[22] N. F. Mott, Proc. Phys. Soc. (London) 49, 258 (1937).
[23] R. J. Harrison and A. Paskin, J. Phys. Radium 23, 613 (1962).

C. Au_3Mn

The alloy Au_3Mn has a critical temperature of approximately 645°C, above which it is statistically fcc. Below T_c it has the Ni_3V structure (DO_{22}) with a tetragonal unit cell ($c/a \approx 2$) composed of two cubic cells of the Cu_3Au structure shifted with respect to each other on the (001) boundary plane by an amount $\frac{1}{2}\mathbf{a}_1+\frac{1}{2}\mathbf{a}_2$, where $\mathbf{a}_3$ is the c axis. It is often referred to as a "long period" superlattice of the Cu_3Au structure with a repeat distance $2M$ equal to two. The notation for this representation is $L1_2(M=1)$. As was discussed in II, the ordered lattice has sets of superlattice peaks at all the Cu_3Au positions as well as at $1\frac{1}{2}0$ and equivalent points, and it shows pseudocubic symmetry because the tetragonality can proceed equally along the $\mathbf{a}_1$, $\mathbf{a}_2$, or $\mathbf{a}_3$ axes of the disordered phase. The diffraction pattern is then characteristic either of a cubic averaging of the DO_{22} structure or of the $L1_2$ structure with the sharp satellites at $1\frac{1}{2}0$ arising from the occurrence of $M=1$ antiphase domains with equal probability along the three cube directions.

For our purposes we would like to phrase the problem in somewhat different terms. Above T_c, with $V_i(i>2)=0$, $V(\mathbf{k}_M)$ occurs at $1\frac{1}{2}0$ for the range $0<V_2/V_1<0.500$. As T_c is approached, the diffuse-scattering maxima at $1\frac{1}{2}0$ will become sharper until, finally, ordering takes place at T_c. For an A_3B alloy, with an interaction energy ratio between 0 and 0.500, the lowest-energy ordered structure proposed to date is DO_{22} [or $L1_2(M=1)$], and this structure has superlattice peaks at 100, 110, etc., as well as at $1\frac{1}{2}0$. Put this way, the discussion of Au_3Mn emphasizes a central point of our approach: It is to the disordered alloy that we look for information about the relative strengths of the interaction energies, with the restriction that this information be consistent with the known ordered structure below T_c. In the case of a $1\frac{1}{2}0$ peak in $\alpha(\mathbf{k})$, the simplest corresponding ordered structure at A_3B is DO_{22}, but we do not claim uniqueness for this correspondence. Although we know of no actual AB structure that orders with a $1\frac{1}{2}0$ superlattice peak, the correspondence at that composition would be unique, namely, both disordered and ordered phases have peaks only at $1\frac{1}{2}0$.

There is, of course, much more available data on the diffraction patterns from ordered alloys than on the diffuse scattering from the associated disordered phases. Au_3Mn, with T_c at ~645°C, seemed an ideal choice since the diffuse scattering above T_c can be measured (the difference in scattering amplitude, for x rays and electrons, of the two metals is large). Tanner has recently made such a measurement of the electron-diffraction pattern from thin (001) single-crystal foils of Au_3Mn.[24] His study was conducted using the hot stage of an electron microscope, and the temperature

[24] L. Tanner, Tech. Note No. 33, Ledgemont Laboratory, Kennecott Copper Corp., 1967 (unpublished).

calibration was very rough, i.e., T_c was defined by the disappearance of the sharp superlattice spots.

We are interested mainly in the shape of the diffuse scattering in the h_1h_20 plane of reciprocal space. The comparison between theory and experiment will be too qualitative to warrant the use of more than V_1 and V_2, and for this case the T_c, for $V(\mathbf{k}_M)$ at $1\frac{1}{2}0$, is given by

$$T_c=(3/2k)V_1(1-\tfrac{1}{2}V_2/V_1\cdots), \qquad (2.5)$$

where $V(\mathbf{k}_M)=V_1(-4+2V_2/V_1\cdots)$. Equation (2.3) was solved for $\alpha(\mathbf{k})$ for various values of V_2/V_1 in the range $0<V_2/V_1<0.500$. Figure 7 shows Tanner's electron-diffraction pattern from Au_3Mn at $T>T_c$. It has been over exposed to reveal the diffuse scattering more effectively, and it is apparent that this scattering is centered not on {100} or {110} but on $\{1\frac{1}{2}0\}$ positions. The intensity shows the usual cubic symmetry (distorted somewhat by size effect), and is elongated along lines between {100} and {110}. These diffuse "cigars" at $1\frac{1}{2}0$ can be reproduced qualitatively using a small value of $V_2/V_1=0.08$, with $T_c/T=0.95$, for which the calculated diffuse-intensity distribution is shown in Fig. 8. It is difficult to say how good the agreement is; certainly both reveal elongated diffuse maxima at $\{1\frac{1}{2}0\}$. Reducing V_2/V_1 enhances the elongation, while increasing this ratio produces a more spherical (actually shieldlike or triangular) shape at $(1,\frac{1}{2},0)$. As with the Cu Au alloys, reducing T_c/T does not change the shape, but changes just the sharpness of the peak.

Au_3Mn would be an ideal candidate for an accurate diffuse x-ray scattering study. The details of the intensity distribution would be very sensitive to higher-neighbor interactions and to the presence of any local tetragonality in the disordered state. For now, it would seem that the qualitative agreement between the theory and Tanner's results establishes roughly the relative magnitude of V_2 (it is probably small compared to V_1),

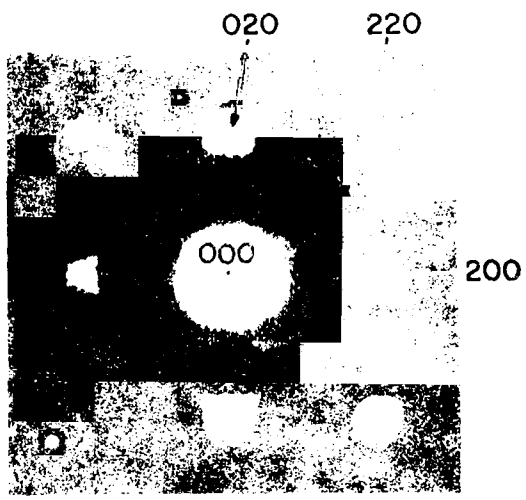

FIG. 7. Electron-diffraction pattern from Au_3Mn above T_c taken by Tanner (Ref. 24). The photograph has been overexposed to emphasize the elongated diffuse maxima at the $\{1\frac{1}{2}0\}$ positions.

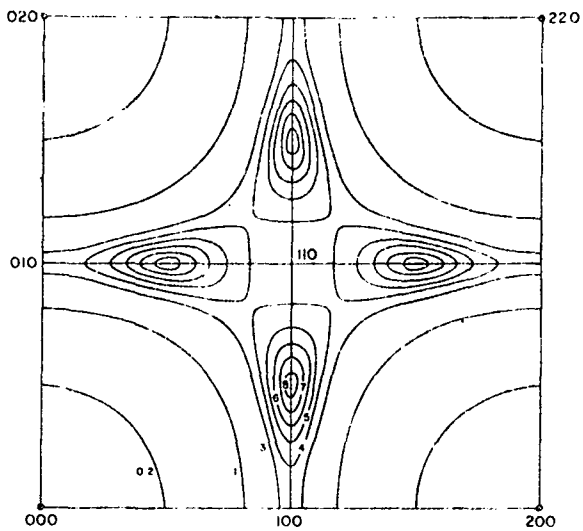

FIG. 8. Theoretical diffuse-scattering map for Au_3Mn with $T_c/T=0.95$ and $V_2/V_1=+0.080$. The intensities are in absolute units.

corroborates the prediction of the disappearance of the 100 and 110 intensity above T_c, and is consistent with the stabilization criterion for the ordered structure.

D. Ni_4Mo

We have chosen Ni_4Mo to compare with theory because of the recent x-ray study of short-range order in a single crystal of this alloy.[25] Ni_4Mo has a more complicated ordered structure[26] than the fcc alloys previously discussed, but the unlabelled atomic arrangement is very close to cubic close packing. All the nickel atoms are crystallographically equivalent, as are all molybdenums. The 12 nearest neighbors of a molybdenum atom are all nickel atoms, and this implies a positive V_1. Of the six second neighbors of Mo, four are unlike and two are like, implying a positive V_2 as well, with the complication that the two like-neighbors are slightly closer than the four unlike ones.

There are many other interesting features of the Ni_4Mo structure. It is body-centered tetragonal (bct) with two formula units per cell, and it can form in 30 distinct, albeit crystallographically equivalent, ways from the disordered fcc phase. Upon ordering, there is a small contraction along the c axis of the bct cell which brings the two like Mo second neighbors along the c axis closer together than the four nickel second neighbors off this axis.

The reciprocal lattice of ordered Ni_4Mo has superstructure reflections arranged in groups of four about the positions $1\frac{1}{2}0$ of the fcc reciprocal lattice. There is therefore no set of superlattice points that are equivalent in the ordered and disordered phases, and this

[25] J. L. Spruiell and E. E. Stansbury, J. Phys. Chem. Solids 26, 811 (1965).
[26] D. Harker, J. Chem. Phys. 12, 315 (1944).

fact makes it difficult to generate predictions of the diffuse scattering from considerations of the ordered structure alone. The discussion here will thus be an attempt to rationalize our preliminary conclusions, based on the diffuse-scattering experiments, with the known ordered structure.

Figure 9 is a reproduction of Fig. 1 from the Spruiell and Stansbury paper.[25] Their Ni_4Mo crystal was rapidly quenched in iced brine from 1000°C, where $T_c \approx 865$°C, and the resulting diffuse-scattering contours are in units of $100 \times \alpha(\mathbf{k})$. Since the ordering reaction is sluggish, the quench probably retains the qualitative aspects of the equilibrium atomic arrangements, with only a slight enhancement of local order taking place. Figure 9 has not been corrected for size-effect scattering, as is apparent from the slight asymmetry in the contours, viz., the intensity is greater at 210 than at 100. The most prominent feature of Fig. 9 is the concentration of intensity in nearly circular contours about the $\{1\frac{1}{2}0\}$ positions. The outer contours are slightly elongated toward 100, 210, etc., and are a bit flattened around 110, so that at 110 the shape of the diffuse scattering is also almost circular.

Figure 9 so obviously indicates a $V(\mathbf{k}_M)$ at $1\frac{1}{2}0$ with $0 < V_2/V_1 < 0.500$, that the corresponding theoretical comparison was made with only V_1 and V_2. As noted in the previous section, as V_2/V_1 increases, the intensity becomes more spherical around $1\frac{1}{2}0$. We calculated intensities using a few different ratios, with T_c/T set at 0.95, until Fig. 9 could be reasonably well reproduced. The final choice, for $V_2/V_1 = 0.300$, is in Fig. 10. We find the agreement satisfactory, and tend to attribute the differences largely to size effect and to the necessity of comparing theory with the scattering from a quenched sample.

It seems that the Ni_4Mo diffuse scattering can be accounted for using just V_2 and V_1, both of the same sign. This result is consistent with, although not predictable from, the ordered structure. The quenched sample apparently has atomic arrangements characteristic of the disordered phase which have been preserved on quenching because on annealing the Ni_4Mo crystal within the ordered region, the diffuse-scattering distribution changes. It begins to flatten out perpendicular to reciprocal lattice lines of the kind $\{1h_20\}$ (Fig. 3 of Ref. 25), and, with increased annealing, diffuse satellites appear at positions identical to the superlattice reflections in the ordered phase, namely, at $\frac{4}{5}\,\frac{1}{2}0$, $6/5\,\frac{1}{2}0$, and all equivalent positions given by the translational symmetry of the disordered reciprocal lattice. As the ordering proceeds, these satellites sharpen into the superlattice spots. This clear distinction in the diffraction patterns from the partially ordered and disordered alloys leads us to believe, in contrast with the appreciable literature on the Cu-Au alloys, that in Ni_4Mo the locally ordered state above T_c is well described by the statistical theory, and that a micro-

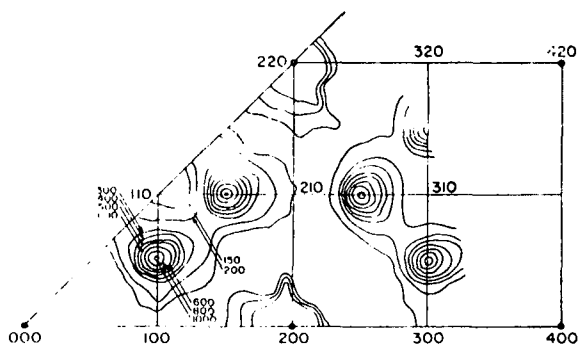

FIG. 9. The diffuse-scattering map for a quenched Ni_4Mo crystal studied by Spruiell and Stansbury (Ref. 25). The contours are in absolute units multiplied by 100, and the data are not corrected for the size effect.

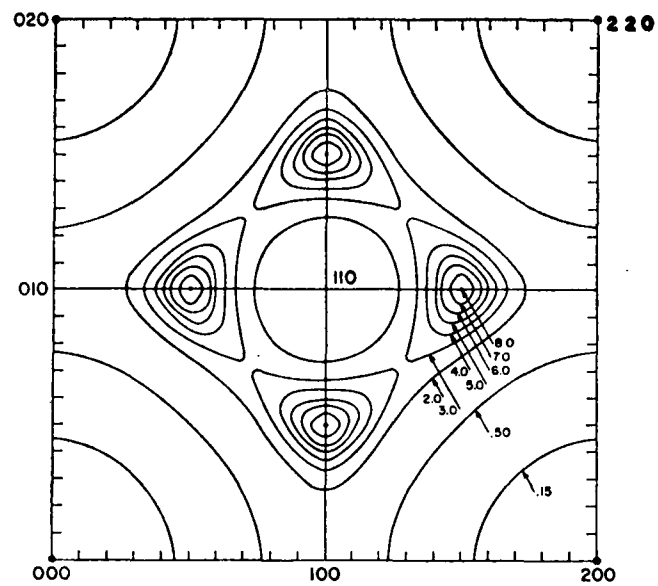

FIG. 10. Theoretical contour map, in absolute intensity units, for Ni_4Mo with $T_c/T = 0.95$ and $V_2/V_1 = +0.300$.

domain theory of short-range order is not a particularly useful concept here.

E. Clustering in CuNi

All of our theoretical calculations have thus far been on ordering alloys that show a preference for unlike nearest neighbors above T_c. Exactly the same formalism can be applied to clustering systems that will have a maximum in $\alpha(\mathbf{k})$, or minimum in $V(\mathbf{k})$, at 000 that sharpens as the critical temperature for phase separation is approached in exact analogy with ferromagnetic critical scattering. For an AB alloy, the critical temperature can be expressed as

$$T_c = (-6V_1/k)(1 + \tfrac{1}{2}V_2/V_1 + 2V_3/V_1 + \cdots).$$

T_c is the temperature below which the solid binary alloy is unstable with respect to infinitesimal composition

fluctuations and begins to phase-separate or unmix. This is also the definition of the coherent spinodal,[27] and the two are the same. The usual treatment of spinodal decomposition is in terms of macroscopic thermodynamic quantities and the kinetics of the process. As in previous sections, however, we shall be concerned here mainly with the correlation functions above T_c.

The evidence for clustering in Cu-Ni alloys has been summarized by Rapp and Maak,[28] who performed the most recent thermodynamic study on this system. By extrapolation of the best available data, they calculated a maximum in the predicted miscibility gap of about 300°C. Below ~300°C (at around 0.7–0.8 at. fract. Ni) phase separation should occur. At exactly the CuNi composition, T_c should be somewhat lower. Very recently, Mozer, Keating, and Moss[29] have studied the diffuse scattering of thermal neutrons from a polycrystalline sample of $Cu_{0.52}Ni_{0.48}$. The results of the neutron investigation of this alloy show that clustering above T_c is indeed observable and that a reliable set of $\alpha(r)$ can be extracted by a least-squares fit directly to the corrected intensity data. The experiment was actually a textbook example of cluster scattering from a powder sample because a null-matrix alloy was used, from which the Bragg intensity and associated thermal-diffuse and Huang scattering were negligible. For all details of the experiment, the reader is referred to the original paper.

The most striking aspect of the experimental short-range order parameters in Table III is the large value of $\alpha_1 = +0.121$ compared to the much smaller values of the other coefficients, all of which are about 10% or less of α_1. The reason for this behavior turns out to be the competition between a negative V_1 and a smaller positive V_2. Since a second neighbor of an origin atom shares four first neighbors with that origin, the change in sign of the interaction energy can bring the second-neighboring occupancy to nearly the random value, and this effect propagates to higher neighbors. By choosing ratios of V_2/V_1 from -1.000 to $+20.000$, Mozer, Keating, and Moss solved Eq. (2.3) for a range of clustering systems in Fig. 6 (II) and for various values of T_c/T, and the calculated α_i were compared with experiment. If $V_2/V_1 \geq 0$, all α_i were positive, thus ruling out that range. The best fit was for $-0.500 \leq V_2/V_1 \geq -0.650$, with T_c/T between 0.70 and 0.75, and a sample comparison from Ref. 29 at $V_2/V_1 = -0.600$ is included in Table III.

The temperature T at which the theory was applied was around 550°C and with $T_c/T = 0.725$, T_c was calculated to be ~325°C. Since the mean-field critical temperatures are all too high, the authors in Ref. 29 chose to place T_c closer to 250°C, in reasonable agreement with the extrapolation of the thermodynamic data.

TABLE III. Calculated and measured short-range order parameters in the alloy CuNi[a]

		α_i		
i	lmn	Perfect clustering	Expt. at ~550°C	Theory: $T_c/T \cong 0.725$ $V_2/V_1 = -0.600$
1	110	1.000	0.121	0.120
2	200	1.000	−0.008	−0.009
3	211	1.000	0.011	0.018
4	220	1.000	0.012	0.018
5	310	1.000	−0.003	−0.003
6	222	1.000	−0.003	0.004
7	321	1.000	0.002	0.003
8	400	1.000	0.005	−0.001

[a] Reference 29.

Because the neutron experiment gave such "clean" results, the derived α_i's should be reliable and the agreement in Table III for both sign and magnitude of the order parameters was considered to be good.

3. bcc ALLOYS

Few detailed studies have been made of the short-range order in bcc alloys other than β-CuZn. Walker and Keating[30] have done extensive neutron-diffraction measurements on this system at several temperatures above the ordering temperature, and more recently Als-Nielsen and Dietrich[31] have made extremely accurate neutron measurements of the short-range-order peak shape at temperatures just above the ordering temperature. This latter work has shown close agreement with the theoretical expression of Fisher and Burford,[10] and would seem to imply that the ordering processes in β-brass are well described by an Ising model employing only nearest-neighbor interactions. However, Harrison and Paskin (HP)[28] have provided theoretical reasons for expecting long-range oscillatory interactions to be significant in this system based on Mott's "polar model" of an alloy. Their work raises the question of whether such long-range forces can be detected from the ordering behavior of β-CuZn.

Paskin[32] has already considered the problem by calculating theoretically the first 40 α_i's at 10% above the ordering temperature for a nearest-neighbor interaction and for the long-range oscillatory interaction given by

$$V(r) = A[\cos(2k_f r + \phi)]/r^3,$$

where k_f is the Fermi momentum, and A and ϕ are adjustable parameters. He used a linearized form of Cowley's equations, which is identical to our expression, to perform the calculations, and arrived at the conclusion that there are significant differences in the two sets of α_i's only for high-order α_i's. Since these are very

[27] J. W. Cahn, Acta Met. 9, 795 (1961).
[28] R. A. Rapp and F. Maak, Acta Met. 10, 63 (1962).
[29] B. Mozer, D. T. Keating and S. C. Moss, Phys. Rev. (to be published).
[30] C. B. Walker and D. T. Keating, Phys. Rev. 130, 1726 (1963).
[31] J. Als-Nielsen and O. W. Dietrich, Phys. Rev. 153, 706 (1967); O. W. Dietrich and J. Als-Nielsen, *ibid.* 153, 711 (1967).
[32] A. Paskin, Phys. Rev. 134, A246 (1964).

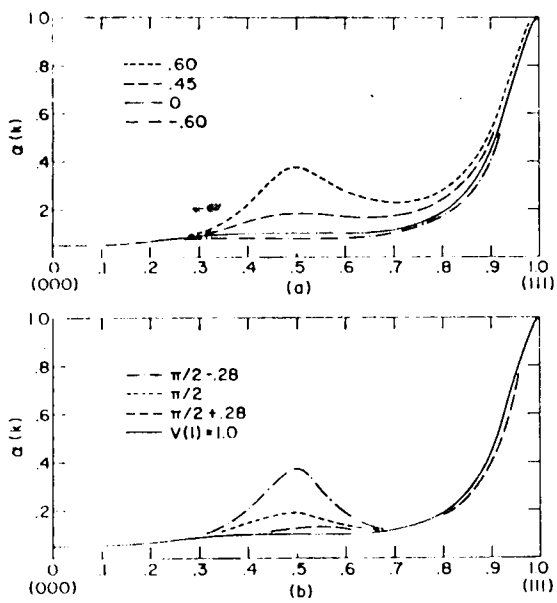

FIG. 11. Theoretical diffuse-scattering profiles for β-brass along a $\langle 111 \rangle$ direction. All cases have been normalized to $\alpha(111)=1.0$. (a) V_1 and V_2 along for several values of the ratio V_2/V_1. (b) A long range oscillatory interaction potential with the indicated choices for the phase factor ϕ compared with a curve for V_1 alone.

difficult to measure with any accuracy, he concluded that long-range oscillatory forces of the type proposed could not be detected experimentally.

We have performed a similar calculation, but have calculated $\alpha(\mathbf{k})$ rather than the α_i's and find that the situation is perhaps not so hopeless as Paskin suggests. Our results for $\alpha(\mathbf{k})$ along a [111] direction are shown in Fig. 11. Three cases have been considered: V_1 alone, V_1 and V_2 alone, and the HP long-range oscillatory potential.

Two of the three values of the phase factor ϕ used here are those that Paskin suggests are the most appropriate for CuZn ($\frac{1}{2}\pi$, $\frac{1}{2}\pi-0.28$). The value of A is immaterial, because it cancels out when Eq. (2.3) is used to calculate $\alpha(\mathbf{k})$. We have truncated $V(r)$ after 20 neighbors in performing these calculations, and all the resulting curves have been scaled to make $\alpha(\mathbf{k})=1.0$ at 111. As is apparent from the figure, a distinct secondary-diffuse peak appears at the $\frac{1}{2}\frac{1}{2}\frac{1}{2}$ position for certain values of the relevant parameters, and careful intensity measurements in this region of reciprocal space should provide a reasonably sensitive test for the presence of higher-neighbor interactions. Although Walker and Keating did make measurements in this region, the measurements were made too rapidly (to avoid the loss of excessive amounts of Zn) to obtain accurate points, so that any details that may have been present were washed out. Consequently, a neutron experiment designed to collect accurate data in the $\frac{1}{2}\frac{1}{2}\frac{1}{2}$ region remains to be done and would appear to be highly desirable. It should be mentioned, however, that in a recent summary of the application of Yvon's theory to binary alloy data, Fournet suggests a ratio of $V_2/V_1=\frac{1}{3}$ for β-brass,[33] based on the measurement by Chipman and Warren[34] of long-range order. Our calculations indicate that this ratio would not produce a measurable peak at $\frac{1}{2}\frac{1}{2}\frac{1}{2}$ and that a ratio in excess of 0.40 is required if only V_1 and V_2 are included.

We have also made calculations of $\alpha(\mathbf{k})$ in the [100] and [110] directions away from the 111 peak and find no appreciable difference between the three cases. As a consequence we have inferred that $\alpha(\mathbf{k})$ is insensitive to the presence of longer-range interactions, except in the neighborhood of the $\frac{1}{2}\frac{1}{2}\frac{1}{2}$ point. This would indicate why the lower-order α_i's do not differ significantly when the range of interaction is increased, and provides a clear case where the diffuse intensity, rather than its Fourier transform, should be studied in order to extract the maximum amount of information about the pair interactions in the alloy.

It is significant that the secondary-diffuse peak occurs at the same position as the superlattice spot for the B32 or NaTl structure (see Figs. 10 and 11, part II). This implies that the energy of the B32 structure is approaching that of the $L2_0$ or β-CuZn structure, and, in fact, if V_2/V_1 had been chosen to be $\frac{2}{3}$ (corresponding to the boundary of the two structures in Fig. 10, part II) the peak at $\frac{1}{2}\frac{1}{2}\frac{1}{2}$ would also have had a value of 1.0. This also occurs if ϕ is chosen to be $(\frac{1}{2}\pi-0.3)$, which represents a lower bound for ϕ in order that $L2_0$ structure be the stable low-temperature form.

4. SUMMARY AND CONCLUSIONS

In the present paper, part III, we have applied the theory of parts I and II to diffraction data on alloys above T_c. This has enabled us to evaluate the importance of interactions beyond nearest neighbors, a feature not readily available to the more exact thermodynamic expressions. The results on the Cu-Au system indicate the presence of a long-range interaction potential which must extend at least to third neighbors in order to explain the x-ray diffuse scattering. This interaction also appears to be oscillatory in nature: positive and rapidly varying in the region of the nearest neighbors, negative at second neighbors, and turning positive again at the third-neighbor distances.

For the Cu-Pt system, we get good agreement with the data of Walker at the CuPt composition, which means a ratio V_2/V_1 in excess of ~ 1.00. In the case of Au_3Mn, predictions based on the ordered structure would require diffuse peaks at $1\frac{1}{2}0$ above T_c with V_2/V_1 between 0.0 and 0.500. Reasonable agreement is obtained with the electron diffraction result of Tanner by using $V_2/V_1 \cong 0.08$. The disappearance, above T_c, of

[33] G. Fournet, in *Phase Stability in Metals and Alloys*, edited by P. S. Rudman, J. Stringer, and R. I. Jaffee (McGraw-Hill Book Co., New York, 1967).

[34] D. Chipman and B. E. Warren, J. Appl. Phys. 21, 696 (1950).

diffuse intensity at the ordered superlattice points of 100, 110, etc., is also confirmed.

The diffuse scattering data of Spruiell and Stansbury on Ni_4Mo is well reproduced by the theory by setting $V_2/V_1=0.300$. This ratio, while not predictable from the ordered structure, is consistent with it. In addition, for completeness, the recent results of Mozer, Keating, and Moss on CuNi are briefly summarized, where it is shown that the theory applies as well to clustering systems as it does to ordering ones.

Finally, the case for a long-range oscillatory interaction in β brass is reexamined. We show that only at the $\frac{1}{2}\frac{1}{2}\frac{1}{2}$ position in reciprocal space will the effect of an interaction beyond V_1 be remarkable. It is thus suggested that very careful neutron-scattering data be collected above T_c at that position in order to test for the presence of longer-range interactions.

We hope by these papers to have demonstrated the usefulness of an approximate theory in generating some interesting information on the pair interactions in a variety of binary alloys. As the techniques for incorporating longer-range interactions into the more exact theories are developed, these will in turn demand more exacting data on binary alloys. It is thus our further hope that a systematic collection of such data will be forthcoming.

J. Phys. Chem. Solids Pergamon Press 1969. Vol. 30, pp. 2589–2598 Printed in Great Britain.

THEORETICAL DETERMINATION OF n-SITE CONFIGURATION PROBABILITIES FROM PAIR CORRELATIONS IN BINARY LATTICES

PHILIP C. CLAPP
Ledgemont Laboratory, Kennecott Copper Corporation, Lexington, Mass. 02173, U.S.A.

(*Received* 5 *February* 1969)

Abstract—A new variational method is presented for determining configuration probabilities of three or more sites in partially ordered binary lattices from pair correlation data. The method is tested for several cases where the exact solution is known by independent means, and it is shown to yield the correct result in each case. It is suggested but not proven that the method is exact for all applications where the configurational energy of the lattice remains constant during the variational procedure. Comparison is made with the Superposition Approximation of Kirkwood and with Monte Carlo studies. In addition, the method is shown to bear an inverse relationship to the Cluster Variation Method. It is concluded that this new variational procedure should be quite useful for obtaining a more complete microscopic description of a partially ordered lattice than is presently available with the pair configurations picture.

1. INTRODUCTION

A BINARY lattice is defined here as any regular lattice whose sites are occupied in one of two ways (e.g. a binary alloy, a lattice gas, or a spin $\frac{1}{2}$ magnetic lattice). A complete description of the lattice configuration is possible only when the lattice is perfectly ordered. At finite temperatures the lattice contains some degree of disorder and since the state of the lattice is now an average over some ensemble of configurations only a statistical description of the lattice arrangement is possible. When only short range order (SRO) is present the usual description of the lattice is based upon the pair correlations (i.e. the Warren SRO parameters in alloys, spin–spin correlations in magnetic systems) which are normally all that can be experimentally measured.* This however gives a very incomplete picture of the state of the lattice because it focuses on only two sites of the lattice at a time. It is clear that a knowledge of the probabilities for larger cluster configurations (triplets, quadruplets, etc.) would provide a much more complete description of the lattice structure at the atomic level.

We shall propose here a general theoretical method for inferring these higher order cluster probabilities from the pair probability data. To give it a name we shall call it the Probability Variation Method (PVM). Our scheme is very closely allied to the Cluster Variation Method (CVM) which has been extensively developed by Kikuchi[1] and collaborators. It may be described in some ways as an inverse of the CVM as we show below.

This inverse operation appears to be new, except for a calculation made by Kikuchi[2] for soap-bubble configurations. Although the CVM as normally used to calculate the configuration entropy of a system is known to be approximate in most cases[3], the inverse application to determine n-site probabilities is not similarly limited and in fact may be exact in all circumstances where one condition is satisfied. This condition is that the configurational energy of the lattice depend only upon the pair correlations that are held

*Recent work by COWLEY J. M. (*Acta crystallogr.* **A24**, 557 (1968)) on kinematical diffraction from solid solutions and field ion microscopy studies by GOLDF. and MACHLIN E. S. on Au–Pt and Ni–Pt alloys (*Phil. Mag.* **18**, 453 (1968)) indicate that it may be possible to obtain larger cluster correlations experimentally in some cases.

constant during the calculation. The exposition of the method is given in Section 2 and it is shown in Section 3 that in the several cases where the exact result for larger cluster probabilities is known, the PVM produces the correct answer.

Previously the work on obtaining the configuration probabilities of larger clusters has taken two paths. The first is also an analytic method first proposed by Kirkwood[4] which yields an approximate value for the triplet correlations in terms of the pair correlations. This technique is known as the Superposition Approximation (SA) and although the SA can be extended to higher order correlations there is some ambiguity in the procedure. We shall demonstrate below that at least for the applications of interest here the SA gives results for the triplet case which are not self-consistent and are often grossly in error in comparison to the exact number.

The second approach is more recent and has been made possible by the advent of high speed digital computers. This is the use of the Monte Carlo method (MCM) to generate configurations of a large number of sites (10^2–10^4) by letting the computer shuffle site occupations according to either a set of hopping probabilities[5] or until the configuration arrived at by the computer satisfies the observed pair correlations of a real system[6]. This method has the great advantage of demonstrating explicitly the configuration of a large number of sites in a partially ordered lattice. There is the difficult question, however, of establishing whether the single configuration map presented by the computer is truely representative of the majority of the millions of other configurations that would also satisfy the constraints. More to the point, perhaps, is the question of which properties of this configuration are typical and which are peculiar to it alone (or to a minority set) and should thus be ignored. We shall return to this problem later when we compare results of our calculations to that of the MCM.

In comparison with the MCM the present approach is limited in regards to the size of cluster which can be handled. The practical computational limit is of the order of ten sites. However, it has the advantage of providing cluster probabilities which are a statistical average over the entire ensemble of configurations of the infinite lattice that satisfy the pair correlation data. Also, the calculations are simpler to perform than the Monte Carlo procedures and if all that is needed are these smaller cluster probabilities then the present method should be completely satisfactory.

2. THEORY

(A) *The Probability Variation Method (PVM)*

We assume that the lattice composition and the pair correlations (or SRO parameters) for some range of the intersite distance are known. The problem is to determine the most probable frequency distribution for clusters of a given kind that will be consistent with the above data. The theory is most easily described by presenting an example and then generalizing to other order clusters. Consider a triplet cluster as shown in Fig. 1.

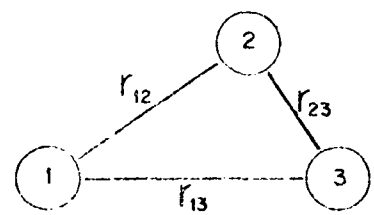

Fig. 1. A triplet

We shall use the notation and some results developed in a previous paper[7] that presented exact expressions for triplet probabilities in the special case of equal composition binary lattices. If site i of the lattice is occupied by an (A, B) object we assign the occupation number σ_i the value $(+1, -1)$. Thus a specification of the σ_i's (for $i = 1, N$) completely describes the configuration of all N sites of the lattice. There will be N triplets of the kind shown in Fig. 1 obtained by letting site 1

successively be each of the N lattice sites while sites 2 and 3 maintain their same relative position and orientation to site 1. Periodic boundary conditions are assumed. There are eight possible configurations for a triplet. Each configuration type is identified by an index k and they are listed in Table 1 along with the values of various σ products in each

$$\sum_k [\sigma_1\sigma_2]_k P_k = \langle\sigma_1\sigma_2\rangle \quad (2e)$$

$$\sum_k [\sigma_2\sigma_3]_k P_k = \langle\sigma_2\sigma_3\rangle \quad (2f)$$

$$\sum_k [\sigma_3\sigma_1]_k P_k = \langle\sigma_3\sigma_1\rangle \quad (2g)$$

$$\sum_k [\sigma_1\sigma_2\sigma_3]_k P_k = \langle\sigma_1\sigma_2\sigma_3\rangle \quad (2h)$$

Table 1. Coefficients for triplet sum rules

Cluster type	k	$[\sigma_1]_k$	$[\sigma_2]_k$	$[\sigma_3]_k$	$[\sigma_1\sigma_2]_k$	$[\sigma_2\sigma_3]_k$	$[\sigma_3\sigma_1]_k$	$[\sigma_1\sigma_2\sigma_3]_k$
	1	+1	+1	+1	+1	+1	+1	+1
	2	+1	+1	−1	+1	−1	−1	−1
	3	+1	−1	+1	−1	−1	+1	−1
	4	−1	+1	+1	−1	+1	−1	−1
	5	+1	−1	−1	−1	+1	−1	+1
	6	−1	+1	−1	−1	−1	+1	+1
	7	−1	−1	+1	+1	−1	−1	+1
	8	−1	−1	−1	+1	+1	+1	−1

cluster. Let the fraction of N triplets of type k be P_k. Then the lattice average of any occupation number product is given by the identity:

$$\langle\sigma_1\sigma_2 \cdots \sigma_n\rangle = \frac{1}{N}\sum_{j=0}^{N-1} \sigma_{1+j}\sigma_{2+j}\cdots\sigma_{n+j} = \sum_k [\sigma_1\sigma_2 \cdots \sigma_n]_k P_k \quad (1)$$

and for our example we can write the following set of sum rules:

$$\sum_k P_k = 1 \quad (2a)$$

$$\sum_k [\sigma_1]_k P_k = \langle\sigma_1\rangle = c \quad (2b)$$

$$\sum_k [\sigma_2]_k P_k = \langle\sigma_2\rangle = c \quad (2c)$$

$$\sum_k [\sigma_3]_k P_k = \langle\sigma_3\rangle = c \quad (2d)$$

where $c \equiv m_A - m_B$ and (m_A, m_B) are the fraction of (A, B) objects in the lattice. The coefficients of the P_k's in equation (2(a–h)) are all known by inspection of the cluster types and the values are listed in Table 1.

Strictly speaking, the averages on the right hand side (r.h.s) of equations (2(b–h)) are for a single lattice configuration, but we shall use the experimentally determined values of these quantities instead, which represent thermodynamic averages over a large ensemble of lattice configurations. However, since it is known from statistical mechanics that an overwhelming number of the states of the lattice which contribute to the average of a macroscopic quantity do not depart significantly from the ensemble average (except in the vicinity of critical points) this

ensures that we are studying the configurational properties of a 'typical' lattice state. Hence the r.h.s. of equations (2(b–d)) are known from the composition, and the r.h.s. of equations (2(e–g)) are assumed known from diffraction data. $\langle\sigma_i\sigma_j\rangle$ in alloys may be calculated from the Warren short range order parameter α_{ij} by the relation: $\langle\sigma_i\sigma_j\rangle = (1-c^2)\alpha_{ij}+c^2$. Clearly a knowledge of $\langle\sigma_1\sigma_2\sigma_3\rangle$ would make the set of equations determinate and the P_k's could then be obtained. Symmetry considerations make a theoretical evaluation of $\langle\sigma_1\sigma_2\sigma_3\rangle$ possible for the special case of $c=0$[7] but for $c\neq 0$ such arguments are no longer valid.

It is convenient at times to have the complementary set of identities which give a particular P_k in terms of occupation number lattice averages. For this purpose we use the projection numbers introduced in [7] and defined as follows:

$$\sigma_i{}^A \equiv \tfrac{1}{2}(1+\sigma_i) = (1,0) \text{ if } (A,B) \text{ is on site } i \tag{3a}$$

$$\sigma_i{}^B \equiv \tfrac{1}{2}(1-\sigma_i) = (0,1) \text{ if } (A,B) \text{ is on site } i. \tag{3b}$$

Then the probability that a cluster will be occupied in a particular manner is given by the lattice average of the corresponding projection numbers, e.g.

$$P_{12\cdots n}{}^{AB\cdots B} = \frac{1}{N}\sum_{j=0}^{N-1}\sigma_{1+j}{}^A\sigma_{2+j}{}^B\sigma_{n+j}{}^B \equiv \langle\sigma_1{}^A\sigma_2{}^B\cdots\sigma_n{}^B\rangle = \frac{1}{2^n}\langle(1+\sigma_1)(1-\sigma_2)\cdots(1-\sigma_n)\rangle \tag{4}$$

which can then be multiplied out and reduced to a sum of occupation number averages. Explicit examples will be given in the next section.

A priori it might be expected that the possible range of $\langle\sigma_1\sigma_2\sigma_3\rangle$ is +1 to −1 but the reality condition that all P_k's are positive semi-definite in the linear equations limits $\langle\sigma_1\sigma_2\sigma_3\rangle$ to a much smaller range. This is also manifested by a narrowing of the allowable range of the individual P_k's. An example of this effect will be seen in Section 3(C) below. In essence the linear equations for the P_k's confine the possible P_k values to a small volume in P_k space (a linear manifold in the case of triplets). This important fact has previously been noted and emphasized by Gehlen and Cohen[6] in their Monte Carlo study of local order in alloys. The volume of the subspace depends upon the particular values of c and the $\langle\sigma_i\sigma_j\rangle$'s. It is largest when the $\langle\sigma_i\sigma_j\rangle$'s are that of a completely disordered alloy (i.e. $\langle\sigma_i\sigma_j\rangle = c^2$) and the volume reduces to a single point when the $\langle\sigma_i\sigma_j\rangle$ values are those of a fully ordered structure. The P_k's then become completely determined.

Regarding P_k as the probability of finding, by random selection, a cluster of type k in the lattice, Information Theory[8] can be used to make a 'best choice' for the values of the P_k's. Since the situation is one of incomplete knowledge (the P_k's are only known within the limits imposed by the linear equations), Information Theory states that the most unbiased value for the P_k's within this range is that set which maximizes the 'ignorance' function $I(P_k)$ given by:

$$I(P_k) = -\sum_k P_k \ln P_k. \tag{5}$$

Information Theory shows that any other choice would imply that there is more information about the P_k's than has been given. More information of a very complicated kind may, in fact, be present due to overlapping cluster conditions that we shall now consider.

This choice can also be interpreted in more familiar terms as a principal of maximum entropy. $I(P_k)$ is proportional to the configurational entropy $W_{\text{CVM}}(P_k)$ obtained by placing NP_1 clusters of type 1, NP_2 clusters of type 2, etc. on a lattice of N sites in all possible ways *without worrying about incompatible overlaps*. This is given by the combinatorial factor:

$$W_{CVM}(P_k) = \frac{N!}{\prod_k [NP_k)!]} \cong N\left[-\sum_k P_k \ln P_k\right] \tag{6}$$

and is recognizable as the combinatorial factor of the Cluster Variation Method (CVM) using this particular cluster as a basis.

Let us assume for the moment that equation (6) correctly evaluates the number of lattice configurations for a given set of P_k's, and also assume that the configurational energy depends only on the $\langle\sigma_i\sigma_j\rangle$'s that are being held constant. Then maximizing $W(P_k)$ with respect to the P_k's (and subject to the constraints of equations (2(a–g)) will yield the most probable value for the P_k's. Furthermore, as the size of the lattice increases, the statistical law[9] of large numbers states that the fraction of lattice configurations having any value of the P_k's other than this optimum set becomes vanishingly small.

We now examine the two assumptions that we have used. It is known from work on the CVM that equation (6) considerably overestimates the number of lattice configurations of given P_k because it includes many configurations containing incompatible cluster placements such as the one shown in Fig. 2. Here we have chosen an equilateral triangle

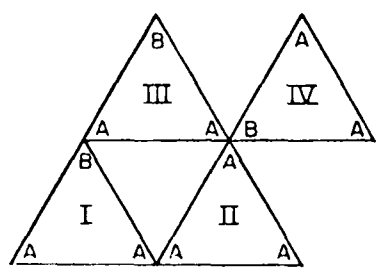

Fig. 2. Superposition of triplets in a lattice.

as the cluster and illustrate only a small region of the lattice. Although clusters I and II are in agreement on the occupation of their common vertex, I and III are incompatible and IV is incompatible with both II and III. Thus W_{CVM} counts not only all the possible lattice configurations but a much larger number which are impossible on a real lattice. If $W(P_k)$ is just the subset of compatible configurations then obviously $W(P_k) \leq W_{CVM}(P_k)$.

However, it is clear that for our purposes we do not need to know the magnitude of $W(P_k)$. All that is required is a knowledge of the P_k values which maximize it! Thus we can reduce our first assumption to a much simpler one, namely that if P_k is changed such that $W_{CVM}(P_k)$ increases (decreases), the subset of compatible configurations $W(P_k)$ also increases (decreases). At this point we are unable to prove the assumption generally but only argue its plausibility on the grounds that increasing the total number of configurations should increase the chance of compatible configurations occurring. The postulate in simplest form is:

Postulate I: In any given subregion of P_k *space the maximum of* $W_{CVM}(P_k)$ *and* $W(P_k)$ *coincide.*

The second assumption required in order that the variational calculation be exact is that the configurational energy of the lattice depends only upon quantities that are being held constant, i.e. the composition and pair correlations spanned by the cluster.

Postulate II: The configurational energy of the lattice is constant over the subregion of P_k *space defined by the linear constraints.*

We can compare the present procedure with the Cluster Variation Method as it is normally applied to illustrate the inverse relationship that they bear to each other. In the CVM the pair correlations are not assumed known but instead are the quantities to be predicted, while the P_k's are used as intermediary variables to accomplish the calculation. A certain size of cluster is chosen, as we have done, and the same linear relationships are written between the P_k's and the pair correlations. The entropy of the system for a particular set of values of the pair correlations is then deduced from equation (6) by maximizing W_{CVM} with respect to the P_k's. This leaves W_{CVM} a function of just the pair correlations which are to be varied later when W_{CVM}

is inserted in a free energy expression. For this process to give the correct result it is necessary that the maximum of W_{CVM} agree with the true $W(P_k)$ not only in location but in magnitude as well (apart from a constant scale factor) over the entire P_k space. This is necessary in order that W (and hence the free energy) have the correct functional dependence on the pair correlations. This latter requirement is the principal cause of error in the Cluster Variation Method and is obviated in the present analysis by taking the pair correlations from measurements, i.e. we stay strictly within a micro-canonical ensemble and proceed in the reverse direction to determine the P_k's from the pair correlations.

(B) The Superposition Approximation

Kirkwood's Superposition Approximation [4] and variants of it have been used by many writers to obtain rough estimates of higher order correlations in analytic form. The general formula is:

$$P(\sigma_1\sigma_2\cdots\sigma_n) = C \prod_{1\le i<j\le n} P(\sigma_i\sigma_j) \qquad (7)$$

where C is a normalization constant which is adjusted to make the sum of n-site probabilities add up to unity. $P(\sigma_1\sigma_2\cdots\sigma_n)$ is the probability of occurrence of the configuration σ_1 for site 1, σ_2 for site 2, $\cdots$, σ_n for site n. For triplets, which is the most frequent application of the SA, equation 5 is:

$$P(\sigma_1\sigma_2\sigma_3) = CP(\sigma_1\sigma_2)\,P(\sigma_1\sigma_3)\,P(\sigma_2\sigma_3) \quad (8a)$$

and for a 4-site cluster, the SA expression is:

$$P(\sigma_1\sigma_2\sigma_3\sigma_4) = CP(\sigma_1\sigma_2)\,P(\sigma_1\sigma_3)\,P(\sigma_1\sigma_4) \times P(\sigma_2\sigma_3)\,P(\sigma_2\sigma_4)\,P(\sigma_3\sigma_4) \quad (8b)$$

It is generally recognized that for weakly correlated systems the SA is a good approximation (at least for triplets) but for non-dilute lattices at temperatures where the pair correlations are finite the SA is rather poor and, in fact, will give results that show serious inconsistencies with the input values of the pair correlations.

3. EXACT RESULTS

(A) Linear chain

The simplest system in lattice statistics is the infinite one-dimensional chain (see Fig. 3) with nearest neighbor interactions, generally

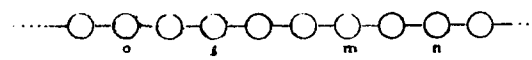

Fig. 3. The one-dimensional lattice.

referred to as the Ising linear chain. In 1925 Ising[10] exactly calculated a number of statistical properties of this lattice including the pair correlation functions. The pair correlation for nth neighbors on the chain is:

$$\langle\sigma_i\sigma_{i+n}\rangle = t^n \qquad (9)$$

where $t \equiv \tanh(-\beta V)$, $\beta \equiv 1/kT$ and V is the nearest neighbor interaction. *The triplet* correlation function $\langle\sigma_i\sigma_{i+m}\sigma_{i+n}\rangle$ is zero for symmetry reasons and thus all triplet probabilities are completely determined from the pair correlations[7]. The quadruplet correlation function $\langle\sigma_i\sigma_{i+l}\sigma_{i+m}\sigma_{i+n}\rangle$ (or simply $\langle\sigma_o\sigma_l\sigma_m\sigma_n\rangle$) has some value q which we shall attempt to determine by our method. The sixteen quadruplet probabilities can be written in terms of the pair and quadruplet correlation functions by use of equation 4 and inserting the values of the pair correlations from equation 9 gives:

$$\begin{aligned}
AAAA = BBBB &= (1 + t^l + t^{m-l} + t^{n-m} \\
&\quad + t^m + t^{n-l} + t^n + q)/16 \\
AABB = BBAA &= (1 + t^l - t^{m-l} + t^{n-m} \\
&\quad - t^m - t^{n-l} - t^n + q)/16 \\
ABAB = BABA &= (1 - t^l - t^{m-l} - t^{n-m} \\
&\quad + t^m + t^{n-l} - t^n + q)/16 \\
ABBA = BAAB &= (1 - t^l + t^{m-l} - t^{n-m} \\
&\quad - t^m - t^{n-l} + t^n + q)/16 \\
AAAB = BBBA &= (1 + t^l + t^{m-l} - t^{n-m} \\
&\quad + t^m - t^{n-l} - t^n - q)/16 \\
AABA = BBAB &= (1 + t^l - t^{m-l} - t^{n-m} \\
&\quad - t^m + t^{n-l} + t^n - q)/16
\end{aligned}$$

$$\begin{aligned} ABAA = BABB &= (1-t^l-t^{m-l}+t^{n-m} \\ &\quad + t^m - t^{n-l} + t^n - q)/16 \\ ABBB = BAAA &= (1-t^l+t^{m-l}+t^{n-m} \\ &\quad - t^m + t^{n-l} - t^n - q)/16 \end{aligned} \tag{10}$$

where $AAAA$ represents P_{1234}^{AAAA}, etc. Each of the 16 P_k's is now a linear function of the single variable q and maximizing equation 5 with respect to q yields:

$$\frac{\partial I(q)}{\partial q} = 0 = \frac{\partial}{\partial q}\left\{-\sum_{k=1}^{16} P_k(q)\, ln\, P_k(q)\right\} \tag{11}$$

which gives upon calculation:

$$\frac{(AAAA)(AABB)(ABAB)(ABBA)}{(AAAB)(AABA)(ABAA)(ABBB)} = \frac{(XYZ+Q)(X\bar{Y}Z+Q)(\bar{X}\bar{Y}\bar{Z}+Q)(\bar{X}Y\bar{Z}+Q)}{(XY\bar{Z}-Q)(X\bar{Y}\bar{Z}-Q)(\bar{X}\bar{Y}Z-Q)(\bar{X}YZ-Q)} = 1 \tag{12}$$

where $X = 1+t^l$, $\bar{X} = 1-t^l$, $Y = 1+t^{m-l}$, $\bar{Y} = 1-t^{m-l}$, $Z = 1+t^{n-m}$, $\bar{Z} = 1-t^{n-m}$, $Q = q - t^{n-m+l}$. Equation (12) has but one real root which is $Q = 0$ or:

$$q = \langle\sigma_0\sigma_l\sigma_m\sigma_n\rangle = t^{n-m+l} \tag{13}$$

$\langle\sigma_0\sigma_l\sigma_m\sigma_n\rangle$ can also be evaluated exactly by the complete summation of a diagrammatic expansion with the same result. For comparison, the Superposition Approx. gives via equation (8(b)) expressions for the quadruplet probabilities which are correct only to lowest order in t, e.g.

$$(AAAA)_{S.A.} = C(1+t^l)(1+t^{m-l})(1+t^{n-m})(1+t^m)(1+t^{n-l})(1+t^n)/16$$

so that the SA does yield the correct high temperature weak correlation limit but is increasingly in error with increasing correlation. Paradoxically the SA also gives the correct result at the zero temperature perfectly ordered limit so that we conclude that the SA is most in error for states of partial order for this example.

(B) Triplets in AB *alloys*

The exact formulae for triplet cluster probabilities in AB binary lattices with pairwise interactions is known [7]. Thus we can test the present method on a more realistic three dimensional problem. Employing equation (4) we may write the eight triplet probabilities of an arbitrary cluster as:

$$\begin{aligned} AAA &= (1+3c+\langle\sigma_1\sigma_2\rangle \\ &\quad + \langle\sigma_2\sigma_3\rangle + \langle\sigma_3\sigma_1\rangle + \tau)/8 \\ BBA &= (1-c+\langle\sigma_1\sigma_2\rangle \\ &\quad - \langle\sigma_2\sigma_3\rangle - \langle\sigma_3\sigma_1\rangle + \tau)/8 \\ ABB &= (1-c-\langle\sigma_1\sigma_2\rangle \\ &\quad + \langle\sigma_2\sigma_3\rangle - \langle\sigma_3\sigma_1\rangle + \tau)/8 \\ BAB &= (1-c-\langle\sigma_1\sigma_2\rangle \\ &\quad - \langle\sigma_2\sigma_3\rangle + \langle\sigma_3\sigma_1\rangle + \tau)/8 \end{aligned} \tag{14}$$

$$\begin{aligned} BBB &= (1-3c+\langle\sigma_1\sigma_2\rangle \\ &\quad + \langle\sigma_2\sigma_3\rangle + \langle\sigma_3\sigma_1\rangle - \tau)/8 \\ AAB &= (1+c+\langle\sigma_1\sigma_2\rangle \\ &\quad - \langle\sigma_2\sigma_3\rangle - \langle\sigma_3\sigma_1\rangle - \tau)/8 \\ BAA &= (1+c-\langle\sigma_1\sigma_2\rangle \\ &\quad + \langle\sigma_2\sigma_3\rangle - \langle\sigma_3\sigma_1\rangle - \tau)/8 \\ ABA &= (1+c-\langle\sigma_1\sigma_2\rangle \\ &\quad - \langle\sigma_2\sigma_3\rangle + \langle\sigma_3\sigma_1\rangle - \tau)/8 \end{aligned}$$

where BBA represents P_{123}^{BBA} etc., τ is the value of the triplet correlation $\langle\sigma_1\sigma_2\sigma_3\rangle$, and we note that for an equi-composition alloy $\langle\sigma_i\rangle = c = m_A - m_B = 0$. Assuming only pairwise interactions in the lattice implies that the configurational energy is dependent only on the pair correlations so that varying τ subject to fixed values of $\langle\sigma_1\sigma_2\rangle$, etc. will ensure that Postulate II is satisfied. Varying equation (5) with respect to τ yields

$$\frac{\partial I(\tau)}{\partial \tau} = \frac{\partial}{\partial \tau}\left\{-\sum_{k=1}^{8} P_k(\tau)\ln P_k(\tau)\right\} = 0 \tag{15}$$

which gives:

$$\frac{(AAA)(BBA)(ABB)(BAB)}{(BBB)(AAB)(BAA)(ABA)} = 1. \quad (16)$$

This equation has but one real solution: $\tau = 0$, which is also the prediction of the exact theory. This result clearly depends on Postulate II being satisfied for if the system contained three body interactions as well τ would be expected to have a non-zero value.

(C) Triplets in Monte Carlo experiments

The Monte Carlo work that has most relevance to the present study is that carried out by Gehlen and Cohen[6]. Using Moss's experimental data[11] for the first, second, and third neighbor pair correlations in Cu_3Au at 450°C they used a computer to shuffle atomic configurations on 4000 sites. They used two starting configurations: perfectly random, and perfectly ordered and allowed the computer to change configurations only if the new configuration was more consistent with the pair correlation data. The process was stopped when the computer configuration had values for the pair correlations sufficiently close to the experimental data. A number of properties of the final computer configurations were then measured, in particular the various fractions of nearest neighbor triplets and quadruplets. Although these few computer configurations undoubtedly represent but a very small fraction of the ensemble of 4000 site configurations that would have the same pair correlations, it is safe to assume that the values for the triplet probabilities derived from the computer configurations are typical of the ensemble for two reasons. First, since there are 32,000 triplets of this kind in a single configuration, the statistical averaging is of a high order. This would not be true of some larger feature of the configuration such as the shape of an antiphase boundary involving several hundred atoms. Second, the results for the triplet numbers varied by insignificant amounts among different final configurations. As a consequence it is practically certain that their Monte Carlo values for the triplet and quadruplet probabilities are very close to the exact values for the Cu_3Au lattice at this temperature. There is, of course, the implicit assumption in their operation that the configurational energy depends on no more than the three pair correlations that were used as input.

Our method is easily applied to the calculation of the triplet probabilities by using equations (14) and (15) which again yield equation (16) but the solution is now different from $\tau = 0$ because $c \neq 0$. We write equation (16) as

$$\frac{(D_1+X)(D_2+X)(D_3+X)(D_4+X)}{(D_1'-X)(D_2-X)(D_3-X)(D_4-X)} = 1 \quad (17)$$

with

$$X = \tau - c$$
$$D_1 = 1 + \langle\sigma_1\sigma_2\rangle + \langle\sigma_2\sigma_3\rangle + \langle\sigma_3\sigma_1\rangle + 4c$$
$$D_1' = 1 + \langle\sigma_1\sigma_2\rangle + \langle\sigma_2\sigma_3\rangle + \langle\sigma_3\sigma_1\rangle - 4c$$
$$D_2 = 1 + \langle\sigma_1\sigma_2\rangle - \langle\sigma_2\sigma_3\rangle - \langle\sigma_3\sigma_1\rangle$$
$$D_3 = 1 - \langle\sigma_1\sigma_2\rangle + \langle\sigma_2\sigma_3\rangle - \langle\sigma_3\sigma_1\rangle$$
$$D_4 = 1 - \langle\sigma_1\sigma_2\rangle - \langle\sigma_2\sigma_3\rangle + \langle\sigma_3\sigma_1\rangle$$

Equation (17) reduces to a cubic, $X^3 + a_2X^2 + a_1X + a_0 = 0$ with $a_2 = c(D_2 + D_3 + D_4)$, $a_1 = ((D_1 + D_1')(D_2D_3 + D_3D_4 + D_2D_4) + 2D_2D_3D_4)/8$, $a_0 = cD_2D_3D_4$. This has one real root, which can be proven by assuming there is more than one and showing that this implies negative values for some of the P_k's. The single real root is extracted by the standard cubic solution method. At this point the solution is applicable to any kind of triplet on a lattice of arbitrary composition. The D_i's are evaluated for Cu_3Au nearest neighbor triplets by setting $c = \frac{1}{2}$ and $\langle\sigma_1\sigma_2\rangle = \langle\sigma_2\sigma_3\rangle = \langle\sigma_3\sigma_1\rangle = (1-c^2)\alpha_1 + c^2$ where α_1 is the measured Warren short range order parameter for nearest neighbors. The three pair correlations are equal because the triplet under consideration has each site a nearest neighbor of the other two. The numerical results are listed in Table 2.

The allowed range for the triplet probabilities has been found from equation (14) by putting in the known values for c and the $\langle\sigma_i\sigma_j\rangle$'s and then determining the range of τ for which all the probabilities remain positive.

Table 2. Nearest neighbor triplet probabilities in Cu_3Au *at*

Triplet type	Range allowed by linear equations at $T = 450°$	Monte Carlo[6] $N = 4000$		This calculation (PVM)	very approx
		Ordered start	Random start		
Cu-Cu-Cu	0·302–0·328	0·3273	0·3275	0·3271	0·3474*
Cu-Cu-Au	0·672–0·594	0·5962	0·5956	0·5964	0·5576*
Cu-Au-Au	0·000–0·078	0·0758	0·0761	0·0759	0·0940*
Au-Au-Au	0·026–0·000	0·0007	0·0007	0·00067	0·1

*Note that these values are outside the allowed range.

The result is that τ has a lower bound at $-0·396$ and an upper bound at $-0·188$. The first values in the table correspond to the lower bound of τ and the second values to the upper, so that by imposing this reality condition alone, the values of the triplet probabilities are already known reasonably well. The PVM solution is $\tau = -0·1941$.

It is apparent from Table 2 that the agreement between the Monte Carlo numbers and the PVM predictions are very good. It suggests that the PVM values are probably the exact results for the infinite lattice ensemble.

Although the SA would appear to give a reasonable estimate of the triplet probabilities, three of the values are impossible because they lie outside the range allowed by equation (1·1). This means that if the SA probabilities were used to determine τ, each one of the linear equations would give a different τ and the inconsistency could not be resolved.

Alternatively, if the SA probabilities are fed back into equation (2) the values of c and α_1 so determined are in error by 2 and 23 per cent respectively. In fact, an arbitrary choice of τ anywhere within the allowed range of τ would be better than using the SA, for this at least would produce a set of values for the triplet probabilities consistent with the known alloy data.

4. SUMMARY AND CONCLUSIONS

We have introduced a new way to determine the statistical probabilities of clusters of more than two sites from pair correlation data in any binary lattice. This approach has been called the Probability Variation Method (PVM) to indicate its kinship to an older method which has been employed in pair correlation determinations, the Cluster Variation Method. The PVM was compared with the Superposition Approximation and Monte Carlo results. It was shown to be more accurate than the former and more easily applied than the latter. A plausibility argument was presented that the PVM represents an exact calculation of the cluster probabilities for lattices where the configurational energy remains constant as the cluster probabilities are varied. The PVM was shown to yield the exact result for all the cases that could be calculated by alternate means. Thus the PVM should become a very useful tool for obtaining a more complete microscopic picture of partially ordered lattices.

In a subsequent paper we shall give results of the PVM applied to larger clusters consisting of a central site surrounded by all its nearest neighbor sites in two and three dimensional lattices. We shall also indicate various calculation short cuts and working techniques that can be employed in these more complex operations.

Acknowledgements—The author would like to thank Professor J. B. Cohen for a conversation and correspondence about cluster probabilities and the Monte Carlo work that were quite informative. He is also indebted to Professor J. M. Cowley for originally stimulating his interest in this subject and to Professor S. C. Moss and Dr. C. B. Walker for valuable discussions.

REFERENCES

1. KIKUCHI R., *Phys. Rev.* **81**, 988 (1951); *J. chem. Phys.* **19**, 1230 (1951).

2. KIKUCHI R., *J. chem. Phys.* **24**, 861 (1956).
3. KURATA, M., KIKUCHI R. and WATARI T., *J. chem. Phys.* **21**, 434 (1953).
4. HILL T. L., In *Statistical Mechanics*, pp. 195, 278. McGraw-Hill, New York (1956).
5. FOSDICK L. D., *Phys. Rev.* **116**, 565 (1959); GUTTMAN L., *J. chem. Phys.* **34**, 1024 (1961).
6. GEHLEN P. C. and COHEN J. B., *Phys. Rev.* **139**, A844 (1965).
7. CLAPP P. C., *Phys. Rev.* **164**, 1018 (1967).
8. KATZ A., In *Principles of Statistical Mechanics*, p. 18. Freeman, San Francisco (1967); also, BRILLOUIN L., *Science and Information Theory*. Academic Press, New York (1962).
9. GUGGENHEIM E. A., In *Thermodynamics*, 4th Edn., p. 63. North-Holland, Amsterdam (1959)
10. ISING E., *Z. Phys.* **31**, 253 (1925).
11. MOSS S. C., *J. appl. Phys.* **12**, 3547 (1964).

Memo from

Philip C. Clapp

This technical report has appeared in published form in the book:
"Ordered Alloys: Structural Applications and Physical Metallurgy", B. H. Kear et al.
Editors - Clator's Press, Baton Rouge, La. (1970) pp.25-36

LEDGEMONT LABORATORY
KENNECOTT COPPER CORPORATION
128 SPRING STREET • LEXINGTON 73, MASS.

A CRITICAL EXAMINATION OF THE VALIDITY OF THE PAIR-WISE INTERACTION MODEL FOR ORDERED ALLOYS

Philip C. Clapp

Ledgemont Laboratory, Kennecott Copper Corporation
Lexington, Massachusetts.

ABSTRACT

The use of central pair-wise interatomic forces of short range to account for the many various configurations of ordered alloys has had a long and generally successful history. It is thus important to determine under what conditions this simple model might be grossly in error. In particular, we shall pose and provide partial answers for the following questions:

a) Is it essential to postulate the presence in some systems of infinite range forces (such as the Brillouin zone-Fermi surface interaction originally proposed by Jones to explain the Hume-Rothery phases and recently used by Sato & Toth to account for long period superlattices) or are these effects reducible to finite range forces?

b) Is there any evidence for the presence of non-central forces in the ordering behaviour of metallic systems?

c) Are the many-atom forces proposed by strain ordering theories for alloys with large atom size disparities essentially reducible to pair-wise interactions or is the observed behaviour an irreducible many-body effect?

Introduction

Any attempt to explain or predict the physical properties of alloys from an atomistic viewpoint, whether it be phase stability, stacking fault energies, kinetics of ordering, mechanical behaviour, microstructure or any other topic that could have been chosen for this conference, must begin with a model of the atomic interactions present.

One that has been used very often in one form or another is the central pair-wise interaction scheme. This is probably more because of its ease of application than because of any strong evidence of its validity. In fact, it has been known for a long time that the violation of the Cauchy relations among the elastic constants in most metals implied that non-central or many-body forces must play some part.

Beginning with the fundamental constituents of a metallic lattice, namely the atomic nuclei and the electrons, all the interactions are simple coulomb forces and thus are entirely central pair-wise interactions. However, when we try to describe the effective force that exists between two atoms in a metallic lattice due to the interaction of one nucleus, its bound electrons and its cloud of conduction electrons with another such object it is very unlikely that the force will still be a simple central pair-wise interaction. All that we can hope is that the dominant part of the interaction will have this character. What we shall examine here to some degree is the question of which alloy properties and which alloy systems are consistent with a predominantly central pair-wise interaction scheme and, conversely, which cases clearly violate the model and show that a more complicated treatment is necessary.

One particularly simple version of this model assumes only a nearest neighbor interaction of constant strength and has been widely used in ordering theories such as the quasi chemical method, regular solution theory and the Ising model. It is now clear that this assumption is an extremely crude one and many authors[1,2] have pointed out its drawbacks. For instance, it cannot explain why most order-disorder transformations are first order transitions, why the critical temperature for ordering is often observed to be a maximum away from the stoichiometric composition or even why a face centered cubic alloy should order at all.[3] These are serious failings and it is apparent that any calculation based on this assumption should be taken with a large grain of salt.

This experience makes it evident that the model must include higher neighbor interactions and also provide for changes in the interaction strengths as the lattice parameter or composition vary.

Central Pair-Wise (CPW) Interactions and What They Can Explain

Two important recent developments in the theoretical work on intermetallic interactions have given a more distinct picture of the general character of these forces. Friedel[4] and others[5,6] were able to show that because the conduction electrons in a metal were limited to wave vectors below the Fermi wave vector k_F, they would not be able to screen out the charge of the metallic ions completely. This incomplete screening leads to a long range oscillatory potential between the metal atoms falling off as r^{-3} and has a CPW character.

The second result has come from a new technique for calculating the interatomic forces in metallic systems and is referred to as pseudo-potential theory[7]. Whereas the Friedel incomplete screening result gives only the character of the interaction at large distances, the pseudo-potential calculations provide an approximation over the full range of the interaction. The principal term in the calculation invariably yields a CPW interaction but higher terms in the perturbation expansion indicate more complex types of interactions (i.e. many-body interactions). A recent pseudo-potential calculation of the Li-Mg system by Hayes et alia[8] gives a CPW interaction

with the near neighbor interactions arising primarily from the direct overlap of atomic orbitals and a Friedel long range oscillatory potential taking over beyond the fifth neighbor distance.

Unfortunately, the pseudo-potential technique is difficult to apply to the transition and noble metals. Consequently no calculations of interatomic interactions in these systems are yet available, but we can hope that the results for these groups will not be radically different. The Friedel interaction is not similarly limited so that for metals generally, we can expect an oscillatory potential falling off as r^{-3} at large distances.

Let us assume then that the CPW part of the interatomic interactions in an alloy have the general features indicated in Fig. 1. Thus the equilibrium interatomic distance for an A-A, a B-B and an A-B pair are all different and the average lattice spacing will be some compromise distance when the alloy is disordered. A second point to note is that the binding energies of each type of pair are different also. The long range oscillatory feature of the potentials has been ignored for the present. We further assume that the potentials at near-neighbor distances are due principally to the overlap of bound electrons so that this part of the curves will remain relatively constant as the composition or temperature of the alloy changes, unless there is some change in valence of the ions.

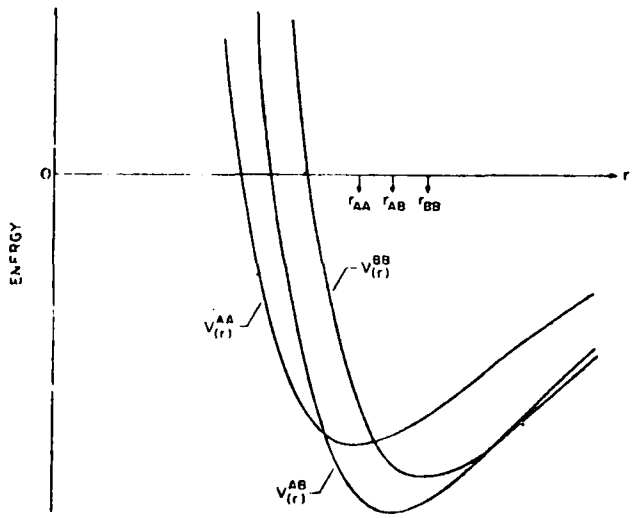

Figure 1:

Interatomic potentials in a binary alloy chosen to have different well-depths (causing a chemical ordering force) and different minima positions (causing a strain ordering force).

What then are the qualitative predictions of this model? The total configurational energy of the alloy is:

$$E_{CONFIG.} = \sum_i [V^{AA}(r_i)\, N^{AA}(r_i) + V^{BB}(r_i)\, N^{BB}(r_i) + V^{AB}(r_i)\, N^{AB}(r_i)] \quad (1)$$

where r_i is the distance between the i-th neighbors in the lattice, $N^{AA}(r_i)$ is the total number of A-A pairs in the lattice separated by that distance, and $V^{AA}(r_i)$ is the strength of the A-A interaction at that distance, etc. If the fraction of (A,B) atoms in the lattice is (m_A, m_B) and the Warren short range order parameters α_i are used, then:

$$N^{AA}(r_i) = \frac{NZ_i}{2}\,(m_A^2 + m_A m_B \alpha_i) \quad (2a)$$

$$N^{BB}(r_i) = \frac{NZ_i}{2}\,(m_B^2 + m_A m_B \alpha_i) \quad (2b)$$

$$N^{AB}(r_i) = NZ_i\, m_A m_B (1-\alpha_i)$$

where Z_i is the coordination number in the i-th shell, and N is the total number of sites in the crystal. This allows us to make a useful separation of the energy into an order independent part and an order dependent part:

$$\frac{2E}{N} = \sum_i Z_i V_o(r_i) + \sum_i Z_i V(r_i) \alpha_i = E_o(r) + E_1(r,\alpha) \qquad (3)$$

where $$V_o(r_i) = m_A^2 V^{AA}(r_i) + m_B^2 V^{BB}(r_i) + 2m_A m_B V^{AB}(r_i)$$

and $$V(r_i) = m_A m_B [V^{AA}(r_i) + V^{BB}(r_i) - 2V^{AB}(r_i)]$$

The functions $V_o(r)$ and $V(r)$ have been plotted in Fig. 2 for the case $m_A = m_B$.

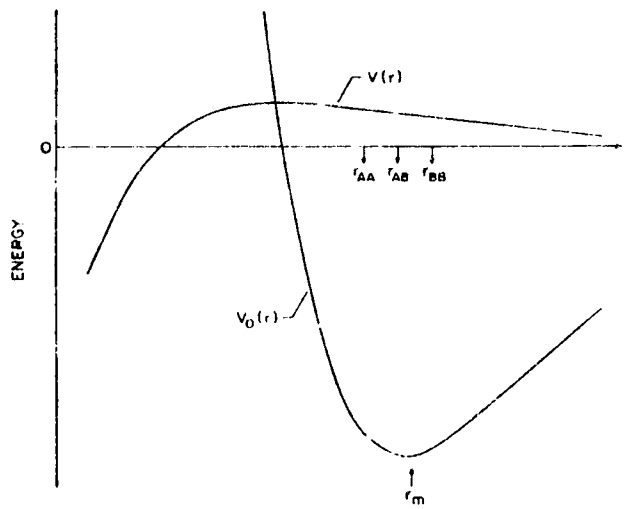

Figure 2:
Plots of $V_o(r) = m_A^2 V^{AA}(r) + m_B^2 V^{BB}(r) + 2m_A m_B V^{AB}(r)$ and $V(r_i) = m_A m_B [V^{AA}(r_i) + V^{BB}(r_i) - 2V^{AB}(r_i)]$ for $m_A = m_B$.

If the alloy is completely disordered then all the α_i are zero and only $E_o(r)$ contributes to the energy. The lattice spacing is then determined by minimizing E_o with respect to lattice size. If we ignore all but first neighbor terms for the sake of illustration, this would place the first neighbor distance at the minimum of the $V_o(r)$ curve i.e. at r_m. The driving force for ordering first neighbors is given by $V(r_m)$ and as the temperature is lowered α_1 will become increasingly negative. As Dienes(9) has pointed out this will cause a change in the lattice spacing because the nearest neighbor distance will always be at the minimum of $V_o(r) + \alpha_1 V(r)$. In the vicinity of the order-disorder transformation temperature (T_c), α_1 changes quite rapidly and in fact the lattice spacing will usually change discontinuously at T_c as shown by Garland and Renard(10). This changes the nature of the transformation from second order to first order. We also note that the ordering energy $V(r_1)$ has changed slowly as the lattice spacing has changed. Changing the composition of the alloy will also have effects on the lattice spacing and the ordering energy because $V_o(r)$ and $V(r)$ will now be different mixtures of $V^{AA}(r)$, $V^{BB}(r)$ and $V^{AB}(r)$ as may be seen from Eq. 3. This can produce asymmetries in the shape of the order-disorder phase boundary and can cause the peak in T_c to be shifted off the stoichiometric composition as is often observed experimentally.

Asymmetric lattice distortions of the ordered phase can also be understood qualitatively from this model in cases like CuAu which orders in alternating [100] planes of Cu and Au atoms. Since the interaction between planes is

principally $V^{AB}(r)$ the interplanar spacing will be determined by this interaction, whereas the spacing within a plane will depend on the features of $V^{AA}(r)$ and $V^{BB}(r)$. Thus we can expect the inter and intra-planar spacing to be different in the ordered phase as is observed. CuPt which is also a* layered ordered structure (on {111} planes) may be a similar example.

Clapp and Moss[11] have shown that the stability of all* of the simple ordered structures of cubic alloys can be explained by including second and occasionally third neighbor interactions. In fact, the ordered structures can be correctly predicted by measuring the interaction strengths in the disordered phase from short range order diffuse scattering data.

Past Criticisms of CPW Interactions

1) Incorrect prediction of the shape and temperature maxima of the order-disorder phase boundary. As we have seen in the previous section this is really an objection to the much more naive constant nearest-neighbor interaction model and does not apply to the full CPW model.

2) Most order-disorder transformations are first, not second, order. This again is a failing of the constant interaction model and is not a difficulty once the variation of ordering energy with lattice parameter is included.

3) AuNi has often been cited as a case that was inexplicable in terms of pair-wise interactions because the short range order (SRO) data of Flinn et alia[12] indicated a driving force for ordering whereas the phase diagram shows a miscibility gap and hence clustering. This paradox was usually dealt with by suggesting that because of the large size effect present in the alloy important "strain energies" had not been included in the pair-wise description. Moss[13] has since shown that the original SRO data were not correctly separated from the large size-effect diffuse scattering and when this operation was done more carefully the SRO data also indicated clustering, in conformity with the phase diagram.

In addition Golding, Moss and Averbach[14] used a CPW ion core repulsion between nearest neighbors to calculate the variation with composition of the shear constants for AuNi concentrated solutions as well as the heat of formation. They got good agreement with experimental data which indicates that the strain energy term in this system is well represented by the changes in the short range CPW repulsive interaction between neighboring ions.

4) Electron phases-Brillouin zone effects-Long period superlattices. The concept that the energy of the conduction electrons can be lowered by introducing a new periodicity into the lattice such that the corresponding Brillouin zone will touch the surface of the Fermi sphere has often been used to explain the stabilization of various ordered structures. Jones[15] proposed this mechanism to explain the Hume-Rothery electron phases, Slater[16] suggested a similar idea to explain the ordering of CuPt and recently Sato and Toth[17] have used this concept extensively to explain the existence of long period superlattices.

Until recently it has been difficult to understand what kind of force is implied by this mechanism. In particular it seemed difficult to relate it to any type of interatomic interaction. However, Krivoglaz[18], Moss[19] and others have shown that the effect of a new Brillouin zone touching the Fermi surface (and thereby flattening it to some degree) can be represented by adding a long range oscillatory potential to the interatomic potentials already present. This additional potential is of the form $A\, r^{-1}\cos(2k'r)$ where $2k'$ is the distance between flats in k space and A is related to the area of the flat face. This potential can dominate the long range region of the

---

*CuPt is an important exception and will be discussed later.

interaction since it falls off much more slowly than the r^{-3} decay of the Friedel interaction. If the energy of formation of antiphase boundaries (APB) is not too large then one might expect them to be introduced at regular intervals corresponding to the period of this new oscillatory interaction.

Clapp and Moss[11] found that the energy of {100} APB formation in normal ordered $Cu_3Au(L1_2)$ and $CuAu(L1_0)$ was quite low based on the calculated strengths of first, second and third neighbor interactions, but in Au_3Cu this energy is much higher. This correlates well with the experimental observation that long period superlattice phases are found in Cu_3Au and CuAu and are generated from the simple ordered phases by the introduction of regularly spaced {100} APB's but no such phases have yet been seen in Au_3Cu.

In summary then, the Fermi surface-Brillouin zone effects on the lattice energy can apparently be well represented by a long range oscillatory CPW interaction between the metal ions and can thus be incorporated into the framework of the CPW model.

Present Criticisms

1) Cauchy relations

As mentioned in the introduction the well known violation of the Cauchy relations among the elastic constants of most metals and alloys implies some interaction in addition to the CPW component. Fuchs[20] made a theoretical analysis for pure copper which indicated that most of the inequality of the Cauchy relations was due to the bulk compressibility of the conduction electron gas. This implied that, at least for copper, as long as the volume remained constant, the energetics of the lattice could be treated in terms of CPW interactions.

Although this result is interesting it is a very difficult theoretical job to make this separation and it is doubtful that such an analysis is generally valid. The current practice in fitting interaction models to elasticity data and phonon spectra is to include non-central or angular forces as well. Although these are written as pair forces they are probably a subtle form of many-body force since the definition of angle requires a knowledge of the simultaneous position of atoms neighboring the pair in question. In any case, it is clear that the inclusion of these more complex forces is essential to adequately fit the phonon spectra of metals. Machlin[21] has proposed an order-disorder theory based upon a first neighbor central and non-central interaction, and uses it: to predict the Cu-Au distance in the $L1_0$ structure, to calculate the relative stability of the $L1_1$ and $L1_0$ structures, and to propose a qualitative model for long period superlattices. However, it appears that these effects may be equally well explained on the basis of the simpler CPW model so that it cannot be said that these results imply the necessity of including non-CPW interactions.

2) CuPt

The ordered form of CuPt has long been an enigma from the viewpoint of a nearest neighbor interaction model since there is no change in the number of nearest neighbors of each type relative to the disordered phase. Solutions of many kinds have been offered for this problem. One is to include second neighbor CPW forces, another is to use angular forces, and there is the suggestion of Slater already cited. All of these suggestions appear to resolve the problem but the paradox actually runs much deeper. This is because there is potentially another ordered form of CuPt* (Fig. 3) which has the remarkable feature that it has the same fraction of each type of atom as the normal $L1_1$ CuPt form in every neighbor coordination shell. This means that no CPW model, regardless of how many neighbor interactions are included, could predict an energy difference for these two structures. Slater's Brillouin zone-Fermi surface explanation also seems to fail since the Brillouin zones of the two structures occur at the same radius in k space.

*First suggested to me by Robin Williams of Oak Ridge.

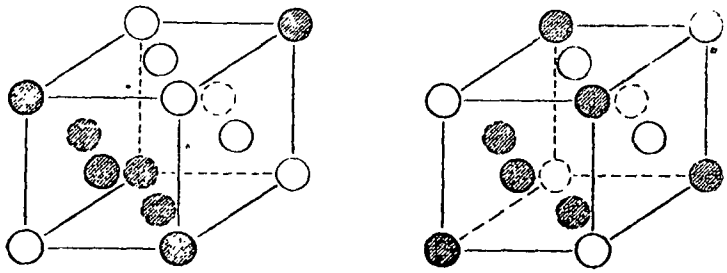

Figure 3: Two ordered atomic arrangements on an fcc lattice that have identical numbers of like and unlike neighbors in every coordination shell and thus will have identical configurational energies in any CPW model.

What appears to be required (since only the $L1_1$ form of CuPt is actually observed in nature) is a many-body interaction. If one begins with the simplest case of a nearest neighbor three-body interaction, this is still not sufficient to produce an energy difference in the two structures since they both have the same number of three body configurations (see Table 1). However, a four-body nearest neighbor interaction will do the trick and this appears to be the minimum model required to explain the stability of the $L1_1$ structure.

TABLE 1

Lattice Fractions of Nearest Neighbor Triangle Configurations

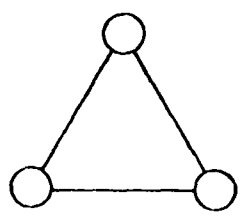

Configuration	$L1_1$	Alternate
Cu-Cu-Cu	1/8	1/8
Cu-Cu-Pt	3/8	3/8
Cu-Pt-Pt	3/8	3/8
Pt-Pt-Pt	1/8	1/8

Lattice Fractions of Nearest Neighbor Tetrahedron Configurations

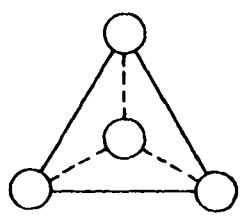

Configuration	$L1_1$	Alternate
Cu-Cu-Cu-Cu	0	1/8
Cu-Cu-Cu-Pt	1/2	0
Cu-Cu-Pt-Pt	0	3/4
Cu-Pt-Pt-Pt	1/2	0
Pt-Pt-Pt-Pt	0	1/8

Another suggestion is that the $L1_1$ structure is stabilized by the contraction of the spacing between the Cu and Pt planes. In the first place, this is in essence a many-body explanation because it requires the simultaneous positioning of a large number of Cu and Pt atoms into the correct layered positions before it can operate, and in the second place, it offers no explanation as to why the Cu and Pt move to these particular positions from the disordered phase.

We may conclude that the $L1_1$ structure is clear evidence of the importance of many-body interactions in at least one alloy system.

3) Strain Energy-Size Effects

In a binary alloy, as we have seen in Fig. 1, the optimum separation of A-A, B-B and A-B pairs are all different and the average separation in the disordered state will be some compromise distance. This departure from the optimum spacings can be regarded as a "strain" resulting from the different "sizes" of the atoms. This strain concept has often been used to explain either ordering or clustering behaviour. Ordering will reduce the strain energy because in the ordered state all (or most) of the first neighbor bonds are A-B and the lattice can relax to the optimim A-B separation. In the clustered state all of the bonds in one region are A-A and all in another region are B-B so that each region can relax separately. These ideas easily fall within the framework of the full CPW model.

However, Warren, Averbach and Roberts[22] noted that A-A, B-B and A-B near neighbor separations are often different from the average spacing and different from each other. This has been called the "size effect" and it contributes to the diffuse scattering spectrum. Thus,

$$r_i^{AA} = r_i(1+\epsilon_i^{AA});\ r_i^{BB} = r_i(1+\epsilon_i^{BB});\ r_i^{AB} = r_i(1+\epsilon_i^{AB})$$

where r_i is the average separation for ith neighbor pairs and ϵ_i^{AA} is the deviation of A-A ith neighbor pairs from that average, etc.

It is sometimes assumed that because of this displacement of atoms from the regular lattice positions any pair-wise ordering theory will be in trouble. This is not necessarily so because the A-A interaction $V^{AA}(r_i)$ can be replaced by $V^{AA}(r_i^{AA})$, etc. As long as the value of r_i^{AA} does not vary according to environment, the configurational energy will still be a simple sum of pair-wise interactions. It is actually possible to construct a lattice having a significant "size effect" but with all the nearest neighbor distances fixed according to type. A portion of such a lattice is shown in Fig. 4. The size of the atoms differ by 8% and the occupation of each site has been decided by the toss of a coin. Thus, although there is undoubtedly a size effect there is no "strain" at least from the viewpoint of nearest neighbors. This construction can also be carried out with a simple cubic lattice, but not with a bcc or close packed lattice.

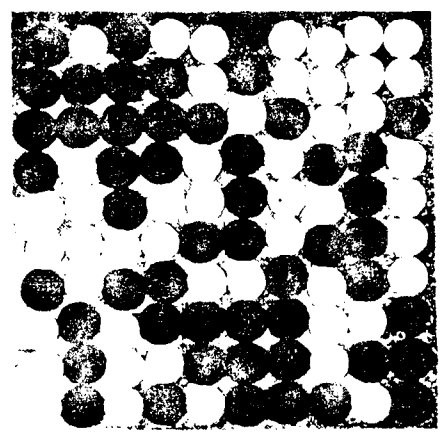

Figure 4: A disordered lattice with an appreciable size effect but no nearest neighbor strain energy.

It is really the variations in ϵ_i^{AA} etc. that cause pseudo many-body effects even when the interactions are purely pair-wise because then each A-A pair that has a different separation will have a different energy and to determine these separations (and hence energies) in a cluster we would have to know how every site in the cluster is occupied simultaneously. For instance we can expect that an A atom surrounded by 10 A atoms and 2 B atoms in a nearest neighbor shell will have a different energy depending on whether the two B atoms are on adjacent sites or on diametrically opposite sites of the shell simply because of variations in the nearest neighbor A-B distances. This is quite apart from the additional many-body effects due to real many-body forces. However as the alloy orders, the number of different atomic environments rapidly decreases, so that variations in ϵ_i^{AA} will decrease and the pseudo many-body effects will diminish as well.

Since there have been measurements only of ϵ_i^{AA} etc. but not of the variations in ϵ_i^{AA}, we can only say that we would expect the pseudo many-body effects to increase with increasing size disparity of the atoms, increasing disorder and increasing close packing of the lattice. The case of CuPt may be the result of such pseudo many-body effects. The size disparity in this case is about 3%.

4) Covalent Bonding-Line Phases

Alloys of transition metals with metalloids such as B, C, N and Si often have extremely narrow homogeneity ranges, high melting points and are quite brittle. All of these aspects indicate that even when the alloy shows metallic conduction there are strong covalent forces present in the lattice. These forces are very inadequately represented by a CPW model because of the strong angular components and because of the fact that a covalent force is essentially an interaction among atom groups (i.e. it is a many-body force). Thus a CPW model cannot really hope to give anything more than the crudest aspects of the behaviour of these compounds.

5) Triplet Correlations in AB Alloys

It has been shown[23] that in an alloy of 50-50 composition having only pair-wise interactions, three atom correlations (other than those directly produced by pair correlations) must vanish. It may soon be possible to measure three atom correlations experimentally either by kinematical diffraction[24] or by field ion microscopy[25]. If the triplet correlations were found to be non-zero this would be direct evidence for the presence of three-body interactions and the magnitude of the triplet correlations could be used to estimate the relative strength of the three-body forces.

Summary

We have shown that as long as the central pair-wise interactions are the dominant forces in an alloy, much of the alloy behaviour can be qualitatively understood. This includes average atomic configurations in the ordered and disordered phases, changes in lattice parameter with ordering, shapes of order-disorder phase boundaries, the existence of electron phases and long period superlattices, and the first order character of order-disorder phase transformations.

Areas of investigation where it was suggested that CPW interactions are not dominant or at least need to be supplemented were the vibration spectra of metal crystals, large size effect alloys, intermetallic compounds with strong evidence of covalent bonding (line phases), and apparently CuPt.

It will be important in the future to develop methods for dealing with many-body forces theoretically and to devise experimental techniques for measuring their relative strength if only to know when we are safe in using a central pair-wise approximation.

References

1. T. Muto and Y. Takagi: Solid State Physics, Vol. 1.

2. L. Guttman: Solid State Physics, Vol. 3.

3. P. C. Clapp: Phys. Rev. Letters, 1966, Vol. 16, p. 687.

4. J. Friedel: Phil. Mag., 1952, Vol. 43, p. 153.

5. J. S. Langer and S. H. Vosko: J.P.C.S., 1959, Vol. 12, p. 196.

6. R. J. Harrison and A. Paskin: J. Phys. Soc. Japan, 1960, Vol. 15, p. 1902.

7. W. A. Harrison: "Pseudo-potentials in the Theory of Metals", Benjamin, 1966.

8. T. M. Hayes, H. Brooks and A. Bienenstock: Phys. Rev., 1968, Vol. 175, p. 699.

9. G. J. Dienes: Acta Met., 1958, Vol. 6, p. 278.

10. C. W. Garland and R. Renard: J. Chem. Phys., 1966, Vol. 44, p. 1120.

11. P. C. Clapp and S. C. Moss: Phys. Rev., 1968, Vol. 171, pp. 754, 764.

12. P. A. Flinn, B. L. Averbach and M. Cohen: Acta Met., 1953, Vol. 1, p. 664.

13. S. C. Moss: Met. Soc. Conferences, 1965, Vol. 36, p. 95.

14. B. Golding, S. C. Moss and B. Averbach: Phys. Rev., 1967, Vol. 158, p. 637.

15. H. Jones: Proc. Roy. Soc., 1934, Vol. A144, p. 225.

16. J. C. Slater: Phys. Rev., 1951, Vol. 84, p. 179.

17. H. Sato and R. S. Toth: Phys. Rev., 1961, Vol. 124, p. 1833; 1962, Vol. 127, p. 469.

18. M. A. Krivoglaz: "Theory of X-ray and Thermal Neutron Scattering by Real Crystals", Plenum Press, 1969.

19. S. C. Moss: Phys. Rev. Letters, 1969, Vol. 22, p. 1108.

20. K. Fuchs: Proc. Roy. Soc., 1936, Vol. A153, p. 622.

21. E. S. Machlin: Trans. AIME, 1966, Vol. 236, p. 185.

22. B. E. Warren, B. L. Averbach and B. W. Roberts: J. Appl. Phys., 1951, Vol. 22, p. 1493.

23. P. C. Clapp: Phys. Rev., 1967, Vol. 164, p. 1018.

24. J. M. Cowley: Acta Cryst., 1968, Vol. A24, p. 557.

25. E. Gold and E. S. Machlin: Phil. Mag., 1968, Vol. 18, p. 453.

DISCUSSION

H. J. Leamy (Bell Labs): The author has shown that many historical objections to the "CPW" interaction model arose as a consequence of the large differences between experimental results and theoretical predictions based on simplified versions of the method. He has also shown that many of these objections are eliminated by application of AA, AB, and BB interactions whose strength varies with interatomic distance. Indeed, this more general formulation has been employed with some success by Leamy (Acta Met., 15, 1839 (1967)) in the analysis of the order dependence of the elastic stiffness of FeAl alloys.

There exists however, strong evidence that "CPW" interactions are not suitable for application to large core metals. In particular, Daniels and Smith (Phys.Rev., 111, 713 (1958)) have shown that the non-central component of the ion core overlap energy in the noble metals increases drastically with core size. The importance of this observation has since been emphasized by several authors (e.g., Trans.AIME, 242, 215 (1968)). It remains to be said, however, that the "CPW" interaction concept is not to be discarded on this basis alone; since the lack of tractable formulations for many body effects make it imperative that it be applied, if only to determine the occurrence and nature of such many body effects. Further, the application of experimentally justifiable "CPW" potentials to the study of the detailed atomic configurations in the neighborhood of defects in alloy crystals is sure to lead to increased understanding of their nature and effects on properties.

P. C. Clapp: I cannot really agree that the work of Daniels and Smith which you cite proves that large non-central forces are present in the noble metals. I believe that they used only a nearest neighbor central force model to fit their pressure data for the elastic constants (after a correction for the conduction electron volume force and the long-range Coulomb force). They ascribed the misfit they found to non-central forces but apparently did not consider the possibility of higher neighbor central forces. I think it would be interesting to re-analyze their data in terms of the general central force model just to see if there really is an irreducible non-central component present in these systems.

I agree with your other comments.

D. S. Lieberman (U of Illinois): Dr. Clapp's analysis seems to explain why order-disorder transformations should be first order. However, in CuAu, although the transformation to the twinned orthorhombic CuAu-II at 380-400°C is indeed first order, the transformation to tetragonal CuAu-I below 380°C is reported to be second order by Smith and Bowles (Acta Met., 8, 405 (1960)). Would Dr. Clapp care to comment as to how his theory can explain this case?

P. C. Clapp: I should hasten to point out that this model does not predict that all o-d transformations must be first order. In Garland and Renard's treatment (10) they show that ΔE (the energy discontinuity) at T_c depends on C_v (specific heat), β(bulk compressibility) and one or two other thermodynamic parameters and that the actual values of these parameters may lead to a vanishingly small ΔE as in β-brass. This may also happen in the case you cite.

S. C. Moss (M.I.T.): In deciding the stability of various forms of a single phase such as CuAu-II → CuAu-I it must always be entropy that we resort to because, as a function of temperature, only the entropy contribution can decide the question. One cannot argue the CuAu-II → CuAu-I reaction on the basis of enthalpy considerations alone.

P. C. Clapp: I agree.

This is reprinted from the book:
"Critical Phenomena in Alloys, Magnets and Superconductors"; R. E. Mills, E. Ascher and R. I. Jaffee eds., McGraw-Hill (1971)

MULTISITE CLUSTER PROBABILITIES IN ISING LATTICES

Philip C. Clapp

Ledgemont Laboratory
Kennecott Copper Corporation
Lexington, Massachusetts

ABSTRACT

If it is assumed that the configurational energy of the lattice depends only upon the pair correlations (i.e., the pair-wise interaction model) then multisite correlations can be inferred from the pair correlations by finding that value of the multisite probability distribution that maximizes the entropy within the microcanonical ensemble defined by the pair correlations.

A variational technique for carrying out this procedure will be described and applied to several examples.

I. INTRODUCTION

The first descriptions of order-disorder transformations around the turn of the century were in terms of a single long-range order

parameter, and for temperatures above the critical temperature T_c where this parameter was zero the configurational state of the system was considered to be essentially random. It soon became apparent from specific heat measurements in the vicinity of T_c that the configurational entropy did not reach the value appropriate to a completely random lattice until the temperature was very far above T_c. This residual order of a "disordered" lattice has been called short-range order (SRO) and the first attempts to quantify and describe it were in terms of a parameter that measured the nearest neighbor pair correlation.

The Ising square lattice results of Onsager[1] and Onsager and Kaufmann[2] were vitally important not only because they finally resolved the question of whether a system having only short-range interactions could achieve a cooperative transition to a state of long-range order, but because it also gave the first exact and detailed description of the propagation of spatial ordering in the SRO state in terms of the range and magnitude of pair correlations.

Characterizing the SRO state of a lattice by means of the pair correlations is now a widespread practice, partly because these are the quantities which can be measured by diffuse SRO neutron or X-ray scattering data, and partly because they are such useful theoretical functions with which to evaluate other thermodynamic properties of the system.

However, there are a number of important questions about the nature of a partially ordered lattice that cannot be answered by the pair correlation description. A frequent and surprisingly frustrating question of this kind is "What does a typical region of the SRO lattice look like?" If one tries to construct the "average" configuration of a region containing more than two sites by adjusting the occupation of sites to satisfy the average nearest neighbor correlation it will then be found that the second and higher neighbor pair correlations are, in general, not correct.

A second question is "What is the distribution in size and frequency of regions in the SRO phase that have a configuration identical to that of the perfectly ordered state?" This question is relevant to our understanding of nucleation processes as well as providing evidence for (or against) microdomain models of the SRO state.

A third question that can be important for real systems where the configuration of the ordered state is not known (usually because atomic mobility has become too sluggish at T_c) is "What is the ordered state configuration that the system is trying to achieve?"

These are all questions that, in general, require a knowledge of the many body correlations present in the SRO state and yet all the information that is normally available is in the form of pair correlations. As we shall show, this information implies a set of sum rules[3] which place definite limits on the range of values that the many body correlations can assume. By using a postulate of Information Theory[4] we can take the further step of determining the "most probable" value of the many body correlations within the range allowed by the known pair correlations and calculate multisite probability distributions for various cases of interest.

The calculation is exact if two conditions are satisfied:

(1) The configurational energy of the lattice is determined by central pair-wise interactions whose range does not exceed the dimensions of the multisite cluster.

(2) The Information Theory choice corresponds to the maximal entropy point in the configurational phase space bounded by the sum rules.

2. THEORY

Consider a cluster of n sites in some fixed geometrical relationship (e.g., a tetrahedral nearest neighbor group, a site and its nearest neighbor sites, etc.). If there are N sites in the lattice and sites are regarded as distinguishable, then there will be N different n site clusters, ignoring boundary effects. The occupation of each site is specified by $\sigma_i (= \pm 1)$. This provides the information of spin alignment (up or down) in magnetic lattices or of atomic configuration in binary alloy lattices. In any case, there will be 2^n possible configurations of the cluster, although many may be symmetrical equivalents if the geometry of the cluster possesses a symmetry.

Denote each configurational type by an index k, and the fraction of n site clusters in the lattice of one type by P_k. P_k can be interpreted equally well as the probability that a cluster chosen at random in the lattice will be of configuration type k. It is obvious that the P_k's must be positive semidefinite and satisfy the simple sum rule

$$\sum_{\{k\}} P_k = 1 \tag{1}$$

The lattice average $\langle \sigma \rangle$ of the occupation numbers σ_i (i.e., the

composition or magnetization) provides n sum rules of the form

$$\sum_{\{k\}} \sigma_j^{(k)} P_k = < \sigma > \quad (j = 1, n) \tag{2}$$

where $\sigma_j^{(k)}$ corresponds to the occupation number of the jth cluster site when it is in configuration k.

In addition, the contribution that each configurational type will make to the lattice averaged pair correlations can be calculated by inspection and leads to other sum rules, $n(n-1)/2$ in number, as follows

$$\sum_{\{k\}} \sigma_j^{(k)} \sigma_{j+p}^{(k)} P_k = < \sigma_j \sigma_{j+p} > \quad (j = 1, n; p > j) \tag{3}$$

In essence, these sum rules confine the possible P_k values to a reduced volume in P_k space. The range of P_k's within this subspace depends upon the composition and pair correlations, being largest when the pair correlations are zero and shrinking to a single point (in most cases) when the pair correlations are those of a perfectly ordered configuration. The P_k's then become completely determined.

Again regarding P_k as the probability that an arbitrarily chosen n site cluster will have the configuration k, a theorem of Information Theory[5] can be used to find the most probable values of the P_k's which are consistent with the information (the sum rules) that we do possess. The theorem states that the least biased choice for the P_k's is that set which maximizes within the allowed subspace the "ignorance function" $I(P_k)$ given by

$$I(P_k) = -\sum_k P_k \ln P_k \tag{4}$$

This theorem is based on a demonstration that any other set of P_k's would imply more information than has been given. More information of a very complicated kind may, in fact, be present due to overlapping cluster conditions that we shall now speak about.

The "ignorance function" can also be interpreted as an entropy function for a particular microcanonical ensemble. Consider the configurational entropy $W(P_k)$ obtained by placing NP_1 clusters of type 1, NP_2 clusters of type 2, etc., on a lattice of N sites in all

possible ways, disregarding overlaps. This is given by the combinatorial factor

$$W(P_k) \quad \frac{N!}{\prod_k (NP_k)!} = {}^{N}\left[-\sum_k P_k \ln P_k \right] \tag{5}$$

and is obviously identical to the "ignorance function" above, apart from the factor of N.

$W(P_k)$ is identical to the combinatorial factor used in the Cluster Variation Method developed by Kikuchi and others[6] using this particular cluster as a basis. The limitations of this expression for calculating the entropy of the lattice are well known since it counts not only all the possible lattice configurations but many more that are impossible because of incompatible overlaps. However, it is clear for our purposes that it is only the location of the maximum and not its magnitude that is of importance.

We shall propose then a postulate which, if true, would make our determination of the most probable set of P_k's an exact procedure. The postulate is: If the value of the P_k's are changed such that $W(P_k)$ is increased (decreased) then the subset of possible lattice configurations will also increase (decrease).

We cannot offer a mathematical proof of this conjecture at present, but we can say that for all the examples where the exact answer is known by other means, the postulate is apparently correct. These include four site clusters on an Ising linear chain, triplet clusters for an equi-composition three-dimensional binary lattice and nearest-neighbor triplet clusters in Cu_3Au. The latter case was determined by Gehlen and Cohen[7] using a computer simulation technique for the SRO state, and our results are compared to theirs and to the predictions of the Kirkwood superposition approximation below.

In summary, if the configurational energy depends only upon the pair correlations spanned by the n site cluster then the sum rules define a microcanonical ensemble of lattice configurations that contain many different sets of P_k's. As N is allowed to increase indefinitely the statistical law of large numbers assures us that the fraction of lattice configurations having any set of P_k's other than the most probable one becomes vanishingly small. Thus, if our postulate about the correspondence of entropy maxima is correct then we have determined exactly the distribution of multisite probabilities characteristic of the system.

3. RESULTS

A computer simulation of a typical lattice configuration in a region of 4000 sites has been carried out by Gehlen and Cohen[7] for Cu_3Au at 450°C (10 percent above T_c) based upon Moss's experimental data[8] for the first, second, and third neighbor pair correlations. Starting from either a perfectly random or a perfectly ordered configuration they used a computer to shuffle atomic configurations, accepting the new configuration only if it was more consistent with the experimental data, until a configuration was reached that had essentially the same pair correlations as the measured values. A number of properties of the final computer configurations were then measured including the various fractions of nearest neighbor triplets. Their results are given in the second and third columns of Table 1. We have calculated from the sum rules the range for the triplet probabilities allowed by the pair correlations and this is given in the first column. The most probable set of triplet probabilities according to our method is shown, as are the predictions of the Kirkwood superposition approximation[9] which is frequently used to calculate triplet probabilities. The latter method approximates a triplet probability as a product of the three pair probabilities as follows:

$$P(\sigma_1\sigma_2\sigma_3) = CP(\sigma_1\sigma_2)P(\sigma_2\sigma_3)P(\sigma_3\sigma_1) \tag{6}$$

where C is a normalization constant adjusted to make the sum of the triplet probabilities unity.

It is apparent from the table that the agreement between our results and the values of Gehlen and Cohen is very good. It suggests that our answer may well be the exact result for the infinite lattice ensemble.

TABLE 1. Nearest Neighbor Triplet Probabilities in Cu_3Au at 450°C

Triplet type	Range allowed by sum rules at $T = 450°$	*Computer Simulation* Ordered start	Random start	This calculation	Superposition approx.
Cu-Cu-Cu	0.302–0.328	0.3273	0.3275	0.3271	0.3474*
Cu-Cu-Au	0.672–0.594	0.5962	0.5956	0.5964	0.5676*
Cu-Au-Au	0.000–0.078	0.0758	0.0761	0.0759	0.0840*
Au-Au-Au	0.026–0.000	0.0007	0.0007	0.00067	0.0011

*Note that these values are outside the allowed range.

TABLE 2. Cu-Centered Cluster Distribution

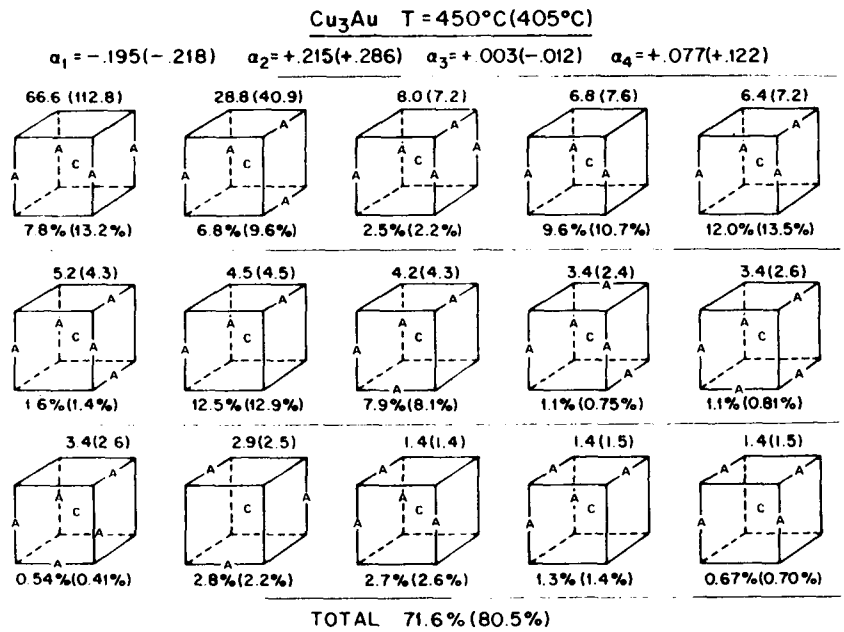

Although the superposition approximation would appear to give a reasonable estimate of the triplet probabilities, the first three values are impossible because they lie outside the range allowed by the sum rules. One may conclude that an arbitrary choice for the triplet probabilities within the allowed range would actually be better than using the superposition approximation, for this at least would produce a set of values consistent with the known alloy data.

TABLE 3. Au-Centered Cluster Distribution

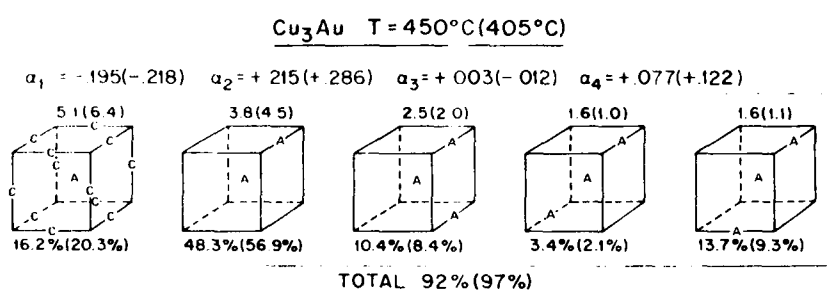

We have also employed the variational method to calculate the probability distribution for the configurations of a cluster consisting of a site and its twelve nearest neighbors in Cu_3Au. It is impractical to display the entire distribution since this would involve over 300 distinct configurations. We have instead shown in Tables 2 and 3 only the most enhanced clusters in order of their enhancement factors (EF). EF is the ratio of a cluster's population in the SRO state to its population in the completely random state.

Moss[8] has measured the SRO parameters at two temperatures above the ordering temperature in this system. Therefore it is possible to study the evolution of the cluster distribution as it approaches the long range ordered (LRO) state. The spectrum for Cu-centered clusters is shown in Table 2 and that for Au-centered in Table 3. The numbers at the lower temperature (3 percent above T_c) are shown in parentheses and those at the higher temperature (10 percent above T_c) without. The numbers above the clusters are the EF's and those below are the actual lattice fraction for each cluster (including its symmetrical equivalents). The total lattice fraction covered by the displayed clusters is given at the bottom of the figures so that the fraction of the lattice that is distributed over the rest of the 300 or so clusters is apparent.

Several interesting aspects of the distribution are immediately apparent. There is a surprising degree of "order" in the nearest neighbor (n. n.) environment even at 10 percent above T_c. In fact, 34 percent of the Cu atoms and 64 percent of the Au atoms have one mistake or less in their n. n. shell (by comparison with the n. n. environment in the perfectly ordered $L1_2$ structure). These fractions increase to 42 and 77 percent respectively at 3 percent above T_c.

The second most enhanced Cu-centered cluster is a particularly interesting type of mistake because it corresponds to the perfectly ordered environment of a different LRO arrangement variously referred to as the DO_{22} structure, the Ni_3V structure or the Cu_3Au long period ($M = 1$) superlattice. Clapp and Moss[10] have previously demonstrated that the pair interactions in Cu_3Au are such that the normal $L1_2$ Cu_3Au structure is only slightly more favored energetically than the DO_{22} structure and this is undoubtedly the source of the "confusion" in the SRO state.

It may be added that as one goes to the lower temperature, although the other Cu-centered clusters either remain at the same lattice fraction or decrease, both $L1_2$ and DO_{22} clusters increase appreciably, so that this competition apparently persists into the LRO state and may be regarded as the source of the very common (100) antiphase boundaries.

4. CONCLUSION

We have provided a set of exact sum rules that are applicable to the probability distribution of any n site cluster. These sum rules provide upper and lower bounds for the n site configuration probabilities that will ensure compatibility with the known composition and pair correlation parameters.

In addition, we have described a variational method for calculating the most probable n site distribution. This method rests upon two postulates; one physical, in the sense that it is an assumption about the nature of the atomic interactions, and the other mathematical, in that it is an assumption about the density of states in two closely related configuration spaces.

The variational method has been used to find the distribution of nearest neighbor 3-site clusters and nearest neighbor 13-site clusters in Cu_3Au. The three-site distribution could be compared to the same distribution previously determined by Gehlen and Cohen by their computer simulation technique and the results were found to be essentially identical. This provides significant support for our mathematical postulate, but not for the physical postulate because it is implicitly assumed in their procedure also.

In fact, if it becomes possible to measure n body correlations directly, any departure from the values calculated within the present scheme will provide important evidence about the relative strength of n body and pair interactions in real systems.

REFERENCES

1. Onsager, L.: *Phys. Rev.*, 65:117 (1944).
2. Kaufmann, B., and L. Onsager: *Phys. Rev.*, 76:1244 (1949).
3. Clapp, P. C.: *Phys. Rev.*, 164:1018 (1967).
4. : *J. Phys. Chem. Solids*, 30:2589 (1969).
5. Katz, A.: "Principles of Statistical Mechanics," p. 18, W. H. Freeman and Co., San Francisco, 1967; also L. Brillouin: "Science and Information Theory," Academic Press Inc., N. Y., 1962.
6. Kikuchi, R.: *Phys. Rev.*, 81:988 (1951); *J. Chem. Phys.*, 19:1230 (1951).
7. Gehlen, P. C., and J. B. Cohen: *Phys. Rev.*, 139:A844 (1965).
8. Moss, S. C.: *J. Appl. Phys.*, 12:3547 (1964).
9. Hill, T. L.: "Statistical Mechanics," pp. 195, 278, McGraw-Hill Book Co., Inc., N. Y., 1956.
10. Clapp, P. C., and S. C. Moss: *Phys. Rev.*, 171:754 (1968), and *Phys. Rev.*, 171:764 (1968).

DISCUSSION *on Paper by P. C. Clapp*

B. McCOY: While you discussed three-particle correlations in detail your method also applies to four-particle correlation. Then, as a

nontrivial check on your method, you can use the exact computation on the four-particle correlation[1] of the two-dimensional Ising model in zero magnetic field.

P. C. CLAPP: I was not aware of this work and I thank you for bringing it to my notice.

C. DOMB: If you are not concerned with the immediate neighborhood of the critical point, you can certainly use series expansions for any of the multiple correlations. It is only when it is necessary to assess critical behavior (say within 1 percent of the critical point) that difficulties arise in assessing the precise asymptotic form of the coefficients. Elsewhere the Padé approximant, for example, should give an approximation accurate enough for testing the hypothesis.

L. ONSAGER: In the Ising model that I solved, one could not only obtain the four-particle correlations but also the three-particle correlations below the critical temperature (where they are nonzero). These could be used to test your own method.

REFERENCES

1. Computed by Y. Y. Stephenson, *J. Math. Phys.*, (1964).

PHYSICAL REVIEW B VOLUME 4, NUMBER 2 15 JULY 1971

Atomic Configurations in Binary Alloys

Philip C. Clapp
Edgemont Laboratory, Kennecott Copper Corporation, Lexington, Massachusetts 02173
(Received 21 January 1971)

The configurational probability distribution of nearest-neighbor configurations has been inferred for a number of cubic binary alloys from their experimentally determined short-range order parameters. The probability variation method, derived previously, was used to perform the calculations. This procedure, which is used to generate n-site probabilities from experimentally measured pair probabilities, requires the physical assumption that the configurational energy of the system can be adequately represented by pairwise interactions whose range does not exceed the diameter of the cluster. Results are presented here for β-CuZn, Cu_3Au, CuAu, Au_3Cu, $Cu_{85}Al_{15}$, $Cu_{52}Ni_{48}$, and $Au_{60}Pd_{40}$, and the implications for ordering (or clustering) behavior are discussed. Finally, tables of coefficients for the bcc and fcc lattice are given to enable one to carry out this type of analysis for any cubic binary system.

I. INTRODUCTION

In a previous paper[1] (hereafter referred to as I) a systematic procedure was presented for using the measured values of Warren short-range order (SRO) parameters $\{\alpha_i\}$ in binary alloys to make a "best" prediction of the probability distribution of n-site atom configurations (where n can be 10 or more). These multisite probability distributions are potentially important for understanding nuclea-

tion processes, unraveling Mössbauer spectra, estimating the distribution of strain fields at the atomic level, or simply visualizing the configurational state of a partially ordered binary system. It also offers a powerful method for predicting the atomic configuration of equilibrium low-temperature phases from high-temperature data, even when such phases are prevented from forming for kinetic reasons.

This predictive procedure was called the probability variation method (PVM), and it can be briefly summarized. If $P_k^{(n)}$ is the probability that an n-site cluster chosen randomly in the lattice is of configuration type k, then the PVM determines the $P_k^{(n)}$ by varying them to maximize the function $I = -\sum_k P_k^{(n)} \ln P_k^{(n)}$ subject to a set of linear constraints that ensure that the composition and SRO parameters of the alloy remain fixed. The method rests upon the physical assumption that the configurational energy of the lattice depends only upon the composition and the α_i's, and thus remains constant during the variation of the $P_k^{(n)}$'s. This is equivalent to assuming that there are no important contributions to the configurational energy from three- or more-body interactions in the crystal. The PVM can then be regarded as a technique for finding the $P_k^{(n)}$'s that maximize the entropy of a microcanonical ensemble of configurational states. It was also shown in I that this microcanonical ensemble contains many more configurational states than are possible on a real lattice. A plausibility argument was given that the maximal entropy point of the real lattice ensemble always coincided with the maximal point of the artificial ensemble used in the calculations. This mathematical assumption could not be rigorously proven but was shown to be valid for a number of cases where the exact result was previously known. At the very least the PVM yields a set of P_k's that are consistent with the experimental data on composition and SRO of the alloy. This is a significant advantage relative to other analytical methods of determining the probability distribution (such as the Kirkwood superposition approximations) that do not satisfy such self-consistency conditions.

In the present paper we have used the PVM to determine the probability distribution of a cluster consisting of a central site and all its nearest neighbors for a number of cubic alloys. In particular we have analyzed β-CuZn, Cu_3Au, CuAu, Au_3Cu, $Cu_{85.5}Al_{14.5}$, $Cu_{52}Ni_{48}$, and $Au_{60}Pd_{40}$ using the available experimental SRO data for these systems. We find that the most enhanced cluster configuration relative to the perfectly random distribution for the alloys β-CuZn, Cu_3Au, and CuAu is the configuration of the perfectly ordered state in each case. The surprising result emerges in Au_3Cu that at a temperature 11% above the ordering temperature the most enhanced configuration appears to be the perfectly ordered configuration of CuAu. We shall offer below several possible explanations of this result.

The $Cu_{85.5}Al_{14.5}$ results show a strong enhancement of a tetrahedral cluster of Al atoms about a central Cu atom reminiscent of the metastable ordered bcc β phase found at the Cu_3Al composition. This supports the picture of the SRO state in this system proposed by Borie and Sparks.[2] It also explains why Gehlen and Cohen[3] found so few of these tetrahedral clusters in a computer mapping of this system since, although the tetrahedral cluster is strongly enhanced, the volume fraction of the lattice occupied in this way is still very small.

The $Cu_{52}Ni_{48}$ distribution shows primarily Cu- and Ni-rich clusters but with a marked tendency to cluster on (111) planes. This agrees with the model proposed by Cohen[4] from his computer mapping of the SRO state. Further evidence in support of the growth of Ni and Cu platelets on (111) planes is given below on the basis of the pair interactions in this alloy previously determined by Moss and Clapp.[5]

The distributions derived for the $Au_{60}Pd_{40}$ alloy indicate a definite tendency for this system to order but it is difficult to decide what the configuration of the hypothetical perfectly ordered state is. The equilibrium phase diagram indicates a single solid solution for all compositions so that the ordering temperature is apparently too low for the ordering reaction to ever go to completion. Lin, Spruiell, and Williams[6] have recently suggested a particular configuration for the ordered crystal on the basis of a computer simulation of the SRO state. Our distribution partially supports their conclusion but also suggests that the real answer may be even more complicated.

II. PROBABILITY VARIATION METHOD

The first step in applying the PVM is to choose the n-site cluster to be studied. A cluster large enough to show many details of the ordering process but small enough for the calculations to be manageable consists of a site and all of its nearest neighbors. The next step is to tabulate all of the possible configurations of this cluster and to evaluate by inspection the contribution that each configuration will make to the lattice composition and pair correlations. This was done in I for the simple example of a triplet cluster and the results were presented there in Table I. Similar tabulations for the nearest-neighbor cluster on bcc and fcc lattices are given in the Appendix. The third step is to construct the linear equations for the P_k's where the jth equation will be of the form

$$\sum_{k=1}^{K} a_j^k P_k = b_j \quad (j = 1, J) \,. \tag{1}$$

The a_j^k's are determined from the cluster tables and the b_j's are set by the composition and SRO

TABLE I. Nearest-neighbor spectrum of Cu atoms in CuZn at $T = 543°C$ $(T/T_c = 1.10)$.

CuZn T = 543°C $(T/T_C = 1.10)$

$\alpha_{111} = -.179$ $\alpha_{200} = +.103$ $\alpha_{220} = +.066$ $\alpha_{222} = +.045$

7.6	3.4	2.0	1.7	1.5
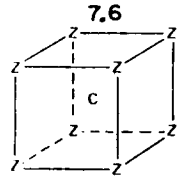	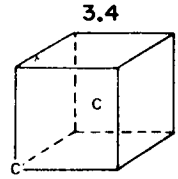	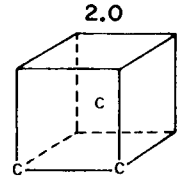	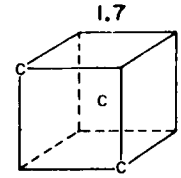	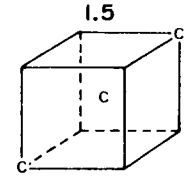
3.0%	10.7%	9.2%	7.8%	2.4%
1.2	1.0	.96	.93	.88
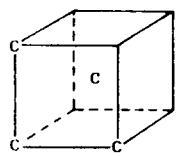	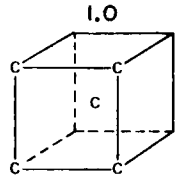	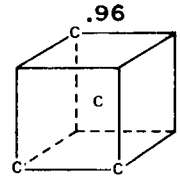	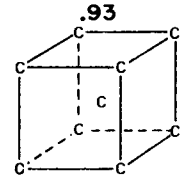	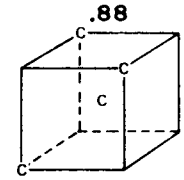
11.8%	2.4%	8.9%	.4%	2.7%
.87	.79	.73	.69	.67
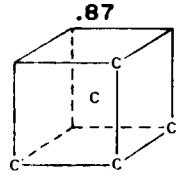	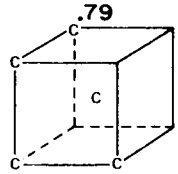	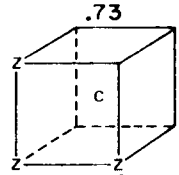	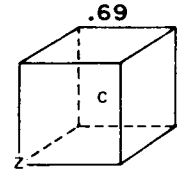	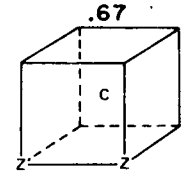
2.7%	7.4%	6.7%	2.2%	3.1%
.67	.61	.56	.56	.51
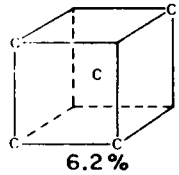	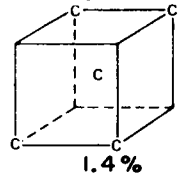	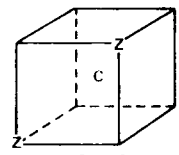	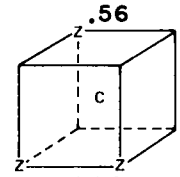	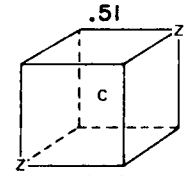
6.2%	1.4%	2.6%	5.3%	.80%
.51	.51			
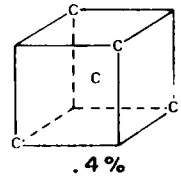	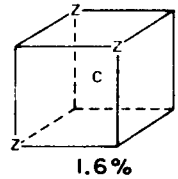			
.4%	1.6%			

TOTAL 100%

data. These equations are also contained in the Appendix.

The number of linear equations J is always exceeded by K, the number of unknowns (the P_k's); with additional conditions that each P_k must not be less than zero, the possible range of each P_k may be quite small. In fact, if the pair correlations are assigned the values corresponding to a perfectly ordered structure, the P_k's will become completely determined.

So far no approximations have been introduced, and any set of P_k's that satisfies the above conditions would represent a possible state of the lattice. If the P_k's are sufficiently limited by these conditions, it may not be necessary to go further. However, when the lattice contains a substantial degree of disorder, it is desirable to determine the most probable set of P_k's. It was pointed out in I that this most probable set will represent the state of the lattice all but a negligible fraction of the time.

It is impossible to proceed further by any method without making some assumption about the configurational energy of the lattice. The basic hypothesis of the PVM has been stated in Sec. I and is essen-

tially that the configurational energy can be expressed as

$$E = \sum_{i=1}^{m} V_i \alpha_i \ , \tag{2}$$

and that m, the maximum neighbor index in the summation, does not exceed the maximum neighbor separation contained in the cluster. For the cluster chosen here, m would correspond to fifth neighbors in a bcc lattice and fourth neighbors in a fcc lattice. The V_i's are pairwise interaction parameters.

The final step is to maximize the PVM entropy measure

$$I(P_k) = -\sum_{k=1}^{K} W_k P_k \ln P_k \tag{3}$$

by variation of the P_k's subject to the linear constraints given in Eq. (1). W_k is the multiplicity of the kth configuration and represents the number of configurations that are equivalent under cubic symmetry. Formally, the variation can be accomplished by the introduction of a Lagrange multiplier λ_j for each constraint, forming the augmented function $I'(P_k)$ given by

$$I'(P_k) = I(P_k) + \sum_{j=1}^{J} \lambda_j C_j(P_k) \ , \tag{4a}$$

where

$$C_j(P_k) = \sum_{k=1}^{K} a_j^k P_k - b_j \ . \tag{4b}$$

The P_k's can now be regarded as independent variables and the maximum of $I(P_k)$ is determined by the equations

$$\frac{\partial I(P_k)}{\partial P_k} = 0 = -W_k(1 + \ln P_k) + \sum_{j=1}^{J} \lambda_j a_j^k \qquad (k = 1, K) \ . \tag{5}$$

Thus,

$$P_k = \exp\left(W_k^{-1} \sum_{j=1}^{J} \lambda_j a_j^k - 1\right) . \tag{6}$$

The λ_j's are now adjusted to satisfy the J linear constraints. This is accomplished by inserting this expression for the P_k's into Eq. (1), giving J nonlinear equations in J unknowns (the λ_j's). An iterative method for determining the P_k's can then be used.

III. ATOMIC CONFIGURATION DISTRIBUTION

In this section the distributions of nearest-neighbor configurations are displayed for a number of alloys as determined by the PVM from available SRO data. In the case of fcc systems it is impractical to present the entire distribution since this would involve over 300 distinct configurations. We have instead shown only clusters having enhancement factors (EF) greater than 1 and have shown only the first dozen or so. The EF is the ratio of a cluster's population in the SRO state to its population in an ideal random alloy of the same composition. The clusters are displayed in the order of their EF's whose magnitudes are given above each cluster. In addition, the percent of atoms in the lattice *of a given kind* that have that particular nearest-neighbor configuration (or one of its symmetrical equivalents) is given in parentheses beneath each cluster. The total percent of the distribution shown is indicated at the bottom of the table. A cluster can have a larger EF but a smaller lattice percentage than another cluster simply because the percentage of the latter cluster was higher in the completely random state. We have also used the convention of indicating the positions of only one kind of atom on the nearest-neighbor shell, the unlabeled positions being occupied by the other atom type.

β-CuZn

The complete nn spectrum of a Cu atom at 543 °C (10% above the ordering temperature) is shown in Table I for this bcc alloy as determined from the SRO parameters reported by Walker and Keating.[7] Although the actual alloy contained 53.7-at.% Cu, the SRO parameters were determined on the basis of an equiatomic model and we have followed this assumption of a 50-50 alloy in our analysis. Thus the distribution for a Zn-center atom is obtained by interchanging Zn and Cu sites everywhere in Table I.

Qualitatively, the distribution is as one would expect. The most enhanced cluster is that representing the nearest-neighbor configuration in the perfectly ordered lattice, the next most enhanced is the "one-mistake" cluster, and the next three are the three possible "two-mistakes" clusters. A model of the SRO state based on the idea of perfectly ordered regions in a disordered matrix does not seem justified for this system. Since only 3% of the Cu (or Zn) atoms see a perfectly ordered nearest-neighbor environment, the volume fraction of such "microdomains" could be 3% at most.

Cu_3Au

Moss[8] has measured the Warren SRO parameters at two temperatures above the ordering temperature in this system. Therefore, it is possible to determine the cluster distribution at these two temperatures and study the evolution of the SRO state as it approaches the long-range ordered (LRO) state. The distribution for Cu-centered clusters is given in Table II and that for Au-centered clusters in Table III. The numbers at the higher temperature (10% above T_c) are shown without parentheses and those for the lower temperature (3% above T_c) are

TABLE II. Nearest-neighbor spectrum of Cu atoms in Cu_3Au at $T = 450\,^{\circ}C$ (405 °C).

Cu_3Au T = 450°C(405°C)

$\alpha_1 = -.195(-.218)$ $\alpha_2 = +.215(+.286)$ $\alpha_3 = +.003(-.012)$ $\alpha_4 = +.077(+.122)$

66.6 (112.8)	28.8 (40.9)	8.0 (7.2)	6.8 (7.6)	6.4 (7.2)
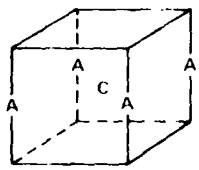	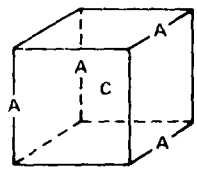	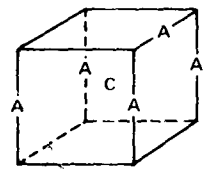	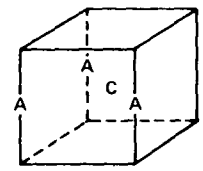	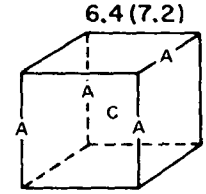
7.8% (13.2%)	6.8% (9.6%)	2.5% (2.2%)	9.6% (10.7%)	12.0% (13.5%)
5.2 (4.3)	4.5 (4.5)	4.2 (4.3)	3.4 (2.4)	3.4 (2.6)
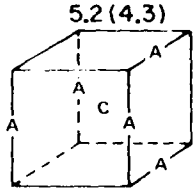	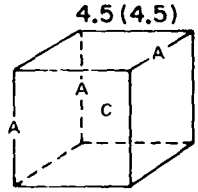	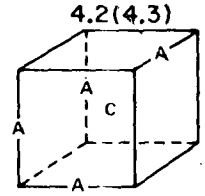	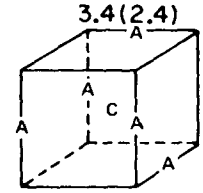	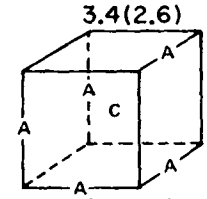
1.6% (1.4%)	12.5% (12.9%)	7.9% (8.1%)	1.1% (0.75%)	1.1% (0.81%)
3.4 (2.6)	2.9 (2.5)	1.4 (1.4)	1.4 (1.5)	1.4 (1.5)
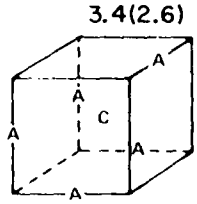	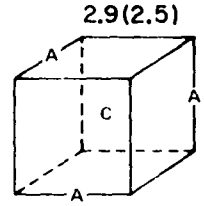	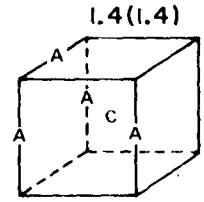	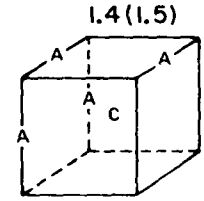	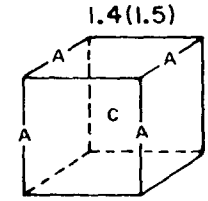
0.54% (0.41%)	2.8% (2.2%)	2.7% (2.6%)	1.3% (1.4%)	0.67% (0.70%)

TOTAL 71.6% (80.5%)

in parentheses.

Several interesting aspects of the distribution are immediately apparent. There is a surprising degree of "order" in the nearest-neighbor environment even at the higher temperature. The Cu-centered perfect-order cluster is very highly enhanced as compared to the comparable cluster in the Cu-Zn distribution at the same relative temperature. In fact, 34% of the Cu atoms and 64% of the Au atoms have one mistake or less in their nearest-neighbor shell at $T = 1.10T_c$. These fractions increase to 42 and 77%, respectively, at $T = 1.03T_c$.

TABLE III. Nearest-neighbor spectrum of Au atoms in Cu_3Au at $T = 450\,^{\circ}C$ (405 °C).

Cu_3Au T = 450°C(405°C)

$\alpha_1 = -.195(-.218)$ $\alpha_2 = +.215(+.286)$ $\alpha_3 = +.003(-.012)$ $\alpha_4 = +.077(+.122)$

5.1 (6.4)	3.8 (4.5)	2.5 (2.0)	1.6 (1.0)	1.6 (1.1)
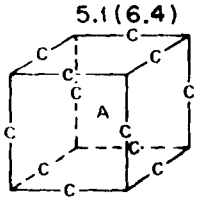	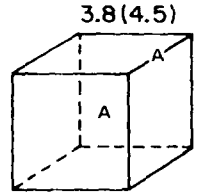	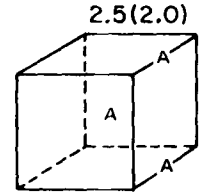	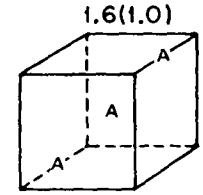	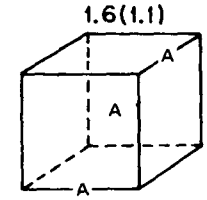
16.2% (20.3%)	48.3% (56.9%)	10.4% (8.4%)	3.4% (2.1%)	13.7% (9.3%)

TOTAL 92% (97%)

TABLE IV. Nearest-neighbor spectrum of Cu atoms in CuAu at $T = 425$ °C ($T/T_c = 1.025$).

CuAu T = 425°C (T/Tc = 1.025)

$\alpha_1 = -.123$ $\alpha_2 = +.048$ $\alpha_3 = +.000$ $\alpha_4 = +.070$

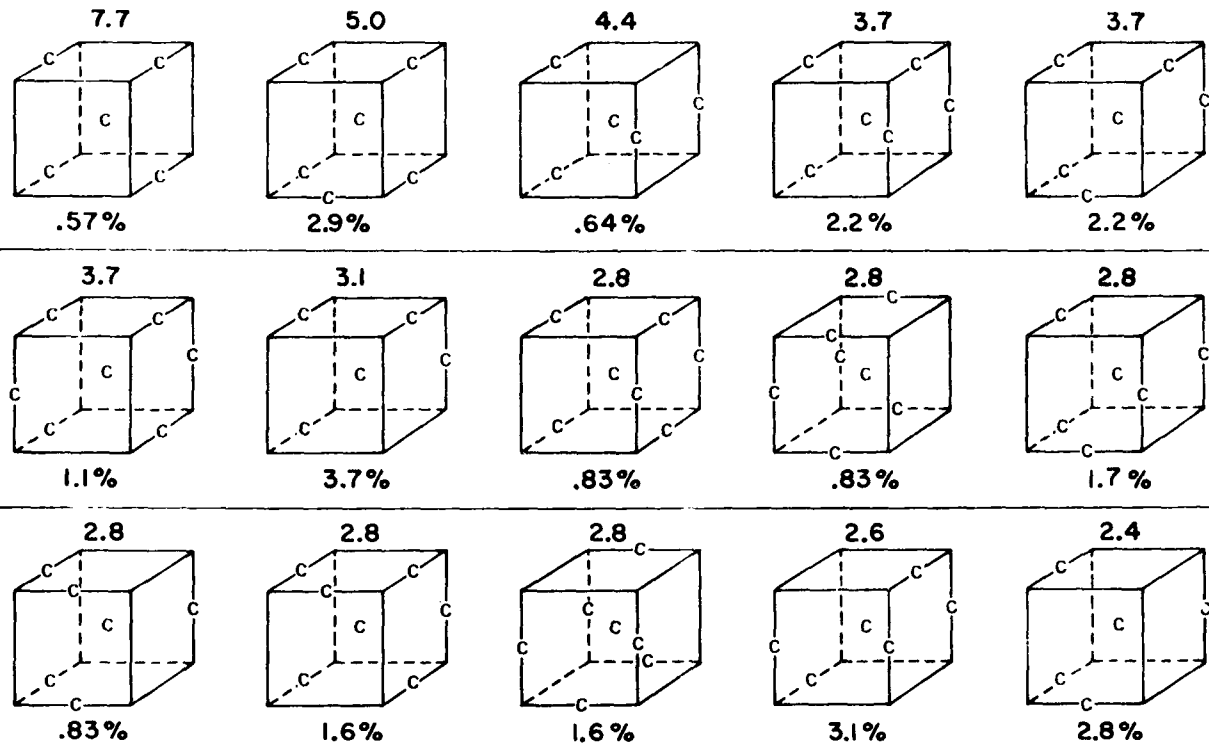

TOTAL 26.5 %

The second most enhanced Cu-centered cluster is a particularly interesting type of mistake because it corresponds to the perfectly ordered environment of a different LRO arrangement variously referred to as the DO_{22} structure, the Ni_3V structure, or the Cu_3Au M 1 long-period superlattice. Moss and Clapp[5] have previously demonstrated that the pair interactions in Cu_3Au are such that the normal $L1_2$ Cu_3Au structure is only slightly more favored energetically than the DO_{22} structure and this is undoubtedly the source of the "confusion" in the SRO state. It may be added that as one goes to the lower temperature although the other Cu-centered clusters either remain at the same lattice fraction or decrease, both the $L1_2$ and DO_{22} clusters increase appreciably so that this competition has a marked persistance and will appear in the LRO state as (001)-type antiphase boundaries.

CuAu

The SRO data of Roberts[9] at $T = 1.025T_c$ were used to generate the cluster distribution shown in Table IV. At this temperature the tendency to order into the $L1_0$ structure is apparent but there is still a considerable degree of disorder present in the nearest-neighbor environment and the perfect-order cluster does not show nearly the same degree of dominance here as compared to the case of Cu_3Au.

Au_3Cu

In Tables V and VI the rather surprising distribution for Au_3Cu is given as derived from the SRO measurements of Batterman.[10] It is normally thought that Au_3Cu orders in the $L1_2$ structure; but the most enhanced Cu-centered clusters are of the $L1_0$ CuAu type, and the fourth most enhanced cluster is even of the Cu_3Au type. The Au-centered cluster distribution is less paradoxical but it also shows a significant number of strongly enhanced clusters of the $L1_0$ CuAu type. If true, this would suggest that the ordering process in Au_3Cu is rather complex and implies that the transformation may actually be to an ordered $L1_0$ CuAu phase intermixed with a Au-rich phase rather than to a homogeneous $L1_2$ Au_3Cu phase. Since the superlattice reflections cannot distinguish between these two possibilities, the

fundamental reflections would have to be examined for appreciable broadening or splitting in the transformed state. The transformation is quite sluggish, however, so that it may require long times before the splitting of the fundamental spots is observable.

On the other hand, the SRO measurements in Au_3Cu are particularly difficult because of large-size-effect scattering and because of the difficulty in achieving equilibrium. Thus, the measured α's may be inaccurate and if the errors were significant this would considerably distort the derived distributions.

Cu-14.5% Al

The α's as determined by Houska and Averbach[11] from powder samples at −190 °C were used to calculate the cluster distribution in Table VII. The SRO structure of this alloy has been of considerable interest ever since the radiation-damage experiments of Wechsler and Kernohan[12] showed that the electrical resistivity first decreases and then increases with increasing exposure time in a reactor. It was surmised that this anomalous behavior was connected with the induced changes in the SRO of the alloy. Houska and Averbach also determined the α's for an irradiated sample and found that all of the SRO parameters increased in magnitude relative to the normal sample, indicating a pronounced increase in the degree of the SRO. However, the value of α_1 that they report is 20% greater than the maximum theoretical limit for an alloy of this composition, which makes it impossible to generate the cluster distribution for the irradiated alloy. This error indicates that either the actual composition of the alloy was in excess of 17-at.% Al or the SRO diffuse scattering was not correctly separated from the other diffuse scattering contributions.

Borie and Sparks[2] afterwards performed a more detailed diffuse-scattering experiment in two planes of reciprocal space for single-crystal samples of Cu–16% Al alloys before and after irradiation. On the basis of their measurements, they suggested an interesting model for the SRO structure. They proposed that the Al atoms for the most part were grouped in tetrahedral clusters (the first cluster shown in Table VII) and that no Al nearest-neighbor

TABLE V. Nearest-neighbor spectrum of Cu atoms in Au_3Cu at $T = 250$ °C ($T/T_c = 1.11$).

Au_3Cu $T = 250°C$ $(T/T_C = 1.11)$

$\alpha_1 = -.06$ $\alpha_2 = +.20$ $\alpha_3 = -.08$ $\alpha_4 = +.14$

18.5	5.1	4.5	3.3	2.8
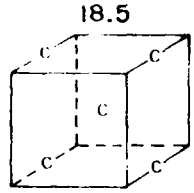	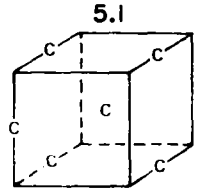	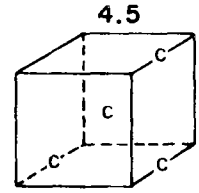	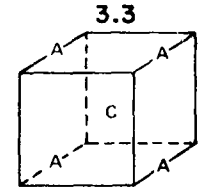	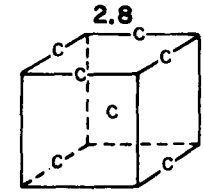
2.16 %	1.59%	6.37%	.005 %	.15%
2.8	[illegible]3	2.1	2.1	1.9
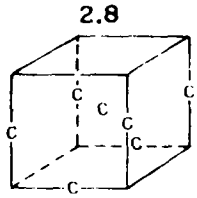	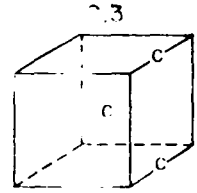	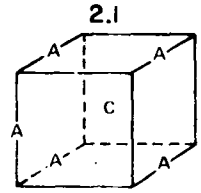	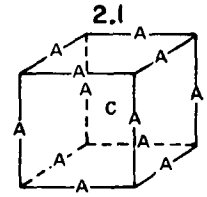	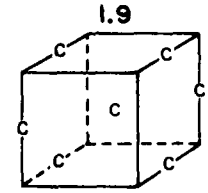
.15 %	[illegible]5%	.08%	6.64 %	.10%
1.7	1.5	1.5	1.5	1.3
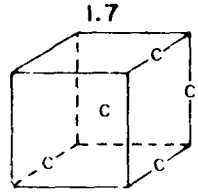	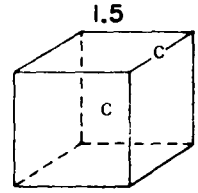	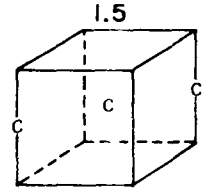	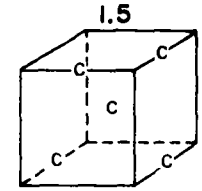	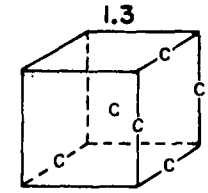
3.21%	19.3%	3.14%	2.75%	.41%

TOTAL 55.6%

TABLE VI. Nearest-neighbor spectrum of Au atoms in Au_3Cu at $T = 250$ °C $(T/T_c = 1.11)$.

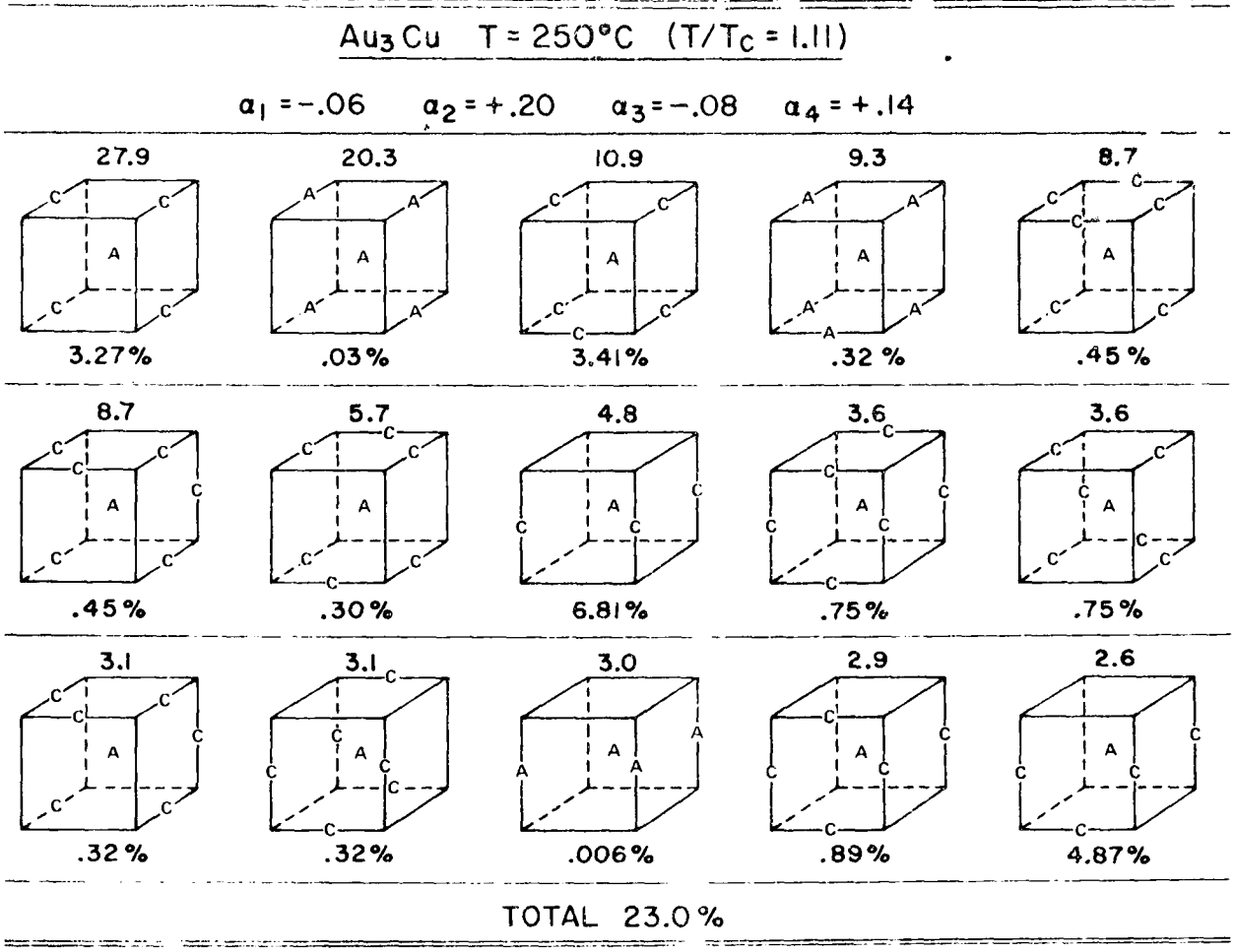

pairs occurred. To further support their model, they observed that the β_1-Cu_3Al metastable phase, which is an ordered DO_3 (BiF_3) structure and appears by quenching the bcc disordered β phase, may be described as an array of regular Al tetrahedra. Although the proposed Al groups in the fcc SRO phase are not regular tetrahedra (two sides are second-neighbor distances and four are third-neighbor distances), they are close to being so and the measured atomic displacements were of the right sign to improve the congruence.

Although their model is provocative, neither of their conjectures can be proven with certainty by their data and even within the framework of their model a considerable degree of freedom remains in the picture of the SRO structure arising from the various ways one can pack the tetrahedral groups.

Gehlen and Cohen[3] took issue with the tetrahedral model on the basis of a computer simulation of the SRO structure that they generated using the SRO parameters of Houska and Averbach[11] (since the diffraction data of Borie and Sparks gives linear combinations of the α's but not the α's individually). By visually scanning their computer-simulated patterns, they concluded that the dominant feature of the SRO structure consisted of linear chains of Al atoms in second-neighbor relationships and that isolated tetrahedral clusters were hardly ever observed.

Our cluster distribution in Table VII supports both models and shows that they are complementary rather than contradictory views of the SRO structure. On the one hand, by far the most enhanced cluster in the distribution is the tetrahedral group proposed by Borie and Sparks, so that the tendency of the system is quite clear. On the other hand, the lattice fraction of such clusters is still very small, so that they would not be a striking feature of an SRO configuration map. The tendency for Al atoms to avoid each other as nearest neighbors is also apparent since the only Al-centered cluster that is enhanced relative to the random state contains no Al atoms in its nearest-neighbor shell and constitutes 72% of the Al sites. This fraction undoubtedly approaches 100% in the irradiated samples.

Furthermore, the Al chains of Gehlen and Cohen will form a tetrahedral group at their point of closest approach if that separation is a second-neighbor distance and the chains are orthogonal. If they are parallel, they will form an array of square groups, which is the second most enhanced cluster in our distribution. Given the high density of chains necessary to account for the Al concentration and realizing that a nearest-neighbor approach of chains is nearly forbidden leads one to the conclusion that second-neighbor chain interactions will occur quite frequently in the Gehlen-Cohen scheme. Finally, one may observe that the Cu_3Al (DO_3) structure can be viewed as either a perfect array of second-neighbor Al chains separated by second-neighbor distances or as a perfect stacking of Al tetrahedra.

$Cu_{52}Ni_{48}$

Recently Mozer, Keating, and Moss[13] have determined the SRO parameters of this alloy at 550 °C from a diffuse-neutron-scattering measurement. The Cu-Ni phase diagram indicates a homogeneous solid solution across the entire composition range but it is now generally agreed from thermodynamic data and SRO studies that Cu-Ni is potentially a clustering system with the predicted miscibility gap maximum at about 300 °C and 70-at.% Ni. Our calculated cluster distributions shown in Tables VIII and IX give further evidence for this tendency and provide some interesting information about the morphology of the pre-precipitation stage (actual precipitation does not occur presumably because of the low transformation temperature).

Although practically all of the enhanced clusters show that the central atom prefers to surround itself with its own kind, the other species appear to segregate on (111) planes. Over half the tabulated configurations can be classified in this manner if no more than one mistake is allowed, and this suggests that the clustering occurs as (111) platelets of each kind. This conjecture is supported by a prior study of Cohen,[4] who made a computer simulation of the SRO state of this alloy and noticed these (111) platelets as a significant feature of his configurations.

TABLE VII. Nearest-neighbor spectrum in $Cu_{85.5}Al_{14.5}$.

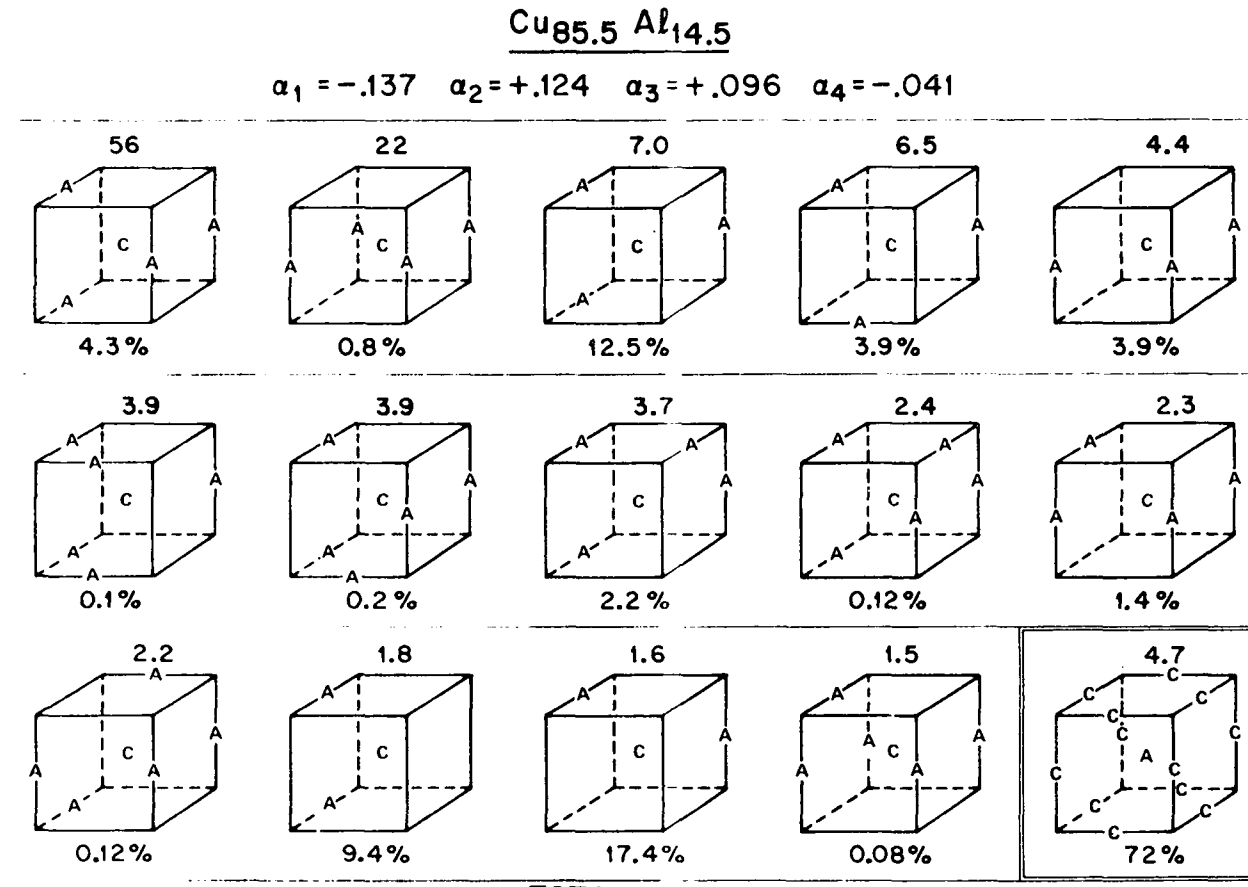

TABLE VIII. Nearest-neighbor spectrum of Cu atoms in $Cu_{52}Ni_{48}$.

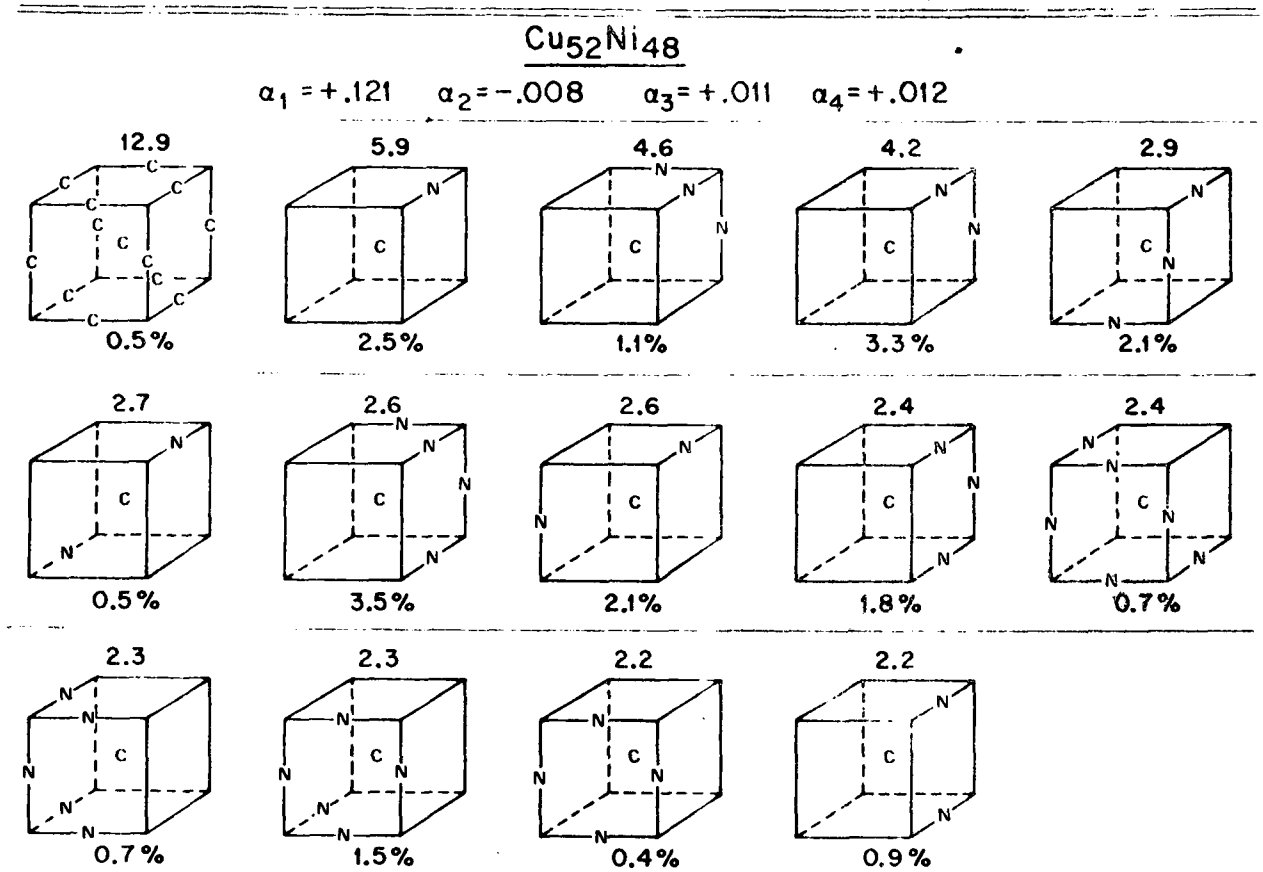

In addition, Moss and Clapp[5] have determined the strengths of first- and second-neighbor interactions in this alloy and found that the second-neighbor interactions (V_2) were negative (meaning that second neighbors prefer to be unlike) and from 50 to 65% as strong as the positive first-neighbor interaction (V_1). This places the alloy close to the limit of stability for phase separation on their lowest-energy structure diagram (Fig. 6 of Ref. 14) and adjacent to the energy region of stability for the $L1_1$ (CuPt-type) ordered structure. The $L1_1$ structure consists of alternate atomic (111) planes of each type and can be regarded as the atomic limit of the (111) platelet morphology.

Assuming that $V_2 = -\frac{2}{3}V_1$, one can calculate that the energy gained by replacing a Cu atom at the edge of a (111) Ni platelet by a Ni atom from the disordered matrix would be $2V_1$, as opposed to only V_1 for the binding energy of a site on the top or bottom surface of the platelet. This calculation assumes the average environment of an edge site would contain two Ni atoms of the platelet as nearest neighbors but no platelet atoms as second neighbors, whereas a surface site would have three Ni nearest neighbors and three Ni second neighbors if the platelet were two or more atom layers thick. Thus one can expect from the energetics that in the nucleation phase the platelets would initially expand their diameter more rapidly than they would thicken, giving large thin regions of each kind of atom lying on (111) planes. We can then explain the structure of the SRO state as being simply the precursor of this predicted mode of growth.

A further prediction can be made that since the relative binding energies of surface and edge sites will be a very sensitive function of the ratio of V_2 to V_1 in this alloy, one can expect large changes in the precipitate morphology (if precipitation can be induced) and large changes in the SRO structure as a result of small variations in V_2/V_1. Pressure or alloy additions should be sufficient to see these effects.

$Au_{60}Pd_{40}$

The Au-Pd binary diagram indicates a homogeneous solid solution at all compositions. However, the relative heats of formation show a maximum negative value at the 40-at.% Pd composition. The

largest anomalous changes in electrical resistivity and Hall constant after cold work and the greatest resistivity recovery upon annealing also occur at this composition. These facts suggest that a significant amount of SRO is present in this particular alloy and led Lin, Spruiell, and Williams[6] to measure the SRO parameters by means of x-ray diffuse scattering. The measurements were made at room temperature on a single-crystal sample that had been slowly cooled from 1050 °C.

We have used the first four SRO parameters determined by Lin, Spruiell, and Williams to generate the Pd-centered cluster distribution shown in Table X and the Au-centered cluster distribution displayed in Table XI. The Pd-centered distribution is more easily analyzed and we shall confine our attention to it.

The most enhanced cluster is a tetrahedral arrangement of four Pd atoms about the central Pd atom. This is precisely the nearest-neighbor environment that an atom would have in the hypothetical AB analog of the DO_{22} structure proposed by Clapp and Moss,[14] and shown below in Fig. 1. On the basis of their analysis, Lin, Spruiell, and Williams have in fact suggested that this is the ordered structure that the system is tending toward and if so would be the first known example of this atomic arrangement in alloys. The ordered structure may also be described as an $M = 1$ antiphase derivative of the $L1_0$ (CuAu) structure. This is perhaps significant because the second most enhanced cluster is the nearest-neighbor configuration of the $L1_0$ structure itself. All but two of the subsequent nine most enhanced clusters are single-defect relatives of one or the other of these first two clusters. Although the $M = 1$ antiphase structure does not contain any $L1_0$-type clusters, an $M = 2$ (and all higher M) antiphase structure will have a mixture of these two cluster types. The $M = 2$ structure is shown in Fig. 2. The proportion of $L1_0$-type clusters increases as M increases and the $L1_0$ lattice may be regarded as the limit as M approaches infinity.

Although Lin, Spruiell, and Williams may be correct in their conjecture that the $M = 1$ structure is the ultimate ordered state of this system, from

TABLE IX. Nearest-neighbor spectrum of Ni atoms in $Cu_{52}Ni_{48}$.

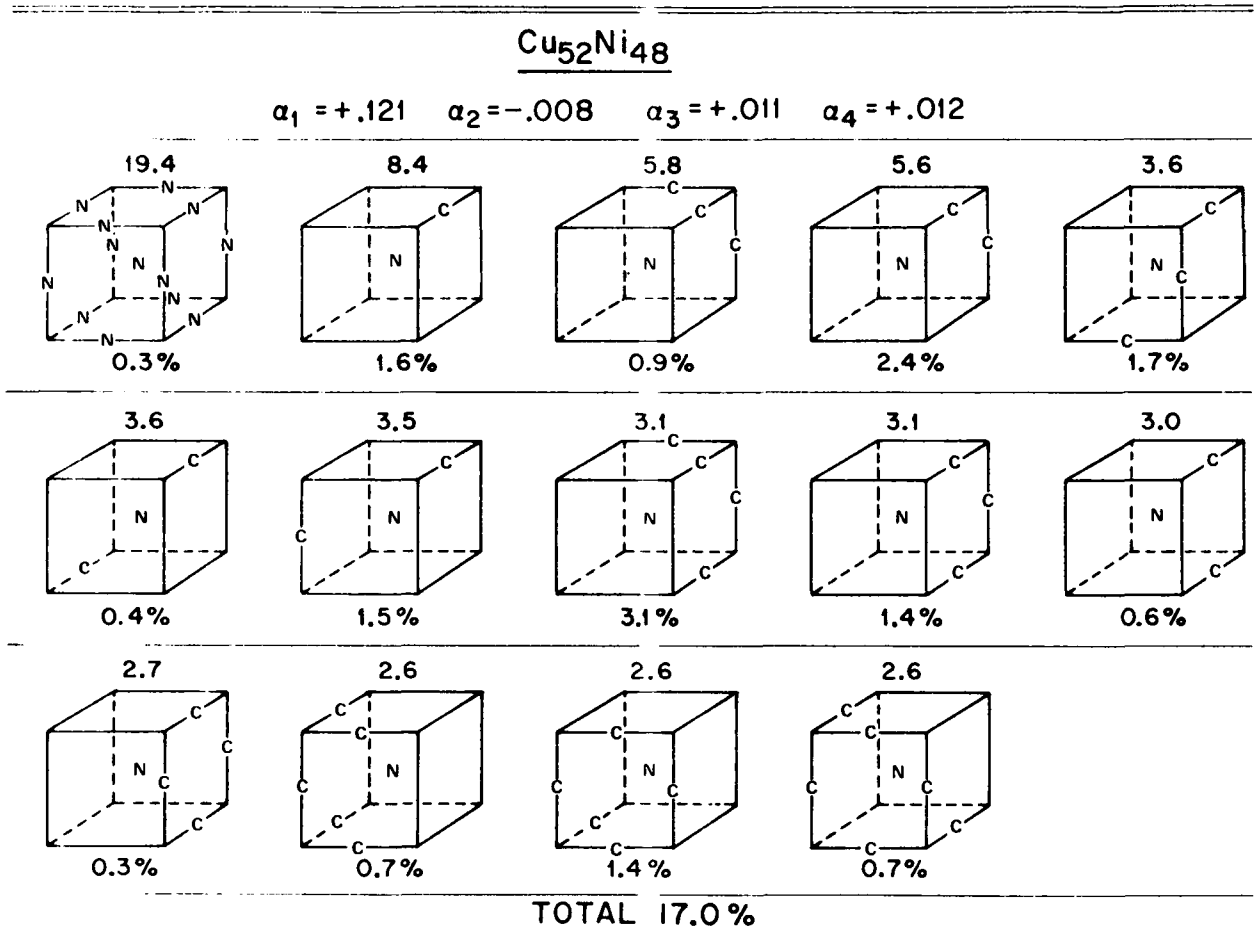

TABLE X. Nearest-neighbor spectrum of Pd atoms in $Au_{60}Pd_{40}$.

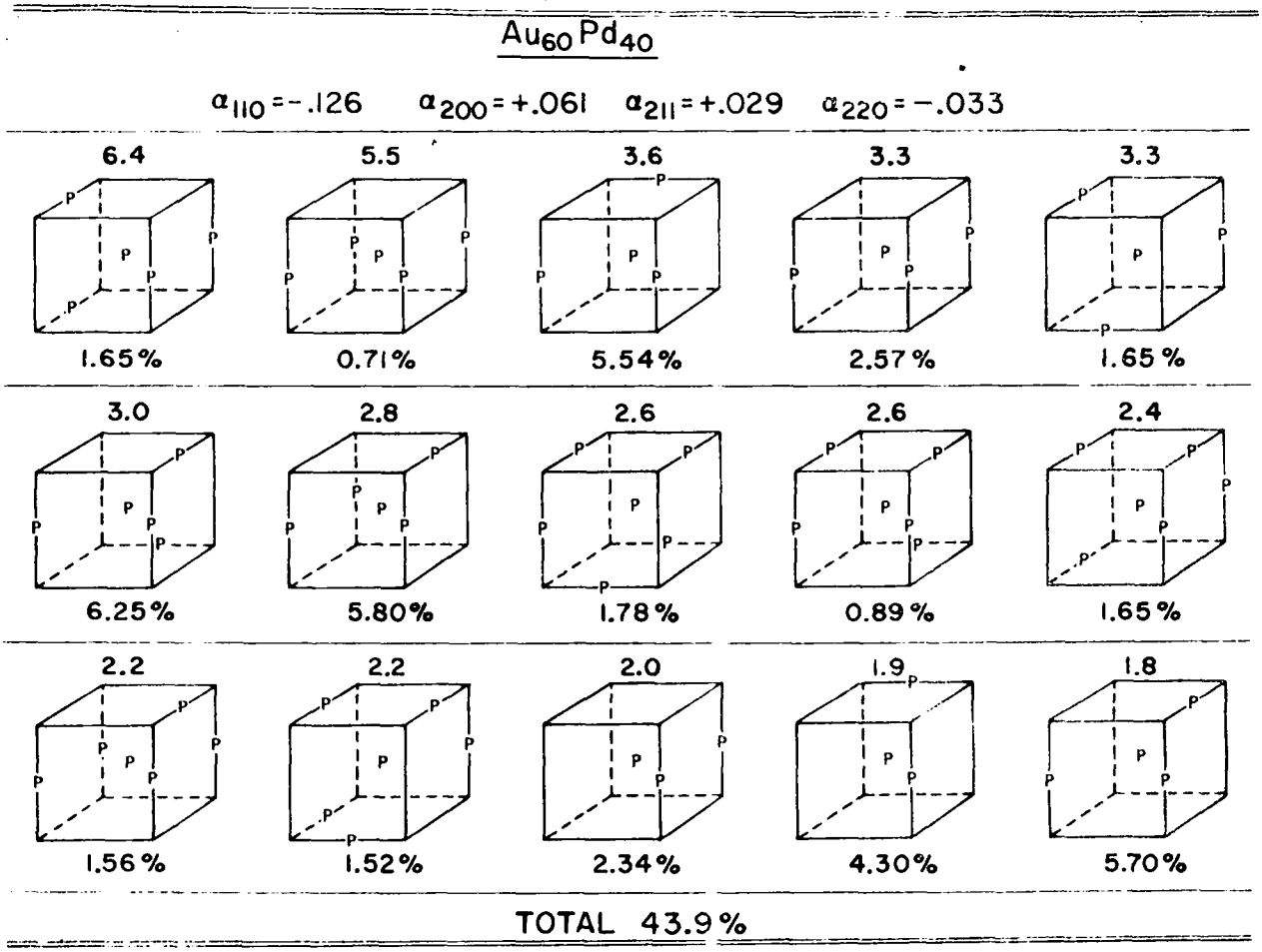

our cluster distribution it would appear that the $M = 2$ structure is just as likely a candidate. An important observation made by the above investigators was that the diffuse SRO peak was actually a double peak lying at $1\frac{3}{8}0$ and $1\frac{5}{8}0$ in reciprocal space. This is not commensurate with the superlattice peak positions of any known structure. The super-lattice positions for the $M = 1$ structure would be at $1\frac{1}{2}0$ and those for the $M = 2$ at $1\frac{1}{4}0$ and $1\frac{1}{4}0$.

The most likely explanation of this phenomenon is along the lines proposed by Moss[15] and recently used by Hashimoto and Ogawa[16] to explain the split diffuse peaks observed above T_c in Cu_3Au. Moss points out that, if the conduction-electron Fermi surface has a large flat region, this will produce a significant contribution to the interatomic ordering energy in the form of a long-range oscillatory potential whose wavelength is related to the diameter of the Fermi "sphere" at the position of the flats. This oscillatory potential will produce composition fluctuations in the disordered phase of the same wavelength, which in general will not be compatible with the integral periods required of an ordered structure. The lowest-energy ordered structure will be the one having an oscillation in composition closest in wavelength to that of the conduction-electron oscillatory potential.

If this is the phenomenon that we are witnessing in the $Au_{60}Pd_{40}$ alloy, it offers some interesting information about the topology of the Fermi surface

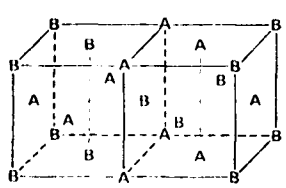

FIG. 1. $M = 1$ antiphase derivative of the $L1_0$ (CuAu) structure.

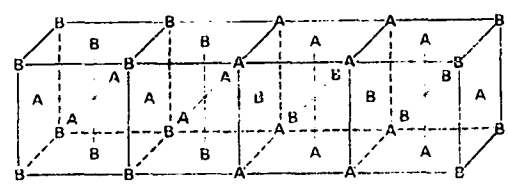

FIG. 2. $M = 2$ antiphase derivative of the $L1_0$ structure.

TABLE XI. Nearest-neighbor spectrum of Au atoms in $Au_{60}Pd_{40}$.

$Au_{60}Pd_{40}$

$\alpha_{110}=-.126 \quad \alpha_{200}=+.061 \quad \alpha_{211}=+.029 \quad \alpha_{220}=-.033$

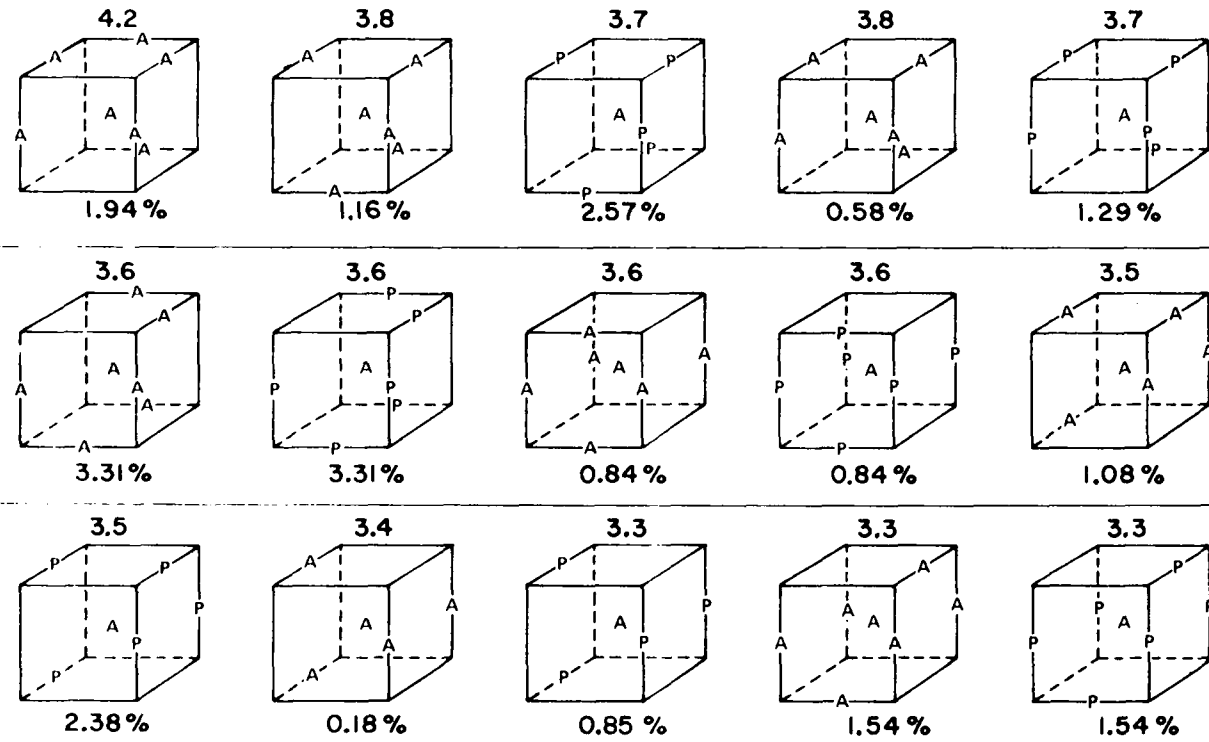

TOTAL 23.4%

and partially explains the sluggish ordering behavior. Our conclusion is, however, that one still cannot decide whether the $M=1$ or the $M=2$ ordered structure will be the ultimate ground state.

APPENDIX: PVM TABLES FOR bcc AND fcc NEAREST-NEIGHBOR SHELL CLUSTERS

Following I, the configuration of a cluster is

TABLE XII. PVM parameters for bcc nearest-neighbor cluster. See Fig. 3 for site indices.

Index k	Sites with $\sigma_i=-1$	Multiplicity W_k	Composition $W_k\langle\sigma\rangle_k$	Second neighbor $W_kC_k^2$	Third neighbor $W_kC_k^3$	Fifth neighbor $W_kC_k^5$
1($\bar{1}$)	...	1	+1(−1)	+1	+1	+1
2($\bar{2}$)	1	8	+6(−6)	+4	+4	+4
3($\bar{3}$)	1, 2	12	+6(−6)	+4	0	0
4($\bar{4}$)	1, 6	12	+6(−6)	0	+4	0
5($\bar{5}$)	1, 7	4	+2(−2)	0	0	+4
6($\bar{6}$)	1, 2, 5	24	+6(−6)	+4	−4	−12
7($\bar{7}$)	1, 2, 8	24	+6(−6)	−4	−4	+12
8($\bar{8}$)	1, 6, 8	8	+2(−2)	−4	+4	−4
9	1, 2, 5, 6	6	0	+2	−2	−6
10	1, 2, 5, 8	24	0	0	−8	0
11	1, 2, 5, 7	24	0	−8	0	0
12	1, 2, 3, 6	8	0	0	0	−8
13	1, 2, 7, 8	6	0	−2	−2	6
14	1, 3, 6, 8	2	0	−2	+2	−2

TABLE XIII. (*continued*).

k	$\sigma_i - 1$	W_k	$W_k\langle\sigma\rangle_k$	$W_kC_k^1$	$W_kC_k^2$	$W_kC_k^3$	$W_kC_k^4$
43($\bar{43}$)	1,6,7,9,11	48	+8(−8)	−8	0	+8	−32
44($\bar{44}$)	1,6,8,9,11	48	+8(−8)	−8	−16	+8	0
45($\bar{45}$)	1,5,6,7,10	24	+4(−4)	0	+8	−8	0
46($\bar{46}$)	1,3,6,10,11	48	+8(−8)	0	0	−8	0
47($\bar{47}$)	1,5,6,7,11	24	+4(−4)	0	0	−4	0
48($\bar{48}$)	5,6,9,11,12	24	+4(−4)	0	0	0	−16
49($\bar{49}$)	1,6,8,10,11	48	+8(−8)	0	−16	0	0
50($\bar{50}$)	1,5,6,11,12	48	+8(−8)	0	−16	0	0
51($\bar{51}$)	1,6,8,10,11	24	+4(−4)	0	−16	0	+16
52($\bar{52}$)	1,4,6,11,12	24	+4(−4)	0	−16	0	+16
53($\bar{53}$)	1,6,10,11,12	24	+4(−4)	+4	0	−8	0
54($\bar{54}$)	1,6,7,10,11	48	+8(−8)	+8	0	−8	−32
55($\bar{55}$)	1,4,6,10,11	48	+8(−8)	+8	−16	−8	0
56($\bar{56}$)	1,2,6,10,11	12	+2(−2)	+4	0	−4	−8
57($\bar{57}$)	1,5,6,10,11	24	+4(−4)	+8	0	−8	−16
58	1,5,6,7,8,10	12	0	−4	+8	−4	+4
59	2,4,5,6,9,11	12	0	−4	+8	−4	+4
60	4,5,6,7,8,11	12	0	−4	+4	−4	+12
61	1,5,6,7,8,11	24	0	−8	+8	−4	+8
62	2,5,6,8,9,11	24	0	−8	+8	−4	+8
63	1,3,5,6,11,12	48	0	−16	0	+8	−16
64	3,5,6,7,9,11	48	0	−16	0	+8	−16
65	3,5,6,9,11,12	24	0	−8	0	+8	−24
66	1,3,6,8,9,11	12	0	−4	−4	+4	−4
67	1,5,6,7,10,12	24	0	−4	+8	−8	+8
68	1,3,6,10,11,12	24	0	−4	+8	−8	+8
69	1,6,7,8,10,11	48	9	−8	0	0	−16
70	2,5,6,9,11,12	48	0	−8	0	0	−16
71	1,3,6,8,10,11	48	0	−8	−16	0	+16
72	1,5,6,8,11,12	48	0	−8	−16	0	+16
73	1,3,6,7,10,11	48	0	0	0	−8	−16
74	1,5,6,8,10,11	48	0	0	0	−8	−16
75	1,6,7,9,10,11	16	0	0	0	0	−16
76	1,4,6,10,11,12	48	0	0	−16	−8	+16
77	1,3,4,6,10,11	48	0	0	−16	−8	+16
78	1,5,6,9,11,12	12	0	0	−4	0	−4
79	1,2,6,8,10,11	12	0	0	−4	0	−4
80	1,4,6,7,10,11	48	0	0	−16	0	−16
81	1,4,6,8,10,11	48	0	0	−32	0	+16
82	3,4,6,8,10,11	4	0	0	−4	0	+4
83	1,4,6,8,11,12	4	0	0	−4	0	+4
84	1,2,6,10,11,12	48	0	+8	0	−16	−16
85	1,5,6,7,10,11	48	0	+8	0	−16	−16
86	1,5,6,9,10,11	24	0	+8	0	−8	−24
87	1,4,5,6,10,11	12	0	+4	−4	−4	−4

k henceforth implies summation over $\bar{k}$ as well. The occupation of the central site is given by σ_0 and so the double index (σ_0, k) serves to specify the complete cluster configurations.

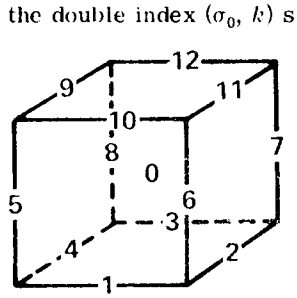

FIG. 4. Site numbering used for fcc clusters in Table XIII.

The multiplicity W_k is the number of symmetry partners that the kth shell configuration has. This is determined by counting the number of different configurations generated by applying the 48 symmetry operations of the cubic point group to the cluster. The less symmetric the cluster the more partners it will have, up to a maximum of 48. Because of the cubic symmetry of the lattice and the input data, these symmetric partners must all occur with equal probability and may thus be grouped together in the calculations. This considerably re-

TABLE XIII. PVM parameters for fcc nearest-neighbor cluster. See Fig. 4 for site indices.

Index k	Sites with $\sigma_i = -1$	Multiplicity W_k	Composition $W_k\langle\sigma\rangle_k$	First neighbor $W_kC_k^1$	Second neighbor $W_kC_k^2$	Third neighbor $W_kC_k^3$	Fourth neighbor $W_kC_k^4$
1($\bar{1}$)	...	1	+1(−1)	+1	+1	+1	+1
2($\bar{2}$)	6	12	+10(−10)	+8	+8	+8	+8
3($\bar{3}$)	6,7	12	+8(−8)	+4	+8	+4	+4
4($\bar{4}$)	5,7	6	+4(−4)	+2	+2	+2	+6
5($\bar{5}$)	6,12	24	+16(−16)	+8	+8	+12	+8
6($\bar{6}$)	6,11	24	+16(−16)	+12	+8	+8	+8
7($\bar{7}$)	5,6,7	12	+6(−6)	0	+8	0	+8
8($\bar{8}$)	5,6,12	24	+12(−12)	0	+8	+8	0
9($\bar{9}$)	1,7,9	8	+4(−4)	0	0	+4	0
10($\bar{10}$)	5,6,11	48	+24(−24)	+8	+16	+8	0
11($\bar{11}$)	4,6,11	48	+24(−24)	+8	0	+8	+32
12($\bar{12}$)	1,5,11	24	+12(−12)	+4	0	+8	0
13($\bar{13}$)	2,6,11	24	+12(−12)	+8	+8	0	0
14($\bar{14}$)	1,6,11	24	+12(−12)	+8	0	+4	0
15($\bar{15}$)	6,10,11	8	+4(−4)	+4	0	0	0
16($\bar{16}$)	5,6,7,8	3	+1(−1)	−1	+3	−1	+3
17($\bar{17}$)	4,6,7,9	6	+2(−2)	−2	+2	+2	−2
18($\bar{18}$)	5,6,8,11	48	+16(−16)	−8	+16	0	+16
19($\bar{19}$)	3,5,6,11	48	+16(−16)	−8	0	+16	−16
20($\bar{20}$)	1,5,10,12	48	+16(−16)	0	+16	−8	+16
21($\bar{21}$)	1,6,7,10	24	+8(−8)	0	+8	0	−8
22($\bar{22}$)	5,6,9,11	12	+4(−4)	0	+4	0	−4
23($\bar{23}$)	1,5,7,10	24	+8(−8)	0	0	0	+8
24($\bar{24}$)	4,5,6,11	24	+8(−8)	0	0	0	+8
25($\bar{25}$)	1,6,9,11	48	+16(−16)	0	0	+8	−16
26($\bar{26}$)	1,5,7,12	12	+4(−4)	0	−4	0	+12
27($\bar{27}$)	1,5,7,11	24	+8(−8)	0	−8	+4	+8
28($\bar{28}$)	2,5,7,12	24	+8(−8)	0	−8	+4	+8
29($\bar{29}$)	2,5,9,10	24	+8(−8)	+4	−8	0	+8
30($\bar{30}$)	1,6,11,12	24	+8(−8)	+4	−8	0	+8
31($\bar{31}$)	1,6,7,11	48	+16(−16)	+8	0	0	−16
32($\bar{32}$)	2,6,7,11	6	+2(−2)	+2	+2	−2	−2
33($\bar{33}$)	1,6,10,11	48	+16(−16)	+16	0	−8	−16
34($\bar{34}$)	5,6,7,8,11	24	+4(−4)	−8	+16	−8	+16
35($\bar{35}$)	4,6,7,9,11	24	+4(−4)	−8	+8	0	0
36($\bar{36}$)	1,4,7,9,11	24	+4(−4)	−8	0	+4	0
37($\bar{37}$)	1,3,6,9,11	24	+4(−4)	−8	0	+8	−16
38($\bar{38}$)	3,5,6,9,11	12	+2(−2)	−4	0	+4	−8
39($\bar{39}$)	2,5,6,9,11	48	+8(−8)	−8	+16	−8	0
40($\bar{40}$)	4,5,6,7,11	48	+8(−8)	−8	0	−8	+32
41($\bar{41}$)	1,6,7,8,11	48	+8(−8)	−8	0	0	0
42($\bar{42}$)	1,3,6,11,12	24	+4(−4)	−4	0	0	0

specified by an occupation number σ_i for each site which can have the value +1 or −1. σ_0 refers to the central site and σ_i (for $i = 1, z$) refers to the z

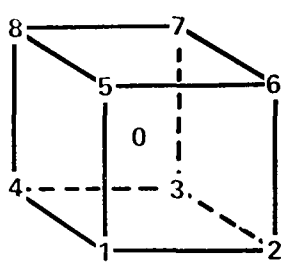

FIG. 3. Site numbering used for bcc clusters in Table XII.

sites in the nearest-neighbor shell around the central site. In the listing of cluster types (see Tables XII and XIII) we have specified only the shell sites having $\sigma_i = -1$ (the remainder of the shell sites are understood to have $\sigma_i = +1$). The various shell configurations are then labeled by the index k. It is not necessary to enumerate those clusters having negative occupation numbers on more than half of the shell sites. These configurations will be the complements of the tabulated clusters and can be generated from them by reversing the sign of σ_i on all shell sites. Each cluster k will thus have a complement which we denote by $\bar{k}$. Any summation over

duces the number of actual configurations to be dealt with.

$\langle\sigma\rangle_k$ is the average "composition" of the shell sites and is given by $\sum_{i=1}^{z}\sigma_i/z$. $\langle\sigma\rangle_k$ is the only tabulated quantity that changes for cluster complements (this being a change in sign) and is indicated by the entries in parentheses.

C_k^n is the average value in the cluster k of the occupation-number pair product $\sigma_i\sigma_j$ (where i, j are any two shell sites that are nth neighbors of each other) and may be determined by direct inspection of the cluster configuration. C_k^n is identical for the complement cluster. Because the coefficients of the PVM linear equations are the products $W_k C_k^n$, these are the quantities we have chosen to tabulate.

The linear constraint equations are as follows:

$$\sum_{\sigma_0}\sum_{k} W_k P(\sigma_0, k) = 1 , \tag{A1}$$

$$\sum_{\sigma_0}\sum_{k} \sigma_0 W_k P(\sigma_0, k) = c , \tag{A2}$$

$$\sum_{\sigma_0}\sum_{k} \langle\sigma\rangle_k W_k P(\sigma_0, k) = c , \tag{A3}$$

$$\sum_{\sigma_0}\sum_{k} \sigma_0\langle\sigma\rangle_k W_k P(\sigma_0, k) = (1-c^2)\alpha_1 + c^2 , \tag{A4}$$

$$\sum_{\sigma_0}\sum_{k} C_k^n W_k P(\sigma_0, k) = (1-c^2)\alpha_n + c^2 , \tag{A5}$$

where c is the difference in atomic fraction of the two components and the α's are the Warren SRO parameters.

If $c = 0$, then $P(\sigma_0, k) = P(\bar{\sigma}_0, \bar{k})$ and Eqs. (A2) and (A3) are redundant.

In Eq. (A5), n takes on the values (2, 3, and 5) for the bcc cluster and (1, 2, 3, and 4) for the fcc cluster.

The quantity to be maximized subject to these constraints is

$$I = -\sum_{\sigma_0}\sum_{k} W_k P(\sigma_0, k)\ln P(\sigma_0, k) . \tag{A6}$$

---

[1]P. C. Clapp, J. Phys. Chem. Solids 30, 2589 (1969).

[2]B. Borie and C. J. Sparks, Jr., Acta Cryst. 17, 827 (1964).

[3]P. C. Gehlen and J. B. Cohen, Phys. Rev. 139, A844 (1965).

[4]J. B. Cohen, J. Mater. Sci. 4, 1012 (1969).

[5]S. C. Moss and P. C. Clapp, Phys. Rev. 171, 764 (1968).

[6]W. Lin, J. E. Spruiell, and R. O. Williams, J. Appl. Cryst. (to be published).

[7]C. B. Walker and D. T. Keating, Phys. Rev. 130, 1726 (1963). Walker and Keating actually measured quantities that are linear combinations of SRO parameters and the Zernike theory of ordering was used to extract the individual parameters. As such they will reflect the inaccuracies of Zernike's formula as well as any experimental errors that may be present.

[8]S. C. Moss, J. Appl. Phys. 35, 3547 (1964).

[9]B. W. Roberts, Acta. Met. 2, 597 (1954).

[10]B. W. Batterman, J. Appl. Phys. 28, 556 (1957).

[11]C. R. Houska and B. L. Averbach, J. Appl. Phys. 30, 1525 (1959).

[12]M. S. Wechsler and R. H. Kernohan, Phys. Chem. Solids 7, 307 (1958).

[13]B. Mozer, D. T. Keating, and S. C. Moss, Phys. Rev. 175, 868 (1968).

[14]P. C. Clapp and S. C. Moss, Phys. Rev. 171, 754 (1968).

[15]S. C. Moss, Phys. Rev. Letters 22, 1108 (1969).

[16]S. Hashimoto and S. Ogawa, J. Phys. Soc. Japan 29, 710 (1970).